Modeling the potential impacts of vegetation change on the future climate of Southern Africa.

Myra Naik

Dissertation presented for the degree of
Master of Science
in
Environmental & Geographical Science

University of Cape Town
February 2015

Supervisor: Dr. B. J. Abiodun

Declaration II

Parts of this dissertation have been submitted for publication in advance of submission of the dissertation for examination. The text of this dissertation includes material from the manuscript entitled "Potential impacts of forestation on the future climate change in Southern Africa", submitted to the International Journal of Climatology. The co-author of the manuscript publication directed and supervised the research that forms the basis for the dissertation.

Abstract

Many studies have projected a future warming over Southern Africa without including the influence of on-going vegetation changes in the region. This study investigates how the vegetation changes may alter the projected warming. For the study, two regional climate models (RegCM and WRF) were applied to simulate the present day (1970-2005) and the future (2030-2065; IPCC RCP 4.5) climate, with and without vegetation change. The study considers two scenarios of vegetation change: the first accounts for the potential impacts of natural bush encroachment and commercial forestation in the eastern part of South Africa, while the second accounts for the expansion of grass cover along the western region of the Grassland Biome in South Africa.

The results of this study agree with that of previous studies in that elevated greenhouse emissions will induce warming over Southern Africa in the future, but further indicate that the ongoing vegetation changes may considerably alter the magnitude of the warming. Forestation may enhance the warming over the forested area and induce cooling elsewhere. It may also produce wet conditions locally and induce dry conditions over other area within the region. In contrast, the expansion of grass cover may reduce the projected warming over the grass covered area and induce warming elsewhere. It may also induce dry conditions locally and produce wet conditions over other areas in the sub-continent. Both vegetation change scenarios (*i.e.* forestation and expansion of grass cover) alter the projected future climate changes through their influences on local surface albedo; while forestation decreases the surface albedo, the expansion of grass cover increases it. However, the changes in

rainfall and temperature from the vegetation changes could enhance the frequency drought over some areas and reduce it over other areas within Southern Africa. This study, therefore, suggests that the vegetation changes may produce unexpected impacts on future climate. It also suggests that before using vegetation changes to mitigate climate change in Southern Africa, the biogeochemical benefits (*i.e.* carbon sequestration) should be carefully weighed against biogeophysical effects (*i.e.* changes in albedo).

Key words: climate change; forestation; grassland; vegetation; Southern Africa

Acknowledgements

First and foremost, I would like to express my sincere gratitude to my supervisor, Dr. Babatunde J. Abiodun, who has provided invaluable advice, guidance, support, and encouragement throughout this degree. Thank you.

I am also very grateful to Mr Ulrich Diasso for sharing his knowledge and expertise in running the WRF climate model. I appreciate all of your help and patience in guiding me through the challenges.

This degree was supported with the financial assistance provided by the Global Change SysTem for Analysis, Research and Training (START), the National Research Foundation of South Africa (NRF), the University of Cape Town (UCT) and the Applied Centre for Climate and Earth Systems Science (ACCESS). Computing facility for the climate simulations was provided by The Centre for High Performance Computing (CHPC) and the Climate System Analysis Group (CSAG), in South Africa. My research would not have been possible without these institutions.

Dr. Neil McKellar, Mrs Anna Steynor and Dr. Pippin Anderson are thanked for their facilitation with the START afforestation stakeholder‘s workshop. Each of the members of the START committee is also acknowledged for useful advice, which steered this project in a positive direction. Special thanks to Prof. Timm Hoffman, Mr James Puttick and Prof. William Bond, in The Botany Department at UCT, for taking an interest in my research and recommending useful literature.

Within the Environmental and Geographical Science Department, I would like to thank Mr Phillip Mukwenha for always being ready to help with software installations and IT-related issues. I am also grateful to Mrs Sharon Adams and Mrs Sharon Barnard, for help with general administration relating to funding, workshop organization and conference travel.

My colleagues in CSAG and friends are warmly acknowledged for advice and support throughout this degree. Last, but not least, I would also like to thank my family, for always being a constant source of support and encouragement throughout my university education.

Table of Contents

List of Figures

List of Tables

List of Abbreviations

DJF – December-January-February

GCM – Global Climate Model

ICTZ – Inter Tropical Convergence Zone

JJA – June-July-August

MAM – March-April-May

RCM – Regional Climate Model

RegCM – Regional Climate Model (ICTP)

SADC – Southern African Development Community

SON – September- October-November

SPEI – Standardized Precipitation

WRF – Weather and Research Forecasting Model (NCAR)

1 Introduction

1.1 Socio-economic factors in Southern Africa

Southern Africa, a geographical area located south of equator in the African continent, accommodates 14 developing countries that unite to form the Southern African Development Community (SADC). Member states of SADC include Angola, Botswana, the Democratic Republic of Congo (DRC), Lesotho, Madagascar, Malawi, Mauritius, Mozambique, Namibia, Seychelles, South Africa, Swaziland, Tanzania, Zambia and Zimbabwe (Figure 1-1). The total population of the region is about 277 million. Although the Gross Domestic Product (GDP) growth in SADC improved by 5.2% from 2000 to 2011, other socio-economic indicators vary considerably between the SADC‘s member nations. For instance, Gross National Product (GNP) per capita is reported to be as much as 60 times larger in high income countries, such as Seychelles, Mauritius, Botswana and South Africa, than in low income countries, such as Malawi, Mozambique, Tanzania, and Angola (SADC, 2001, 2012; Chishakwe, 2010). The SADC political ensemble is committed to achieving economic growth, sustainable development, and social equity for the people of Southern Africa through regional cooperation and integration between the countries (SADC, 2001).

The socio-economic development of the subregion is heavily dependent upon the performance and growth of various production sectors. Since these sectors utilize natural resources directly, they are often vulnerable to and constrained by weather and climate

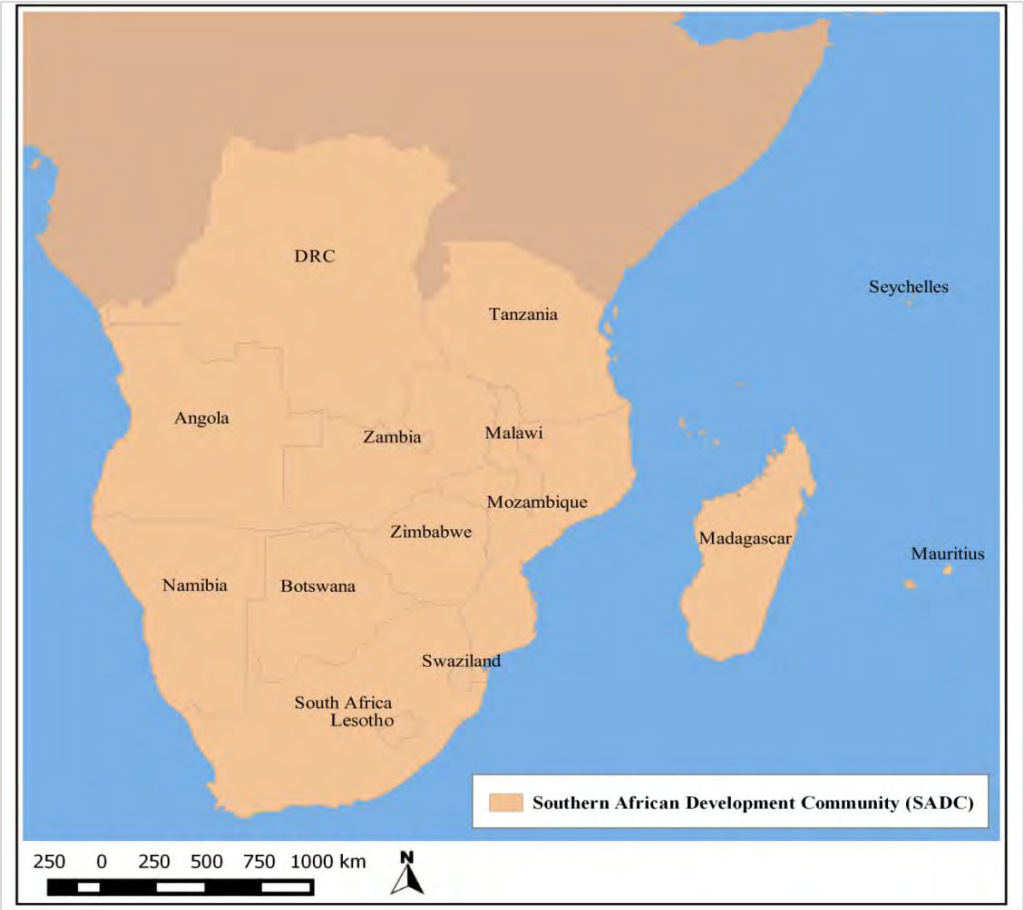

Figure 1-1 The Southern African Development Community. (Adapted from: TDRP, 2015)

extremes. For instance, agriculture is a major sector for many countries in Southern Africa and is particularly vulnerable to climate shock. Agriculture contributes between 4 to 27% of the subregional GDP, 70 to 80% of labour force and about 13% of the region‘s earnings from exports (SADC, 2012). About 60% of the livelihoods in the region depend on agriculture, practiced largely under rain-fed conditions (Cooper, 2008; Zinyengere, 2013). Despite the importance of agriculture to SADC economies, crop production in the SADC has stagnated in the last two decades, threatening food security in the region. Several factors have contributed to the decline in yield and food production, including inappropriate macroeconomic food policies, political unrest, environmental degradation,

as well as erratic rainfall patterns, droughts, and floods (Van Rooyen and Sigwele 1998). For instance, the decline in cereal production in Botswana, Lesotho, Malawi, Swaziland and Zimbabwe was largely attributed to a lack of rainfall in the 2001/2 cropping season (SADC, 2001). With the exception of South Africa, cereal production shortfalls occurred in most of the SADC member states due to adverse weather conditions (SADC, 2001). In order to address the shortage and avoid a humanitarian crisis, several million people in the region received emergency food aid. The increase in the frequency of these dry spells, as well as the lack of drought tolerant crop varieties, has contributed to poor harvest and exacerbated food insecurity in the region (Kandji, *et al.,* 2006). Pre-existing stressors, including human and social developmental challenges, chronic poverty in the region and the HIV/AIDS pandemic, only compound the food crisis, making populations more vulnerable to extreme climates and weather (Kandji, *et al.,* 2006).

The mining sector is also crucial to several SADC economies and accounts for 10% of the region‘s GDP and 5% of employment (SADC, 2001). Mineral processing and resource extraction, influencing the economy in the production of energy and electricity, are also industries vulnerable to changes in weather and climate. For example, the South African economy is heavily reliant on coal, which contributes to the country‘s energy production (71%) and a large proportion, 90%, of the nation‘s electricity (Scholvin, 2014). When exceptionally heavy rainfall soaked the fuel stock of the nation‘s major coal-fired power plants in 2014, the country‘s energy crisis was highlighted (Worthington and Maluleke, 2014). National power rationing was necessary and the electricity supply to major industrial customers tightened. This caused direct, adverse impacts on the

national economy. Other industries utilizing natural resources directly include the forestry and fisheries sectors. Thus, many important socio-economic sectors of Southern African countries depend of weather and climate.

1.2 Factors influencing the weather and climate of Southern Africa

1.2.1 Physical features

Southern Africa, located between about 0–35°S and 10–40°E, exhibits diverse patterns of weather and climate. The region is bound to the west and east, respectively, by the Atlantic and Indian Oceans. Sea Surface Temperatures (SSTs) are largely influenced by the cold Benguela current, flowing toward the equator along the western coastline (as far as Angola), and the warm Mozambique-Agulhas Current, flowing poleward along the eastern coast to the Cape Agulhas (Figure 1-2) (Bhaktawar and Van Niekerk, 2012). The contrast between the two sea surface temperatures of the Oceans contributes to the differences in climate found along the same latitude. A major feature of the Southern African geography is the Great Escarpment. The topography forms a horseshoe shaped boundary between the interior plateau and the narrow coastal margins (Figure 1-2). The mean height of the escarpment, ranges from about 1500 meters above sea level in the southwest to about 3500 meters in the Kwa-Zulu Natal Drakensburg, while the plateau is characterized by wide plains, about 1200 meters above sea level (Bhaktawar and Van Niekerk, 2012). The surrounding oceans and the topography of the region are both primary controls that modulate the climate of the region.

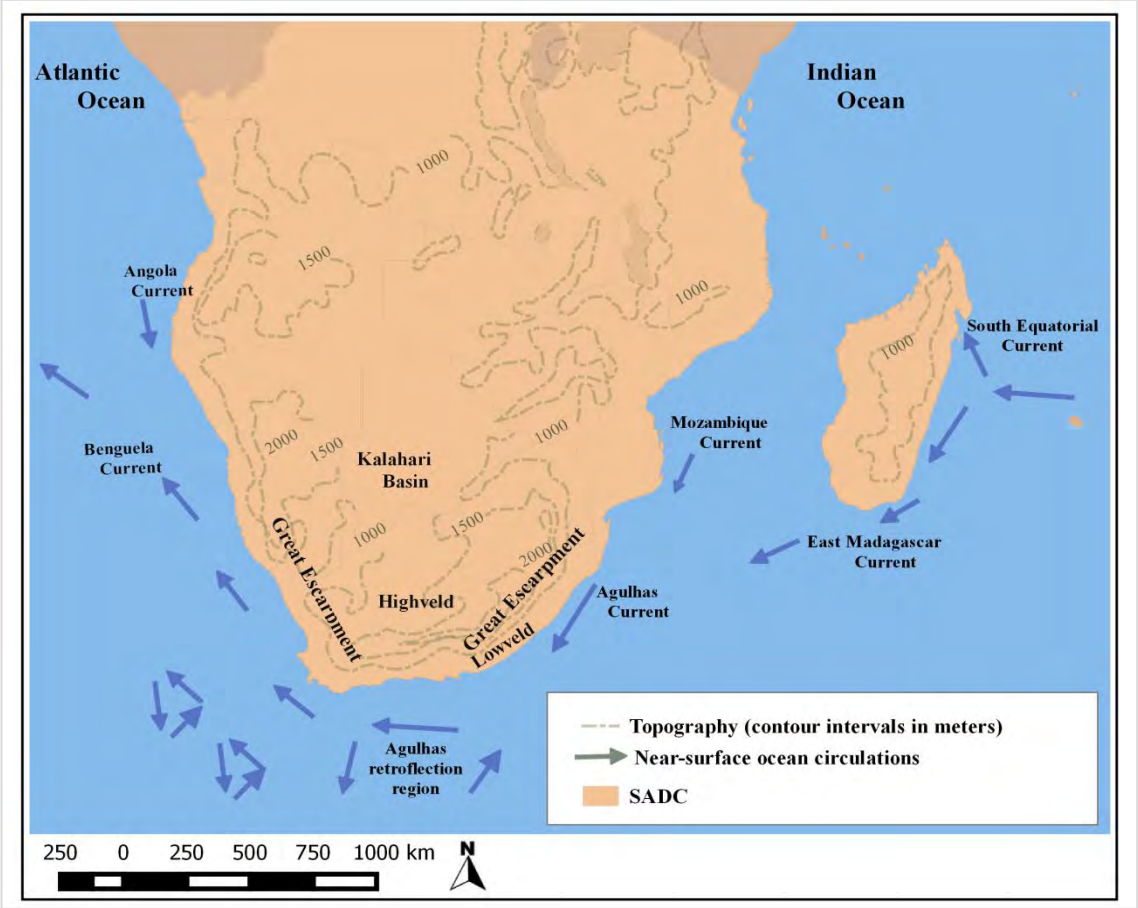

Figure 1-2 Physical features influencing the Southern African climate include the unique topography and surrounding oceans. (Adapted from: Mason *et al.,* 1999; Walker, 1989 and South Africa Travel, 2015)

1.2.2 Seasonality

The Southern African climate is influenced by synoptic features that span from the tropics to temperate regions (Crétat and Pohl, 2012). Large-scale synoptic features drive the climatology of the region and characterize the seasonal cycle. The seasonal migration of the Inter Tropical Convergence Zone (ITCZ; *i.e.* the region where the northeastern and southeastern trade winds converge) and the descending limb of the Hadley cell are both important controls for conditions over the region. Typical conditions that occur during the austral summer season (December-January-February; DJF) include the permanent South

Atlantic High (SAH; west of Namibia) and semi-permanent South Indian Ocean High (SIOH; east of Mozambique) (Figure 1-3). The SIOH is associated with southeasterly trade winds which are responsible for the transport of moist air into the northeast part of Southern Africa (including, for example, Zimbabwe, Limpopo and the South African Free State areas) (Kruger, 2004a). These southeasterly trade winds converge with the cooler and drier southwesterly flow from the SAH, at the –Moisture boundary, inducing vertical motion, precipitation and heavy rainfall. Since the ITCZ has migrated to its most Southern location in DJF, the region also receives large amounts of incoming solar radiation. The insolation causes heating at the surface and induces the presence of a heat low that often forms over the Kalahari Desert and western coastal regions (Figure 1-3). Another important feature of the Southern African climate in this season is the Tropical Temperate Trough (TTT) and the Limpopo Valley thermal trough. The former occurs over the continental interior and permits moisture flow from the tropics to mid-latitude regions (largely in the form of convective thunderstorms and tornadoes), while the latter is responsible for the _draw in' of warm, moist tropical air off the SIOH and acts as a strong modulator between the east and west coasts of the subcontinent.

During the winter season (June-July-August; JJA), the ITCZ and associated high pressure systems are displaced further north and surface heating is weak due to the reduction in insolation. There is an absence of heat lows over the interior, hence the thermal trough weakens or disappears (Kruger, 2004a). The Indian and Atlantic Highs may _merge' over the interior, favouring conditions of a high pressure system, including subsidence and clear skies (Figure 1-4) (Kruger, 2004a). A subsidence inversion may also occur over the

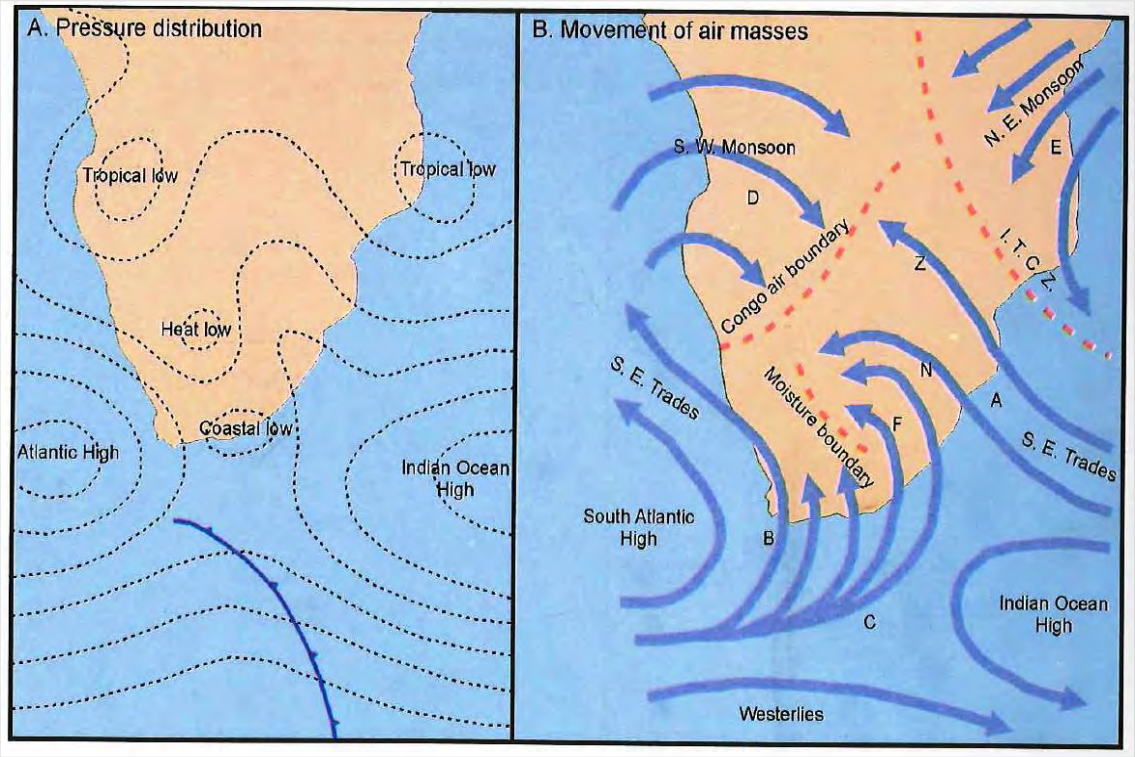

Figure 1-3 Pressure distribution and basic movement of air masses over Southern Africa during summer. (Source: Hurry and Van Heerden, 1982; in Kruger, 2004a; p.13)

interior of the subcontinent (induced by coastal topography), which creates generally drier conditions and less rainfall over most of the region. Coupled to this northward shift of the ICTZ is the enhanced interaction of mid-latitude cyclones and greater penetration of frontal systems further inland (occasionally even as far north as Zimbabwe). It is worth emphasizing that although much of the Southern African subcontinent receives almost all its rainfall during DJF, the southwest region of the Western Cape Province (which receives frontal rainfall from the passage of mid-latitude cyclones during JJA) and a small margin along the south coast of South Africa (where all-season rainfall patterns occur) differ (Tyson, 1986).

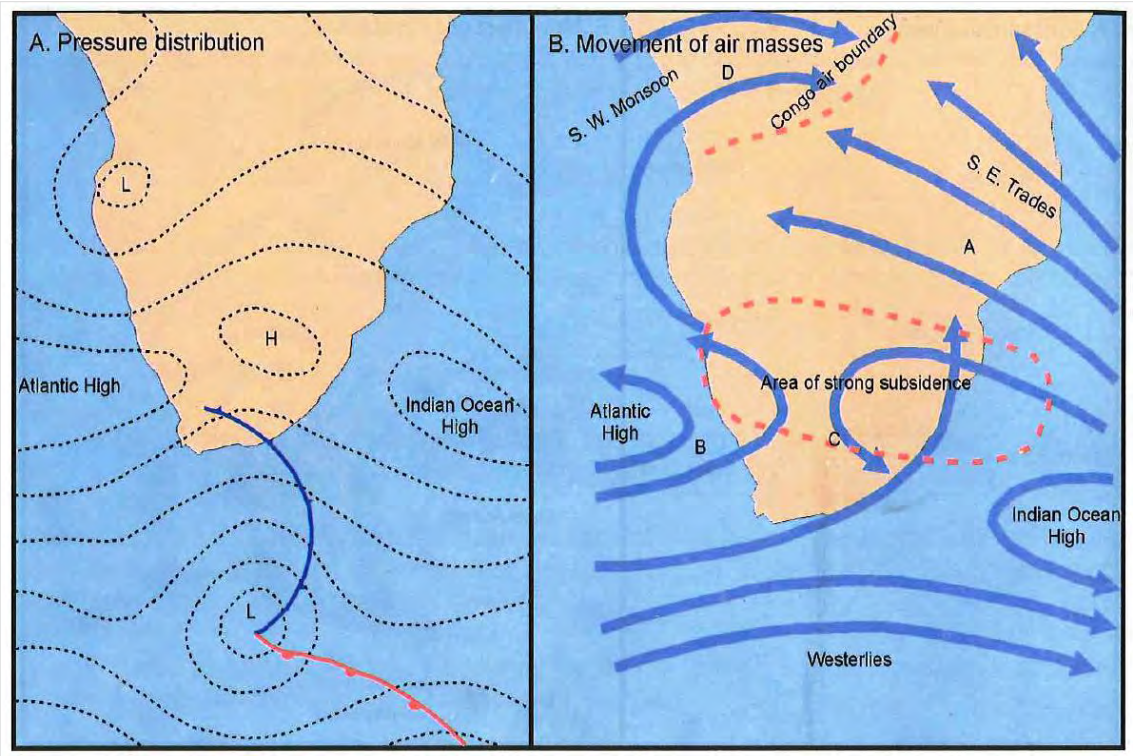

Figure 1-4 Pressure distribution and basic movement of air masses over Southern Africa during winter. (Source: Hurry and Van Heerden, 1982; in Kruger, 2004a; p.14)

1.2.3 Teleconnections and feedbacks

Global modes of variability and feedback processes regulate the regional and local variability of the Southern Africa climate from intraseasonal to interdecadal timescales. Important teleconnections that influence the climate of the region include the Southern Annular Mode (SAN) and the Madden–Julian Oscillation (MJO). The El Nino Southern Oscillation (ENSO) events in the equatorial Pacific are also an important control of rainfall variability associated with the occurrence of frost, floods (during La Nina years) and droughts (during El Nino years) over the region. Moreover, atmospheric stability and regional circulation patterns may also be altered as a result of various feedback mechanisms. For instance, biogenic emissions, often emitted from the burning of

vegetation and by dust particles from deserts and ephemeral lakes (such as the Makgadigadi Pans of Botswana), are a significant source of aerosol particles and trace gases (*e.g.* Bryant *et al.,* 2007; Li, *et al.,* 2003; Tummon, 2011). These particles alter the scattering of insolation, the formation of cloud condensation nuclei and the hydrological cycle through various feedback processes. Through long-range transport and mean air circulation pathways, these particles can feedback to influence both local and regional climates. Another important feedback process and controlling factor in the climate of the region is the distribution of land cover and vegetation type.

1.3 Vegetation of South Africa and its relation to climate

The distribution of vegetation in South Africa represents a synthesis of many climatic elements (Kruger, 2004b). The vegetation is often classified into nine broadly recognized biomes: Fynbos, Succulent Karoo, Desert, Nama Karoo, Grassland, Savannah, Albany Thicket, Indian Ocean Coastal Belt and Forest (Figure 1-5). The biome concept is rooted in a long history of seminal work conducted by Acocks (1988), Rutherford and Westfall 1994), and Low (1998). The biome classification is defined primarily by a uniform life or growth forms and secondarily on the basis of major climatic features influencing the biota (Mucina and Rutherford, 2006).

The vegetation biomes in the country are highly disparate in size. The Savanna and Grassland Biomes tend to dominate, covering, respectively, about 33% and 28% of the country‘s land surface (Mucina and Rutherford, 2006). These biomes are confined largely

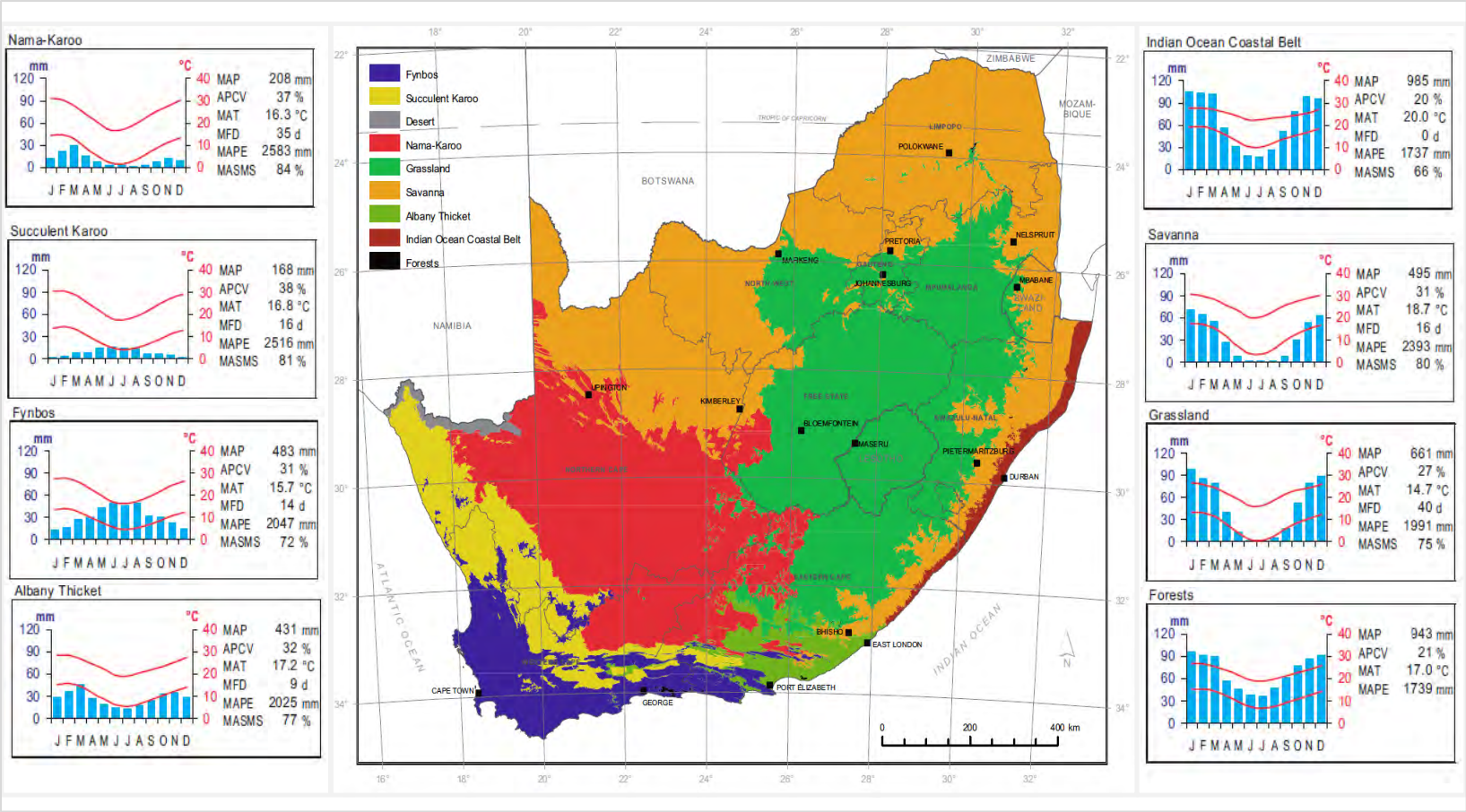

Figure 1-5 Biomes of South Africa, Lesotho and Swaziland. Climate diagrams of biomes excluding Desert. Blue bars show monthly median precipitation. The upper and lower red lines show the median daily maximum and minimum temperature, respectively. MAP: Mean Annual Precipitation; APCV: Annual Precipitation Coefficient of Variation; MAT: Mean Annual Temperature; MFD: Mean Frost Days; MAPE: Mean Annual Potential Evaporation; MASMS: Mean Annual Soil Moisture Stress (% of days when evaporative demand was more than double the soil moisture stress) (Adapted from: Mucina and Rutherford, 2006; p.33, 40)

to the northern and eastern summer and strong-summer rainfall regions of the country (Mucina and Rutherford, 2006). The Savanna biome extends across the northwestern parts of Limpopo, Gauteng, eastern Mpumalanga and parts of KwaZulu-Natal, while that of the Grassland biome extends from the Northwest Province southwards (Dry Highveld Grassland), to the higher elevation regions of Gauteng, Mpumalanga and the southeastern Free State (Moist Highveld Grassland) (Kruger, 2004b). The Grassland Biome exhibits a similar climate to that of the Savanna, except that annual temperatures are generally lower (Figure 1-5) (Mucina and Rutherford, 2006). Grasslands are prone to very low temperatures, particularly during winter (Kruger, 2004b). More specifically, mean minimum temperatures during the coldest months are characteristically higher than 2^{o}C for Savanna regions. Rainfall also varies considerably over this region. Mean annual precipitation in Grasslands regions is between about 400 and 2000 mm, but that of the Savanna region is about 235 mm (Kruger, 2004b). This is due to the influence of topography and the production of orographic rainfall over some regions and not others.

Forest, Albany Thicket and Fynbos Biomes occur mainly along the southern and eastern periphery of South Africa. These biomes cover only about 0.3%, 2.2% and 6.6%, respectively, of the country‘s land surface (Mucina and Rutherford, 2006). Forest, Thicket and Indian Ocean Coastal Belt regions occur in areas of high rainfall (>800 mm per annum). Forest regions, for example, occur in areas where mean annual precipitation exceeds 525 mm, as well as areas of strong summer rainfall where mean annual precipitation exceeds 725 mm (Kruger, 2004b). The extent of forest vegetation in southern regions of the country is regulated by shelter from the Cape Fold Mountains and

proximity to the surrounding ocean. The southwestern regions of the Western Cape (a Mediterranean-type region) and the eastern coastal regions of the Eastern Cape and KwaZulu-Natal typically receive frontal rainfall, during the winter and all year round (Kruger, 2004b). These regions are typically frost free and have mild temperatures (Figure 1-5).

The Nama Karoo and Succulent Karoo Biomes are largely limited to the southern and western regions of South Africa, including northern regions of the Northern Cape and the western part of the Northwest Province. The biomes cover about 20% and 6.5%, respectively, of the country‘s land surface (Mucina and Rutherford, 2006). Both the biomes experience a more semi-arid or arid climate, erratic rainfall and extreme temperatures. The Nama Karoo Biome is found in conditions of all year, summer and strong summer rainfall (about 100-520 mm MAP), while that of the Succulent Karoo is restricted to all year, winter and strong winter rainfall (20-290 mm MAP) (Kruger, 2004b). Although the mean minimum temperature of the coldest month is characteristically higher than 2°C in both Succulent Karoo and Desert biomes, the Nama Karoo biome is subject to very low temperatures, particularly during winter (Figure 1-5). This information demonstrates that vegetation in the region is both a good indicator and integrator of climate in South Africa (Kruger, 2004b).

1.4 Biogeophysical impacts of vegetation change on climate

The structural and functional properties of vegetation on the land surface influence climate (Smith, 2014). Changes to vegetation on the land surface regulate the climate of a

region through different biogeophysical processes. These processes involve the exchange of water and momentum fluxes, greenhouse gas exchanges and atmospheric chemistry, across different spatial and temporal scales (Mahmood *et al.,* 2014; Viterbo, 2002). The net radiation received by the earth‘s surface, for instance, is partitioned depending on the biogeophysical properties of the earth‘s surface. Bare soil and the type of vegetation present alter the energy budget through changes in surface variables, such as soil moisture, albedo (the proportion of insolation that is reflected by the land surface), sensible heat (the flux of heat via conduction and convection processes) latent heat (the flux of heat due to the effects of evapotranspiration or condensation) and Bowen ratio (the ratio of sensible and latent heat) (Zhao and Jackson, 2014). These changes in energy and moisture at the surface are summarized by Pielke (2002) and Warner (2010) in two closely coupled equations:

$$RN = QG + H + L(E + T) \qquad (1)$$

$$P = E + T + RO + I \qquad (2)$$

where RN represents the net radiative flux; QG is the soil heat flux, H is the sensible heat and L is the heat of vaporization (from evapotranspiration (E) and transpiration (T)), P is precipitation, RO is run off, I is infiltration, Qs is incoming solar radiation, α is albedo, QLW and QLW is downwelling and upwelling long wave radiation, respectively, and T is temperature.

Any change to vegetation on the land surface modifies at least one variable and thereby influences climate. Irrigation agriculture could, for example, increase E, T and I in (2)

and decrease QG and H in (1) (Pielke *et al.,* 2002). The biogeophysical changes to the surface energy budget feedback to modify surface variables (such as temperature, humidity, wind-speed and cloud cover) and the structure of the planetary boundary layer. In combination with various biogeochemical feedbacks (*i.e.* those involving changes to the atmospheric chemistry, such as changes in carbon dioxide concentration), the biogeophysical effects may alter the atmospheric temperature and moisture and, thus, the regional weather and climate (Mahmood *et al.,* 2014).

1.4.1 Biogeophysical impacts of forestation

Forestation includes afforestation (planting of forest on land that has not recently or has never been forested) and reforestation (planting of forests on land that was once forested but has recently been converted for a different use) (World Bank, 2010). Many forestation efforts offer ancillary benefits, such as more sustainable livelihoods for local communities and opportunities for environmental conservation (Canadell and Raupach, 2008; Topfer, 2001). Forestation is also often recognized as a reasonable, effective and affordable climate change mitigation option because of its biogeochemical benefits (Lenton and Vaughan, 2009). Forestation can sequester atmospheric carbon dioxide, a major greenhouse gas, and offset fossil fuel emissions (Bathiany *et al.,* 2010). Under the United Nations Framework Convention on Climate Change (UNFCC) and the Kyoto Protocol, many efforts have been made to implement forest-related carbon mitigation projects. Clean Development Mechanism (CDM) and Reducing Emissions from Deforestation and Forest Degradation (REDD) have also created financial incentives to store carbon in forests. Therefore, forestation not only offers emissions reductions, but

also creates economic opportunities generating monetary returns in carbon trading markets (Anderson *et al.,* 2011). However, many of these forestry projects overlook the biogeophysical effects of forestation on climate.

Forests and non-forest vegetation produce contrasting biogeophysical properties (Zhao and Jackson, 2014). This is because the land-atmosphere interactions of a forested region typically differs from that of regions otherwise vegetated, such as cropland, due to differences in the exchange of water and heat between surfaces and the air (more latent heat, less sensible heat), thermal radiation, surface roughness, leaf areas and rooting systems. The different biogeophysical properties influence changes in energy fluxes and their partitioning, and may alter a variety of atmospheric processes; such as evapotranspiration, precipitation and the lifting condensation level (cloud base height) that alters the chances of cloud formation (Figure 1-6), (Mahmood *et al.,* 2014; Zhao and Jackson, 2014). Since these atmospheric processes may span various spatial and temporal scales, the biogeophysical impacts of forestation may modify both the local and regional climate.

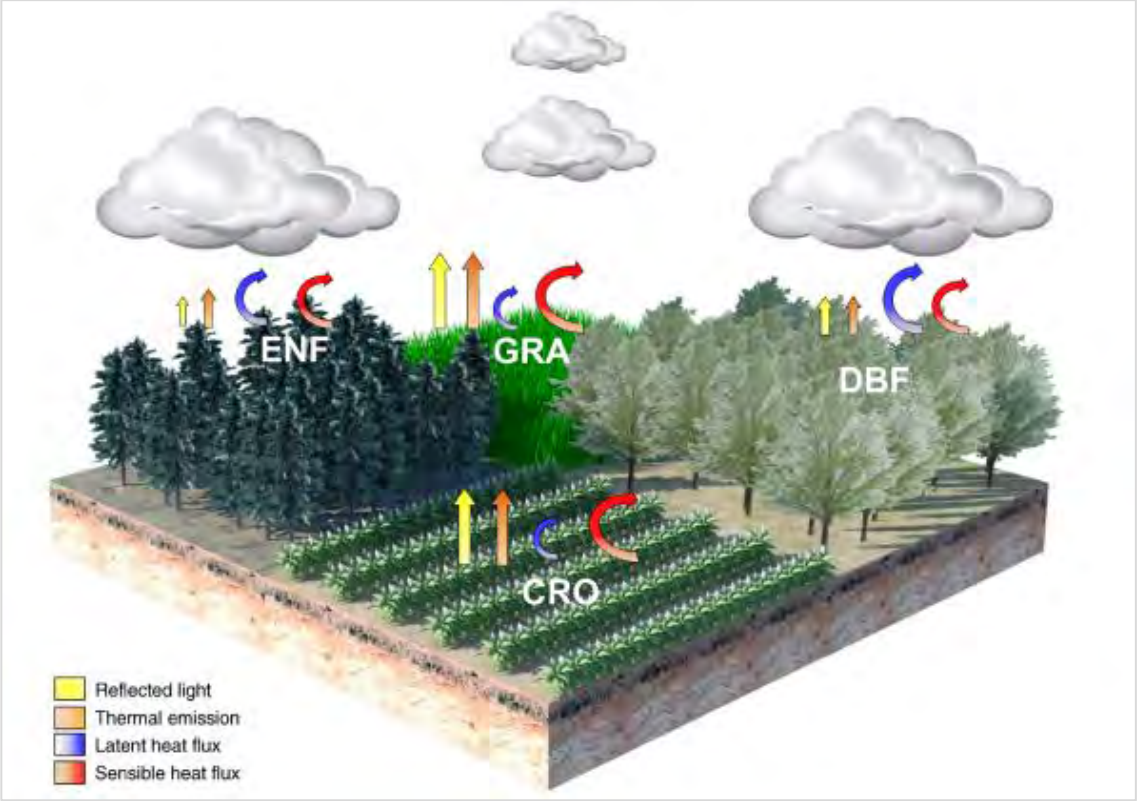

Figure 1-6 The relative magnitudes of surface energy fluxes for four vegetation types (grasslands [GRA], deciduous forests [DBF], croplands [CRO], and evergreen forests [ENF], as depicted clockwise from the top in the graph) are indicated by the sizes of arrows. These biogeophysical differences highlight that forestation impacts climate via biogeophysical pathways in addition to carbon sequestration. (Source: Zhao and Jackson, 2014; p.331)

1.5 Regional climate modeling and land surface representation

Climate models are used by a large number of researchers in almost every region of the world (Rummukainen, 2010). Global Climate Models (GCMs) and their complements, Regional Climate Models (RCMs), are sophisticated numerical tools used to explore the climate system and understand a variety of processes. These computer models are designed to represent physical atmospheric processes by complex mathematical equations that are solved using numerical methods (Trenberth, 1992). The models provide a 3-D representation of different climate variables in the atmosphere and simulate the

conservation of energy, mass and momentum (Figure 1-7). Pioneering work towards RCM development was started by Giorgi and Mearns (1991). RCMs have developed over the last two decades to represent various processes at finer temporal and spatial scales. RCMs are typically forced by time-variable data along lateral boundaries, either in the form of a parent GCM or a global reanalysis product, which constrain the RCM simulation, through various mathematical formulae (Fesser, 2011). This technique, often termed dynamical downscaling, has several strengths and weaknesses, but essentially allows RCMs to capture aspects of regional and local climate often missed in coarse resolution GCM simulations (Rummukainen, 2010). This includes, for instance, representing the effects of mountain ranges, vegetation, and soil characteristics (Figure 1-7). The ability of the models to capture small-scale atmospheric processes in detail is particularly useful for the simulation of vegetation-land-atmosphere processes.

Different land surface schemes and land surface models (LSMs) form an integral component of modern Global Climate Models (GCMs) and Regional Climate Models (RCMs) today (Warner, 2010). These models account for different variables and simulate changes in the physical processes described in equations (1) and (2). Early research conducted by Charney *et al.* (1977) used a series of Global Circulation Model (GCM) simulations in a sensitivity analysis to examine the effects of surface albedo and desertification in the Sahel. Since the 1980s, however, complex biogeophysical packages (such as Dickinson‘s Biosphere Atmosphere Transfer Scheme and Sellers‘s Simple Biosphere Model (in the late 1980s)) have been developed and these provide more realistic models for the radiative transfer, turbulent processes, and the transport of heat

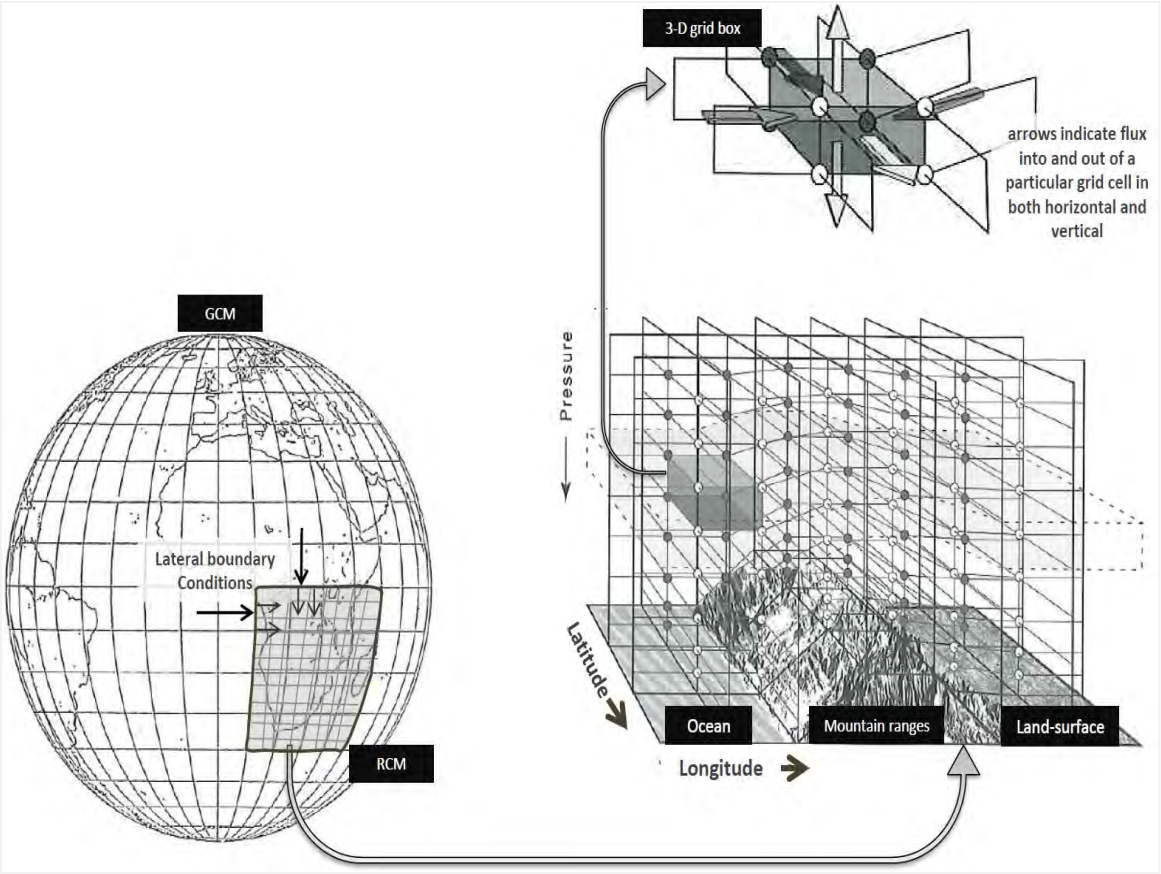

Figure 1-7 Dynamical downscaling, where GCM output is used to drive a RCM at finer horizontal resolution (left), which therefore is able to simulate local conditions (including mountain ranges and land surface processes) in greater detail (right). The atmosphere is divided into a finite number of 3-D grid cells in the vertical and horizontal (top), dots inidcate vertices of grid cells. (Adapted from: Coiffier, 2011; p.35 and Neelin, 2010; p.146)

and water vapour between the atmosphere and the land surface (see Trenberth, 1992 for a complete description). Over the last few decades, model development has also been propelled by rapid developments in computing power and architecture. Numerical models of the atmosphere are now capable of simulating the various processes in the interaction between vegetation on the land-surface and the atmosphere, as well as ocean and sea-ice processes, carbon cycling, and atmospheric chemistry. To date, a variety of models exist aiming to incorporate increasingly comprehensive representations of earth system

processes. A new generation of global earth system models (ESMs), for example, incorporate various aspects of the climate system and include vegetation dynamics and biogeochemistry (especially carbon cycle) components. Although RCMs are optimized for application at fine grid resolution (sufficient to account for vegetation, topography and regional-scale dynamics), they have lagged behind this progress of global climate modeling community (Smith, 2014). Regional ESM development is currently on-going, and there are good prospects to incorporating such functionality into RCMs in the near future (Smith, 2014). Nevertheless, current RCMs are still attractive tools for examining regional scale land-atmosphere processes, and to date, numerous studies have used these models to unpack the complexity of land surface and atmosphere interactions and assess some of the climate implications of future land surface change.

1.6 Vegetation and climate interactions in Southern Africa

1.6.1 Future projections of climate change

Many studies have projected a future warming over Southern Africa. For instance, a warming of about 2-3°C by 2050 is projected over the borders of South Africa and Botswana, and the warming may exceed 4°C over some parts of the interior by the end of the century (Boko, *et al.*, 2007; Hudson and Jones, 2002; Midgley *et. al.,* 2007; Archer *et al,.* 2010). In addition, a drier condition is projected over many areas of Southern Africa in the future (Haensler *et al.*, 2011a; Ringrose *et al.*, 2002). Even so, these studies have projected a warmer and drier climate over Southern Africa without including the influence of future vegetation changes.

1.6.2 Vegetation-climate interactions

From the information provided in earlier sections, it is clear that the distribution of vegetation is both a good integrator and indicator of climate in Southern Africa. However, only a very limited number of studies have investigated how changes to vegetation could influence the future climate of the region. To date, many modeling experiments on vegetation-climate interactions over the region have shown that the biogeophysical properties of vegetation (albedo, evapotranspiration, soil moisture content *etc.*) are important controls of the Southern African climate (*e.g.* Drew, 2004; Chikoore, 2005; Richard and Poccard, 1998). Previous study by Mackellar *et al.,* (2008, 2010) investigated the climate impacts of historical vegetation change, while that of Williams and Kniveton (2011) was the unique in that it studied the impacts of land surface change over Southern Africa in the future. Williams and Kniveton (2011) examined the sensitivity of rainfall variability to increasing aridity associated increase in desert dune expansion. Less clear, however, is how the biogeophysical effects associated with changes to the distribution of vegetation may influence climate change in the future.

Recent research has shown that the current distribution of vegetation in South Africa is dynamic In particular the Forest, Savanna and Grassland Biomes are particularly sensitive to influenced by both climatic and non-climatic factors, that may alter the distribution of vegetation in the future (Midgley and Thuiller, 2010; Rutherford *et al.,* 1999). Important vegetation changes that have been detected in these regions include: on-going forestation activities (*e.g.* DWAF, 2007), which have resulted in increased tree density in the eastern parts of South Africa, as well as the expansion of grass cover along

the border between the Nama Karoo and Grassland Biome in South Africa (*e.g.* Masubelele *et al.*, 2014). However, the biogeophysical feedbacks and potential impacts on climate have not been included in these assessments of vegetation change. This dissertation intends cover these gaps by investigating how the vegetation changes may influence the projections of future climate change.

1.7 Aim and Objectives

The aim of this study is to examine the potential impacts of vegetation changes on the future climate of Southern Africa using two regional climate models.

The specific objectives of the dissertation can be summarized as follows:

1. To examine the regional climate model‘s ability to simulate the Southern African climate.
2. To project the future climate change due to elevated greenhouse gasses.
3. To examine the potential impacts of vegetation changes on the future climate of Southern Africa. This objective will:
    a. Examine the potential climatic impacts of natural and commercial forestation in South Africa.
    b. Examine the potential climatic impacts of grass cover expansion along the western border of the Grassland Biome in South Africa
4. To assess the potential impacts of elevated greenhouse gasses and the vegetation changes on drought in the future.

The dissertation is divided into eight chapters to address the objectives. Following the introductory chapter, Chapter Two presents a literature review on regional climate modeling activities over Southern Africa. Studies that have modelled the potential impacts of vegetation change on climate are also discussed. Chapter Three details the methodology of the study, including a description of data, the regional models used and their setup for simulations. Chapters Four to Seven present and discuss the results of the present study. Chapter Four evaluates the ability of the regional models to reproduce the present-day climate over Southern Africa (model validation). Chapter Five discusses the projected changes due to elevated greenhouse gasses. Chapters Six and Seven present the potential impacts of vegetation change on climate and the potential impacts of vegetation change on drought, respectively. Chapter Eight provides a summary of the key findings, suggestions for future avenues of research and offers concluding remarks.

2 Literature Review

This chapter provides an overview of regional climate modeling activities over Southern Africa. It discusses the observed trends in climate and drought phenomena in the region as a background to the central theme of RCM evaluation and assessment. The focus of the chapter is on studies that have modelled vegetation and climate interactions. An illustrated review is also provided on the potential changes to the distribution of vegetation in South Africa in the future.

2.1 Regional climate modeling over Southern Africa

Since their development in the 1990‘s, regional climate models (RCMs) have proven useful tools for adding detail to global climate simulations (Giorgi and Mearns, 1991; McGregor, 1997). However, regional climate modeling activities in the Southern Hemisphere have lagged behind, relative to many other regions of the world. In particular, research focused on Africa has often been limited, largely as a result of computational facilities, but also due to a lack of human resources and inadequate climate data (Boko *et al.,* 2007). Although the earliest dynamical downscaling effort over Southern Africa was in the early 1990s, extensive climate modeling research focused on Southern Africa only began in earnest over the last decade. Early research conducted by Joubert *et al.* (1999) nested the Commonwealth Scientific and Industrial Research Organization (CSIRO) Division of Atmospheric Research Limited Area Model (DARLAM) in a GCM over the Southern African domain. This pioneering study demonstrated that, notwithstanding some biases, downscaling could capture the pattern of

observed rainfall over most parts of the subcontinent and improve on the GCM simulated climatology.

In recent years, however, much research has evaluated the performance of different individual RCMs. Performance studies typically examine the internal variability of the models and the effect this produces on the model biases. The sensitivity of the simulated regional climate to the RCM‘s physics has been the focus of recent research. For example, Crétat and Pohl (2012), Pohl *et al.* (2014) and Ratna *et al.* (2014) show that the biases in the WRF model, particularly for rainfall, are highly dependent on the physical packages and convective parameterization used. Other studies have quantified the internal variability of regional model simulations using simulations of model ensembles at various timescales (for example, using RegCM: Kgatuke *et al.,* 2008 and WRF: Crétat *et al.,* 2011). These studies describe the sensitivity of the RCM solution to lateral boundary conditions, the size of the simulation domain and physical parameterizations used.

Different timescales in simulations have been explored. Many studies suggest that commonly used RCMs (such as RegCM and WRF models) capture the regional climate at seasonal, annual and interannual timescales well, (Crétat *et al.,* 2011; Sylla *et al.,* 2009; 2012; Yuan *et al.,* 2013), but emphasize that accurate simulation of intra-seasonal variability and the diurnal cycle (particularly for variables like precipitation) is a common deficiency in some of the models. Different spatial resolutions have also been explored with the variable resolution global models, like the conformal-cubic atmospheric model (CCAM; Engelbrecht *et al.,* 2009; 2011), CAM_EULAG Ogier, (2014), and REMO — a

model capable of adequately simulating the long-term climate of Southern Africa at very high resolution (18 km) (Haensler *et al.,* 2011b). Thus, several RCMs have been applied at different scales. Various temporal and spatial resolutions provide the opportunity to compare and better characterize the uncertainty in climate model simulations over the region.

Numerous studies have also focused on RCMs ability to simulate important atmospheric features and large-scale modes of variability influencing the Southern African climate. For instance, preliminary efforts by Hansingo and Reason (2008) used the MM5 regional climate model to examine the atmospheric response to SST dipole patterns in the South Indian Ocean. More recently, Vigaud *et al.* (2012) used the WRF model to examine the origin and development of Tropical Temperate Troughs (TTT) events — which provides a substantial proportion of summer rainfall over the region (Tozuka *et al.,* 2014) — while the study by Boulard *et al.* (2013) used the same model to assess the contribution of ocean SSTs in simulating the regional effects of the El Nino/ Southern Oscillation (ENSO) events. Modeling studies that evaluate the representation of these atmospheric features and large-scale modes of variability are important if RCMs are to provide a realistic representation of the atmosphere and regional climate.

The RCM downscaling technique has matured over the last two decades and the assessment of individual RCMs is likely to continue in the near future as an on-going effort. However, the global scientific modeling community is now making progress towards model inter-comparison projects and coordinated multi-model ensemble

projections at regional scales (Laprise, 2008). Coordinated, international efforts and modeling frameworks have gained traction in recent years and some of these, such as The Coordinated Regional Climate Downscaling Experiment (Giorgi *et al.,* 2009), have focused on Southern Africa. The CORDEX-Africa initiative represents a major collaborative endeavour aimed at developing downscaled climate projections and producing a comprehensive evaluation of climate change consisting of experts from the West African, East African and Southern African region who evaluate the performance of multi-model ensembles of regional climate projections (CORDEX, 2015; Lennard and Kalognoumou, 2013). The RCM simulations over Southern Africa are all performed for a similar domain, driven by ERA-Interim reanalysis (1989-2008) at a spatial resolution of 50 km and then compared to observed datasets. Many of the recent studies from the early findings of the CORDEX project have focused on the ability of the models to capture the spatial and temporal variability of rainfall over the region. The early findings are encouraging, as they suggest that the RCMs can provide useful information and add value to their driving boundary condition data. For instance, Kalognomou *et al.* (2013) and Nikulin et al. (2012) showed that the CORDEX ensemble mean generally outperforms individual RCMs that tend to exhibit wet or dry biases over particular regions. The biases that occurred in these studies were linked to the model configuration and simulation of moisture transport over the region. Although the models also captured important teleconnections that influence rainfall over the region, such as El Nino and La Nina events, a common problem was that the models showed some deficiency in representing the temporal variability in the diurnal cycle of precipitation. Moreover, a recent study by Shongwe *et al.* (2014) suggests the CORDEX models perform well in simulation of

monthly rainfall variability during the austral summer seasons. The study found that, although some biases occurred in a few models, the RCMs were able to simulate the spatial migration of the seasonal rainfall and interannual variability. Nonetheless, other studies have examined the ability of the ensemble to capture patterns in the frequency and intensity of precipitation extremes (for example, Kjellström *et al.;* 2013 Pinto *et al.,* 2013). It is likely that as initiatives such as CORDEX mature they will continue to help improve the quality of individual model simulations, to identify the major deficiencies of RCMs, and to contribute to general progress in regional climate modeling over the region in the future (Solman, 2013).

2.2 Climate trends and drought in Southern Africa

2.2.1 Observed trends in climate

Although the analysis of longterm trends in Southern Africa is restricted by the availability of longterm station data and spatial coverage of stations (MacKellar *et al.,* 2014), some research has focused on examining the observed climatic trends in temperature and rainfall variables in South Africa. These studies suggest that warmer conditions have occurred in many regions across the country since about 1960. Kruger and Shongwe (2004), for example, found positive trends in the annual mean maximum temperature, with increases higher in central, rather than coastal, locations of South Africa. The authors also note positive trends in the annual average temperatures and the annual mean minimum. MacKellar *et al.* (2014) reported significant increases in maximum and minimum temperatures, for all seasons, at several weather stations across

South Africa. However, the authors report significant decreases in minimum temperatures across the central interior.

Longterm trends in rainfall over Southern Africa are more complex due to the region‘s high interannual and multidecadal variability (Boko *et al.,* 2007). Some studies suggest Southern Africa has experienced both intense and widespread drought periods and heavy rainfall events. Usman and Reason (2004) suggest an increase in the frequency of heavy rainfall events, between 1979 and 2002, over eastern (Angola, Namibia) and western (Tanzania and Mozambique) regions, but decreases over the central regions of Southern Africa. Mason *et al.* (1999) found an increase in the intensity of high rainfall events along the east coast of South Africa (between 1931-1969 and 1961-1990), although decreases in extreme rainfall events were noted in some parts of the northeast and northwest of the country. Although these observational trends cannot simply be extrapolated to give indications of future climate, they do help to characterize the climate of the recent past and provide valuable context for interpreting future projections of climate change over the region.

2.2.2 Drought

Drought is often described as a naturally occurring phenomenon resulting from a deficiency in precipitation over a prolonged period of time that causes a ―significant deviation from the normal hydrologic conditions of an area” (Mishra and Singh, 2010; Palmer, 1965). Several studies classify drought into four main categories: meteorological, related to the lack of precipitation over a region; agricultural, when the lack of soil

moisture during the growing season results in crop failure; hydrological, when runoff and percolation affect the groundwater supply and water reservoirs; and socioeconomic, when the supply and demand of economic goods is impacted due to the reduction in water supply (American Meteorological Society, 2004; Field, 2012; Mishra and Singh, 2010).

A variety of drought indices have developed in recent years to better characterize the intensity, magnitude, and duration of drought episodes and improve current understanding of drought phenomena. A review of the usefulness of commonly used drought indices and their limitations is discussed in Mishra and Singh (2010). Indices include, for example, the Palmer Drought Severity Index (PDSI; Alley, 1984), Standardized Precipitation Index (SPI; McKee *et al.,* 1993) and the Standardized Precipitation Evapotranspiration (SPEI; Vicente-Serrano *et al.,* 2010). SPEI is unique, however, in that it can be applied in several different contexts. Much like SPI, it is a useful method for assessing drought severity according to intensity, duration, onset and cessation period. However, SPEI is particularly useful because it discriminates between different drought types (*e.g.* agricultural, hydrological or environmental) and is suitable under conditions of global warming. SPEI represents the climatic water balance of an area and is calculated as the difference between the precipitation and potential evapotranspiration (Vicente-Serrano *et al.,* 2010).

Rouault and Richard (2003) recognize drought as a natural hazard and a recurring feature in Southern Africa a region where the environmental and socioeconomic implications of drought are particularly severe. Widespread drought periods in the region have been

recorded between 1982-1984, 1991-1992 and 1994-1995. These had devastating impacts on national economies in the region, impacting agriculture and livestock, water resources, and industry (Ungani and Kogan, 1998). The need to understand and mitigate the impacts of drought in Southern Africa has motivated many studies. Recent research over Southern Africa has highlighted the value of using SPEI as a drought index for a variety of applications. For instance, Araujo *et al.* (2014) examined the impact of drought on grape yields in the Western Cape Province of South Africa, Ujeneza and Abiodun (2014) examined the capability of GCMs in simulating drought regimes over the region, while Meque and Abiodun (2014) used RCMs to examine the link between ENSO events and summer drought in Southern Africa. These studies suggest that the SPEI index is a useful tool for monitoring and detecting the spatial and temporal characteristics of drought in the region (Araujo *et al.,* 2014). This study will also employ the SPEI to compute the potential impacts of vegetation changes on drought over Southern Africa.

2.3 Potential impacts of forestation

Several modeling studies that have examined the biogeophysical effects of forestation show that the impacts of forestation on regional and global climate are complex. Both positive and negative biogeophysical feedback mechanisms exist. These feedbacks can modify both the local and regional climate of an area, to a degree comparable with future climate change due to greenhouse gasses (Smith, 2014). At different latitudes, various feedbacks and climate variables account for the biogeophysical and biogeochemical processes that occur.

Forestation in tropical regions is often thought to have a positive effect on climate (Bonan, 2008; South *et al.,* 2011; Wang *et al.,* 2014). This is because forestation decreases air temperature through a double cooling effect; firstly, through sequestration of carbon dioxide from the atmosphere and, secondly, through changes in evapotranspiration that increase cloud cover (Betts *et al.,* 2007; South *et al.,* 2011). In both instances, more incoming solar radiation is reflected because of the change in radiative forcing, inducing a local cooling effect. For instance, in a global analysis, Arora and Montenegro (2011) assessed the combined effect of latitudinal forestation on the carbon-cycle and climate. This study showed that temperature reductions from forestation could be as much as three times higher in the tropics as compared to boreal and northern temperate regions. Bala *et al.* (2007) also showed that deforestation of tropical regions could warm earth's atmosphere (by about 0.7^{o}K) through the release of carbon dioxide and reduction in cloud cover. In contrast to these findings however, other regional modeling experiments in tropical regions suggest that these biogeophysical impacts may be more complex. For instance, in West Africa, Abiodun *et al.* (2012) show that forestation may reduce the projected warming over the forested region. Despite the favourable effects, this study also shows that forestation may also enhance the global warming north of forested regions and induce negative impacts on the regional climate in the future.

Forestation at high northern latitudes (45-60°N), such as in arctic and boreal regions, may also produce a significant global warming effect (Wang *et al.,* 2014). This is because forestation induces a complex snow-vegetation-albedo and sea-ice-albedo feedback

mechanism (Claussen *et al.,* 2001). For instance, simulations by Betts *et al.* (2007) suggest that forestation in snow covered regions, such as Canada and eastern Siberia, reduce the surface albedo and induce a positive radiative forcing that exceeds the potential for carbon sequestration. Forestation efforts in these regions could thereby enhance rather than reduce the projected warming. Swann *et al.* (2010) examined the impacts of broadleaf forestation at high latitudes (>60°N latitude) and found that that darker stems and leaves of the forest could mask the bright snow, reducing surface albedo. The authors also recognized an additional mechanism of equal magnitude: through increased atmospheric water vapour, via transpiration of leaves, a positive feedback loop from the ocean and melting sea-ice occurred, not only over the land surface, but also over the ocean, through the turbulent mixing of air.

There is still some uncertainty as to the effectiveness of forestation in temperate zones (South *et al.,* 2011). While still the subject of current debate, some studies suggest that temperature and rainfall response is likely to be more marginal in these regions than at lower latitudes. For instance, Wang *et al.* (2014) used a complex ESM to examine the latitudinal effects of extreme forestation. Biogeophysical impacts in temperate regions of the northern hemisphere forestation (between 0-15°N) produced a relatively small impact on global and regional temperature. However, forest expansion between 45-60°N and 30-45°N caused significant global warming and detectable regional warming, respectively (Figure 2-1).

This warming response is in line with the results from some regional climate modeling experiments in other temperate regions in the Northern Hemisphere. For instance, Gálos *et al.* (2011) and Chen *et al.* (2012) found that forestation may induce a net cooling effect and reduce the severity of projected drought over Hungary and over the southeast United States, respectively. This local surface cooling effect results from hydrological feedback and changes in evapotranspiration.

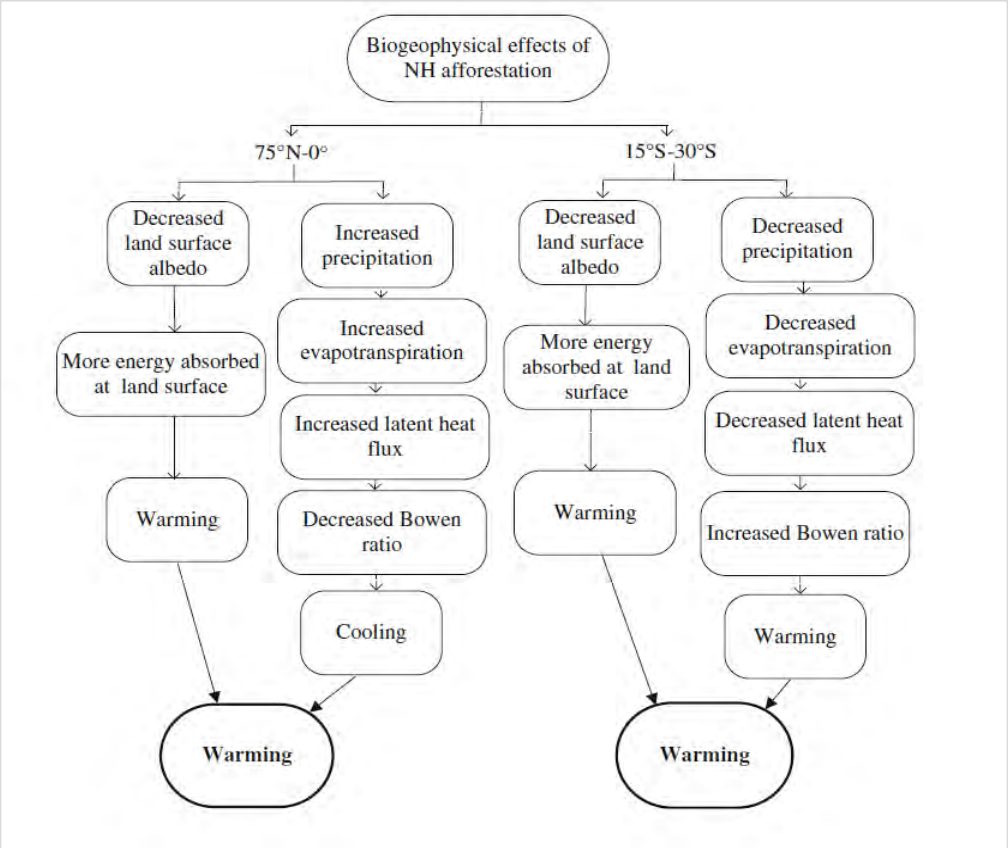

Figure 2-1 Biogeophysical processes influenced by afforestation in the Northern Hemisphere. (Source: Wang et al 2014; p.9)

Limited research has investigated the impacts of forestation in temperate regions of the Southern Hemisphere. Recent study by Wang *et al.* (2015) examined the latitudinal effects of extreme forestation in the Southern Hemisphere. Forest expansions between

30-40°S decreased land surface albedo and induced warming that outweighed the effects of cooling associated with increased precipitation. The warming effect is in line with observational study by Houspanossian *et al.* (2013) over central Argentina which suggest that, in contrast to forestation, the removal of forests (and replacement with croplands) could also produce a strong biogeophysical cooling effect large enough to counterbalance the biogeochemical effects of the deforestation. However, RCM simulations over southern South America (Beltrán-Przekurat *et al.,* 2012) and Australia (Ornstein *et al.,* 2009; Pitman, 2004), show that, large–scale forestation could induce cooler temperatures, increase rainfall and provide other climatic benefits.

Overall, the literature surveyed here lends support to the notion of a zonal gradient to the effectiveness of forestation as a climate mitigation option (Table 2-1). There are, however, latitudinal contrasts due to the different variables and climate processes in different regions. That is, for example, although evapotranspiration and the albedo effect of clouds are significant factors in tropical regions, the dynamics of sea-ice and snow melt are important considerations at high latitudes.

Numerous studies have also highlighted that the biogeophysical impacts on climate may extend to regions adjacent to and remote from the location directly modified, through changes in large-scale circulation and teleconnections (*e.g.* Swann *et al.*, 2012, Zhao *et al.,* 2001 and Wang *et al.,* 2014). Because the biogeophysical impacts of forestation do not recognize political boundaries, there is further motivation for further study to understand where the positive and negative impacts of forestation occur and how the

Table 2-1 Summary of some of the potential impacts of forestation

Region	Summary of potential forestation impacts	Relevant References
Low latitude (0°N—23°N)	Negative radiative forcing from carbon sequestration and negative radiative forcing from reduction in surface albedo. Reduction in regional and/or global temperature.	Arora and Montenegro (2011); Bala *et al.* (2007); Betts *et al.* (2007); South, *et al.* (2011); Swann *et al.* (2010); Wang, *et al.* (2014);
High latitude (60°N—90°N)	Negative radiative forcing from carbon sequestration does not exceed the positive radiative forcing from reduction in surface albedo. Increase in regional and/or global temperature	
Mid-latitude (30°N—60°N)	Negative radiative forcing from carbon sequestration unlikely to exceed the positive radiative forcing from reduction in surface albedo. Increase in regional temperature (uncertain)	

changes influence climate (Abiodun *et al.,* 2012; Wang *et al.,* 2015). Thus, results from model simulations may also vary in a given region depending on whether the ―global" and/or ―local" effects are under consideration (South *et al.,* 2011). This suggests there is still some uncertainty regarding the potential impacts of forestation and the effectiveness of forestation efforts as a climate mitigation option. Since improved detection and attribution of regional forestation effects can help identify areas where forestation mitigates projected climate change most effectively, these studies also have implications for future forest mitigation strategies (Molen *et al.,* 2011; Wang *et al.,* 2015).

2.4 Future changes to the distribution of vegetation in South Africa

Considerable research has been dedicated to understanding the history and dynamics of vegetation change in these regions. Paleoecolgical and sedimentological evidence suggests that the Savanna and Grassland ecosystems, characteristic of the Southern African region today are in fact particularly dynamic and sensitive to climate change (Breman *et al.,* 2012; Neumann *et al.,* 2010). Various factors including temperature, atmospheric carbon dioxide concentrations, fire and different photosynthetic efficiencies have influenced the distribution and co-dominance of shrubs, trees and grasses that are observed in these biomes today (Bond *et al.,* 2003, 2005; Beerling and Osborne, 2006; Ehleringer *et al.,* 1997, 2002). For example, during the late Holocene, the vegetation landscape of the summer rainfall region of South Africa transitioned from a stable state Forest Savanna/Grassland mosaic to one increasingly dominated by grasses (Breman *et al.,* 2012). The extent and distribution of the Grassland-Savanna ecotone has also been shaped by factors including fire regime, anthropogenic pressures and changes in climate and sea level (Neumann *et al.,* 2010). Much like in the past, both climate change and non-climatic factors are expected to continue to influence the structure, composition and function of Southern African biomes in the future (Midgley and Thuiller, 2010; Rutherford *et al.,* 1999).

2.4.1 Forestation activities in South Africa

Although natural and commercial forestation occurs in various parts of Southern Africa, no study has investigated the biogeophysical impacts of forestation on the regional climate. The Eastern Cape Forestry Sector Profile (Figure 2-2) (DWAF, 2007) suggests that while the distribution of forestry activities in the Eastern Cape Province of South

Africa is at present scattered, and the creation of new plantations sites has been minimal, large areas of land in the Eastern Cape show good potential for commercial forestation. Current estimates suggest that more than 44000 ha have been planted over the past decade and the pace is expected to increase in the near future (DWAF, 2007). Moreover, in the mesic and semi-arid Savanna regions there has been a significant increase in the density of woody plants over the last 50 years as a result of increasing atmospheric carbon dioxide concentrations (Wigley *et al.,* 2010; Buitenwerf *et al.,* 2012). This natural phenomenon, known as bush encroachment or thicket expansion (Sankaran *et al.,* 2005), has been reported in open ecosystems around the world (*e.g.* Silva *et al.,* 2008; Bowman *et al.,* 2010), and in Southern African Savanna and Grassland regions, where evidence of the increase in the density (size and number) of woody plants is supported by satellite imagery and repeat photography (Figure 2-3, Figure 2-4) (Bond and Midgley 2012; Buitenwerf *et al.,* 2012; Hoffman and Todd*.,* 1999; Roques *et al.,* 2001; Wigley *et al.,* 2010). The potential increase in tree cover is also reinforced by Higgins and Scheiter (2012) and West *et al.* (2012), who estimated that by the end of the century a ten-fold increase in woody vegetation could occur in some of Africa‘s Savanna regions. This increase in tree density, resulting from commercial forestry plantations and the natural bush encroachment, could potentially feedback and modify both the local and regional climate in the future; however, no study has investigated the potential biogeophysical effects.

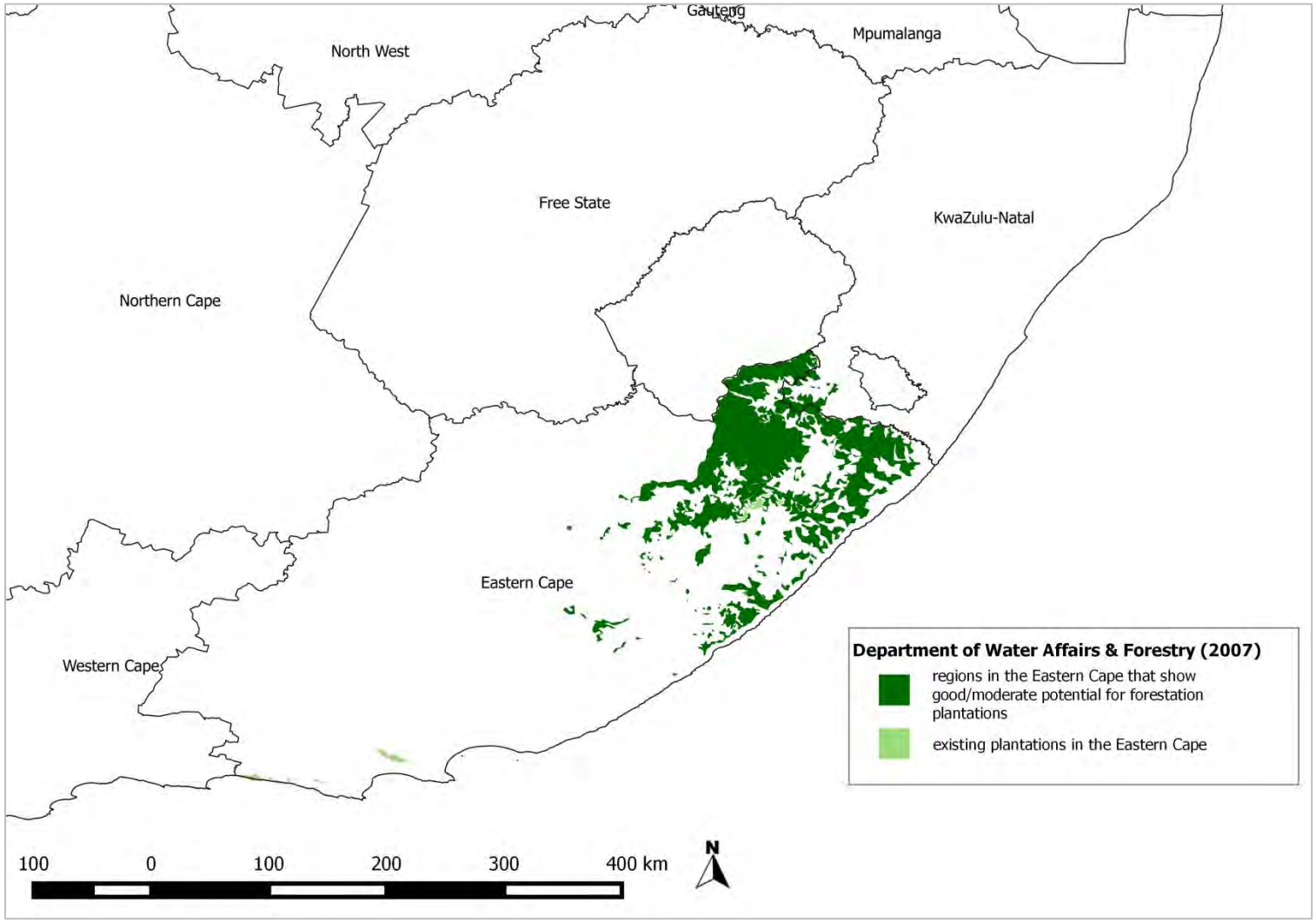

Figure 2-2 Sites in the Eastern Cape recognized as suitable for forestation. (Adapted from: Department of Water Affairs and Forestry, 2007)

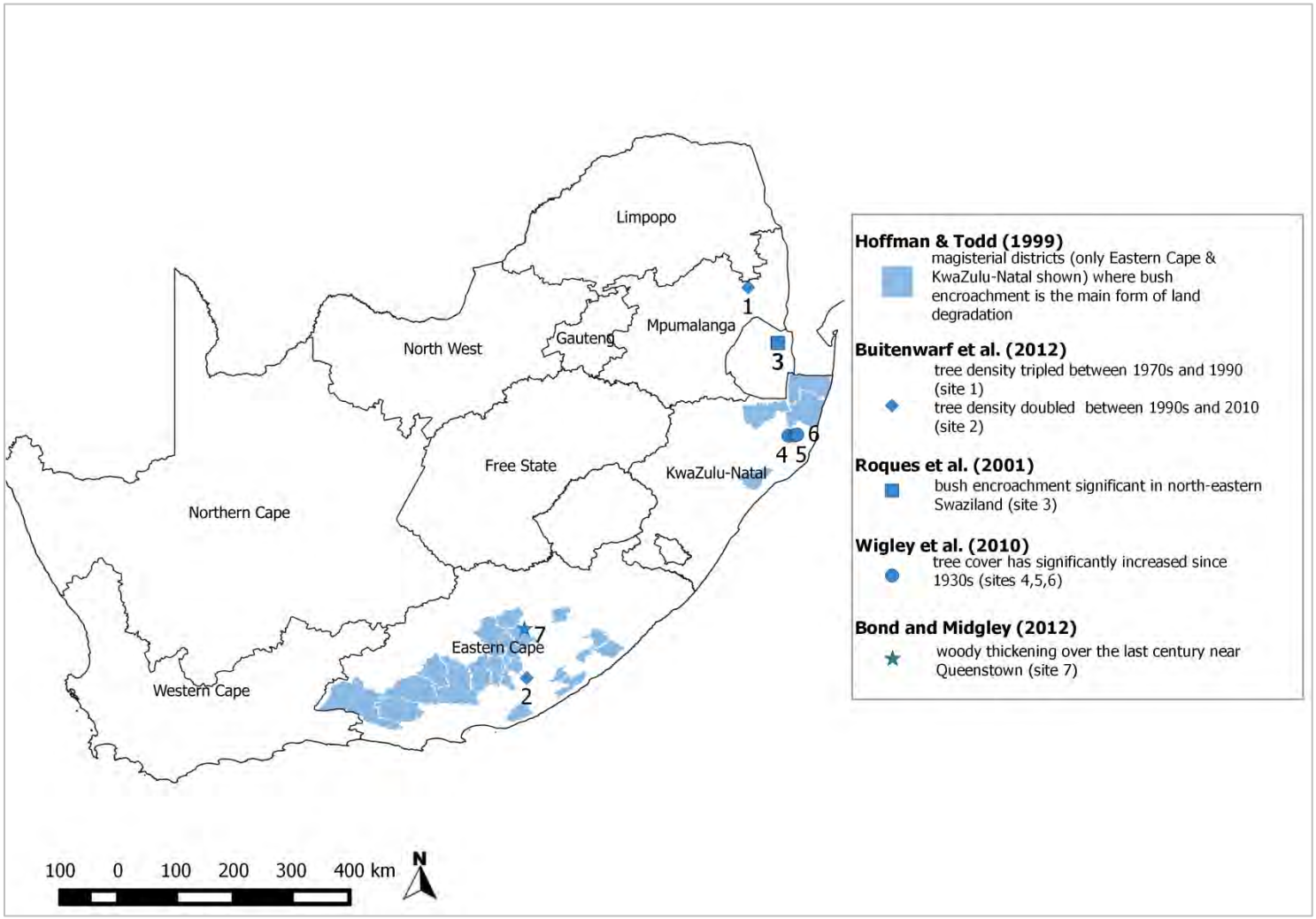

Figure 2-3 Sites in the Eastern Cape and Kwa-Zulu Natal Provinces where bush encroachment has been reported. (Adapted from: Hoffman and Todd, 1999; Buitenwerf *et al.,* 2012; Roques *et al.,* 2001; Wigley *et al.,* 2010; Bond and Midgley 2012)

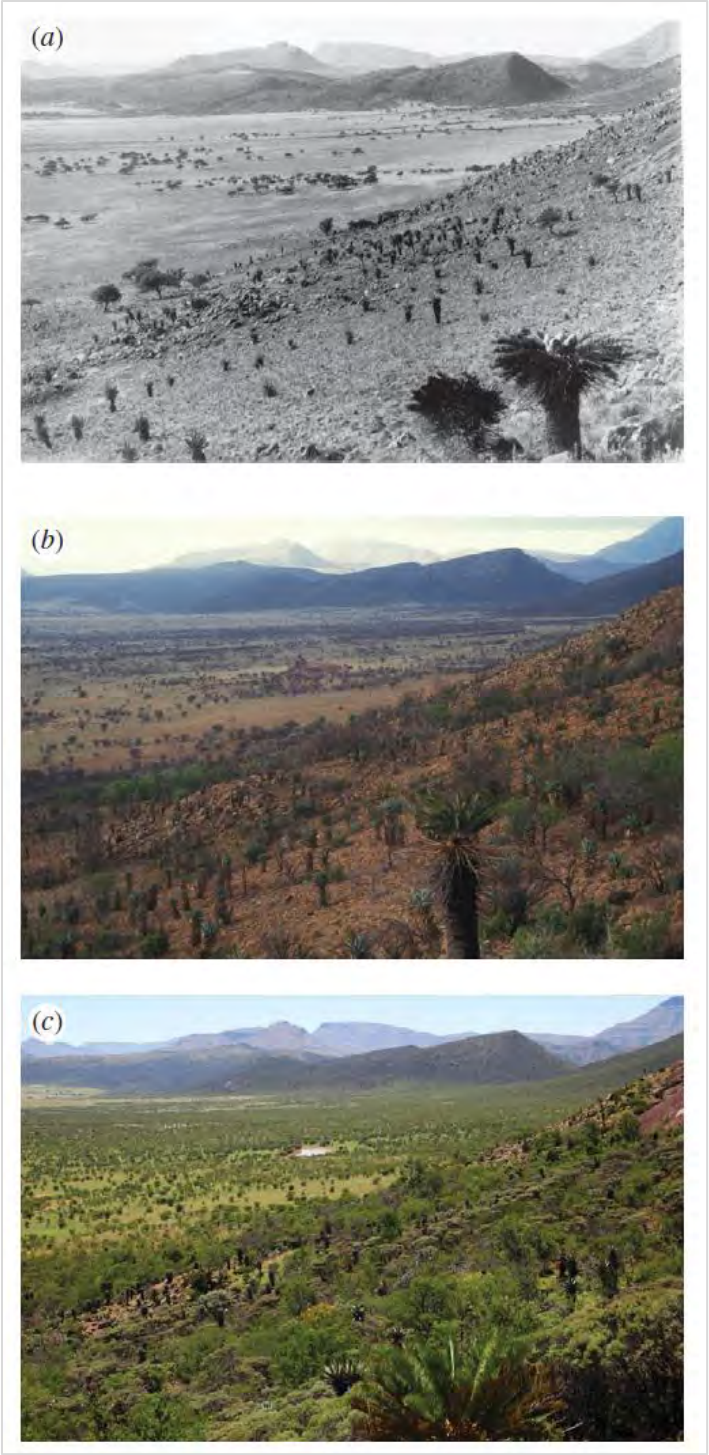

Figure 2-4 Woody thickening has occurred over the last century near Queenstown, Eastern Cape (South Africa) (a) 1925, (b) 1993, and (c) 2011. Note the large woody increase since the early 1990s. The original photograph was taken by the late IB Pole Evans (South African National Botanical Institute) and repeat photos are courtesy of Timm Hoffman and James Puttick (Plant Conservation Unit, University of Cape Town). (Source: Bond and Midgley 2012; p.602)

2.4.2 The Grassland Biome in South Africa

Although changes to the extent and composition of vegetation in South Africa's Grassland Biome are expected in the future, no study has investigated the potential biogeophysical feedbacks of the changes on the regional climate. For instance, Ellery *et al.* (1991) suggests that under future conditions of climate change (a 2^{o}C increase in temperature and 15% decrease in rainfall), the Grassland Biome could be invaded by Savanna vegetation both east and west of the Great Escarpment (see Figure 1-2 and Figure 2-5). This change to the distribution of vegetation would leave only the high altitude Grasslands of the Drakensburg and extensions along the Northern Escarpment (Mucina and Rutherford, 2006). Moreover, Mucina and Rutherford (2006) estimate that the Grassland Biome could contract by between 33-55% of its current extent by 2055, and that this change would occur disproportionately along the western region of the biome. These studies both propose that with increasing aridification, associated with future climate change, the spatial extent of Grassland regions would contract. Recent research by Masubelele *et al.* (2014), however, draws contrast to the aridification hypothesis, as it provides some evidence of an increase in total vegetation cover in the Karoo Midlands region (a region along the ecotone between the Nama-karoo and Grassland Biomes in South Africa) (see Figure 1-5 and Figure 2-5). According to the Masubelele (2012), these observations are in line with those of other researchers, including work by Hoffman and Cowling (1990) and Hoffman and Ashwell (2001) that suggest a detectable change in the trajectory of increased grass cover over time and a decline in dwarf shrub elements, particularly on the low lying plains and slopes.

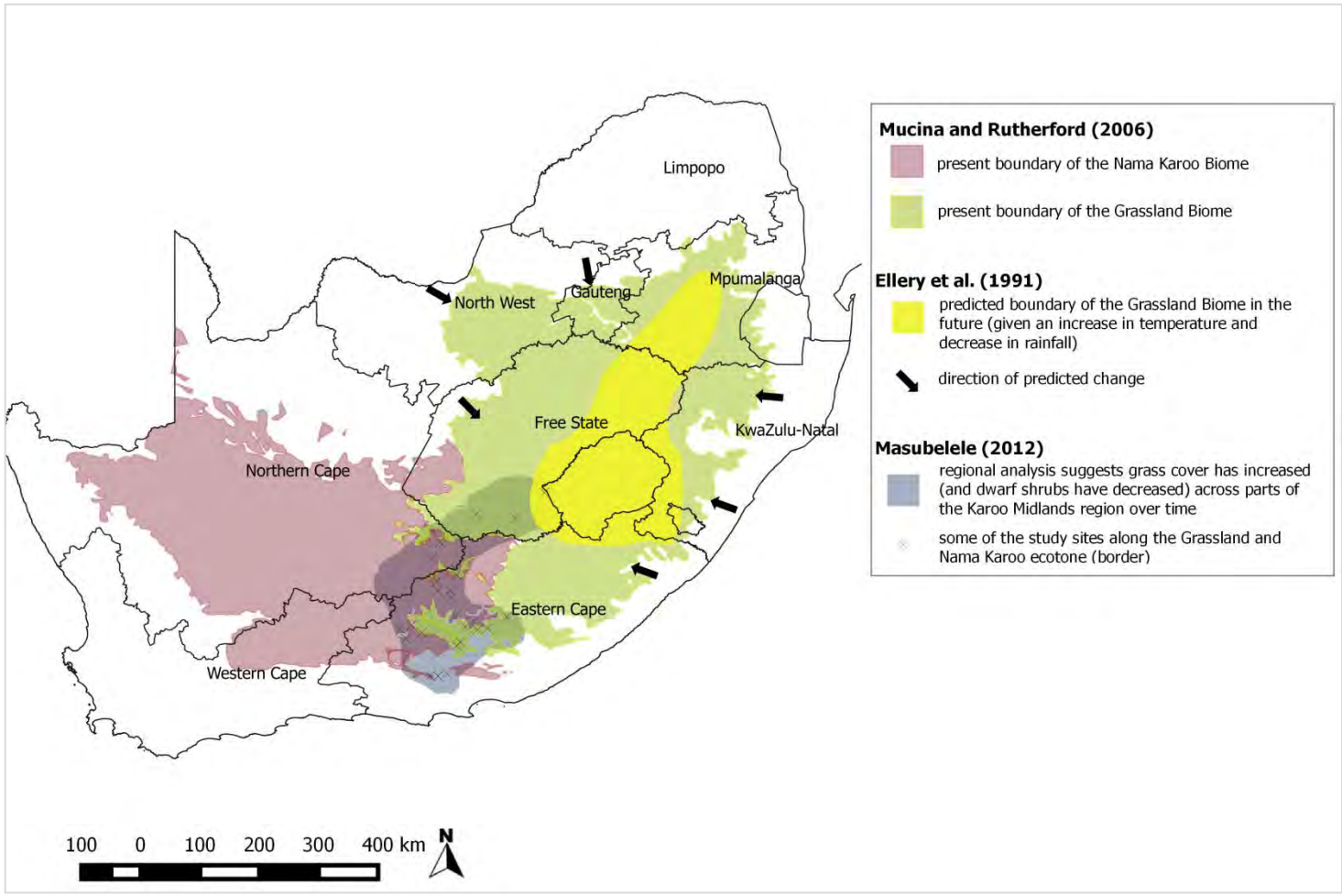

Figure 2-5 Potential future changes to the Grassland Biome. (Adapted from: Mucina and Rutherford, 2006; Ellery, *et al.,* 1991; Masubelele, 2012)

Factors contributing to the observed changes include an increase in seasonal summer rainfall, change in extreme rainfall events in the region, more conservative land use practices and possibly even increasing atmospheric carbon dioxide concentrations (which would cause changes to the water use efficiency of the grasses while also allowing them to survive in more arid regions). The potential expansion of the grass cover could cause a feedback effect and modify both the local and regional climate in the future; however, no study has investigated these potential biogeophysical effects.

3 Methodology

This chapter provides a detailed description of the datasets, models, and method used in the study. It begins with a brief description of the types of datasets used followed by a full description of the simulation domain and physics parameterization schemes for the RCMs. A summary of the experimental design is then provided, the scenarios of vegetation change are explained, and the contextual research that reinforces each is detailed. An overview of the calculations for added value and drought is also provided.

3.1 Data

For this study, three types of datasets were analysed: observation, reanalysis and model simulations. The observed datasets were produced by the Climate Research Unit (hereafter, CRU; Mitchell and Jones, 2005; Harris *et al.,* 2014) at the University of East Anglia. CRU consists of monthly observations from meteorological stations across the global land surface, but gridded at a 0.5^{o} x 0.5^{o} resolution for the period 1901-2009. In this study, we used CRU temperature and precipitation for the period 1971-2004 to evaluate the model simulations. The reanalysis dataset, the NOAA-CIRES 20^{th} Century Reanalysis Data Version 2 (hereafter, NOAA; Compo *et al.,* 2009), was obtained from NOAA/OAR/ESRL PSD, Boulder, Colorado, USA (ESLR, 2015). This product consists of global atmospheric data at 2.0^{o} x 2.0^{o} horizontal grid spacing, and extends from 1871 to date, at 6-hourly intervals (Compo *et al.,* 2006; 2011). We used NOAA winds for the period 1971-2004 to evaluate the simulated winds. The model simulation datasets

comprise two GCMs and two RCMs simulations. The two GCMs are the Met Office Hadley Centre Model (HADGEM2-ES, hereafter HAD; Martin *et al.,* 2011) and the Max-Planck-Institute for Meteorology Model (MPI-ESM-LR, hereafter MPI; Marsland *et al.,* 2003). The simulations for both GCMs (HAD and MPI) were obtained from the Coupled Model Intercomparison Project (CMIP5) and were used to provide the initial and lateral boundary conditions for the two regional climate models.

3.2 Regional climate models description

The two regional models used in the study are the International Centre for Theoretical Physics (ICTP) Regional Climate Model version 4.3 (hereafter, RegCM; Pal *et al.,* 2007) and the Weather Research Forecasting Model version 3.1.1 (hereafter, WRF; Skamarock *et al.,* 2008). Using two models provides the opportunity to compare simulation results and determine whether the results obtained are model dependent. Both RCMs are suitable for downscaling global climate datasets over the Southern African region (see, for example, the CORDEX Africa initiative; Kalognomou *et al.,* 2013) and for examining the potential impacts of vegetation changes on regional climate (see, for example, Abiodun *et al.,* 2012; Trail *et al.,* 2013). However, the two models differ in their dynamics; RegCM is a hydrostatic model while WRF is a non-hydrostatic model.

3.2.1 RegCM

The RegCM system is as a community model that is recognized as flexible, portable and easy to use with a wide range of application for use by scientists in both developed and developing nations (Pal *et al.,* 2007). Since the 1980s, when RegCM1 was created,

successive updates and new physics parameterizations have been added. The dynamical component of the first generation RegCM was based on National Centre for Atmospheric Research (NCAR) Mesoscale Model (MM4), while the physics schemes of RegCM2 are rooted in the NCAR Community Climate Model 2 (CCM2), and the mesoscale model MM5 (Kgatuke *et al.,* 2008). New model versions (since RegCM2- in 1990 and RegCM3- in 2006) have improved on model physics and parameterizations for climate application. This includes improvements in the model‘s representation of land surface, radiative transfer, and, most recently, a new parameterization for sub-grid scale variability in clouds (Kgatuke *et al.,* 2008). The model is currently under development and improved physics schemes, including convection and cloud microphysics, are expected to be released in a new generation of RegCM by 2015 (version 5; ICTP, 2014). In this study, the most recent version of RegCM (v 4.3) is used.

RegCM is a hydrostatic, terrain-following (sigma) coordinate model with various physics and parameterization options (Giorgi *et al.,* 2012) (Table 3-1). For the present study, we used the Community Climate Model (CCM3) scheme of Kiehl *et al.* (1996) for radiative transfer and the Holtslag *et al.* (1990) parameterization for the planetary boundary layer. Emanuel (1991) scheme is used for convective parameterization and the SUB-grid EXplicit moisture scheme (SUBEX; Pal *et al.,* 2000) for precipitation processes. RegCM simulations were set up with a time step of 100s and a horizontal grid space of 40 km using a Lambert conformal projection (Figure 3-1). The Southern African domain extends from about 20^{o}W to 60^{o}E and from 5.0^{o}N to 55^{o}S, with 18 vertical grid point spacing from the surface to a 50 hPa level.

Land surface processes in RegCM are represented by the Biosphere Atmosphere Transfer Scheme (BATS). Dickinson *et al.* (1993) provides a full description of this package representing the exchange of momentum, energy and water between the surface, vegetation, soil and the atmosphere. BATS includes 20 different vegetation/land cover types (the characteristics of the land cover are in Appendix A: see Table 10-1, Table 10-2), 3 soil categories (sand, loam and clay) and different soil colours (ranging from light to dark). Elguindi *et al.* (2011) provide a full description of the computations for canopy and foliage temperature, which are calculated diagnostically from radiative, sensible and latent heat fluxes. Calculations for sensible heat, water vapour and momentum transfer rely on surface drag coefficients, roughness length, and stability in the boundary layer. Soil moisture is a function of surface runoff and saturation and influences evapotranspiration at the surface.

Table 3-1 Physics and parameterization references for the regional climate models used in this study. (Adapted from Kalognomou *et al.,* 2013)

	RegCM	WRF
Model	Regional Climate Model, version 4.3	Weather Research and Forecasting Model, version 3.11
Developing Institute	Abdus Salam International Centre for Theoretical Physics, (ICTP) Italy	National Centre for Atmospheric Research, (NCAR) USA
Projection	Lambert Conformal	Lambert Conformal
Horizontal Grid Resolution (km)	40	40
Vertical Coordinate /levels	terrain-following sigma coordinate, /18	terrain-following hydrostatic pressure, Eta/40
Advection	Eulerian	Eulerian
Time step (s)	100	180
Convective scheme	Emmanuel (1991)	Kain–Fritsch (new Eta scheme); Kain (2004)
Radiation scheme	Kiehl, *et al.* (1996)	Dudhia (1989) scheme; Mlawer *et al.* (1997)
Turbulence vertical Diffusion	Holtslag *et al.* (1990)	Hong, *et al.* (2006)
Cloud microphysics scheme	SUB grid EXplicit moisture scheme (SUBEX); Pal, *et al.* (2000)	WRF single-moment 5-class scheme (WSM5); Hong *et al.* (2004)
Land surface scheme	Biosphere–Atmosphere Transfer Scheme (BATS1E); Dickinson, *et al.* (1993)	Unified Noah land-surface model; Tewari, *et al.* (2004)
Latest reference	Pal, *et al.* (2007)	Skamarock, *et al.* (2008)

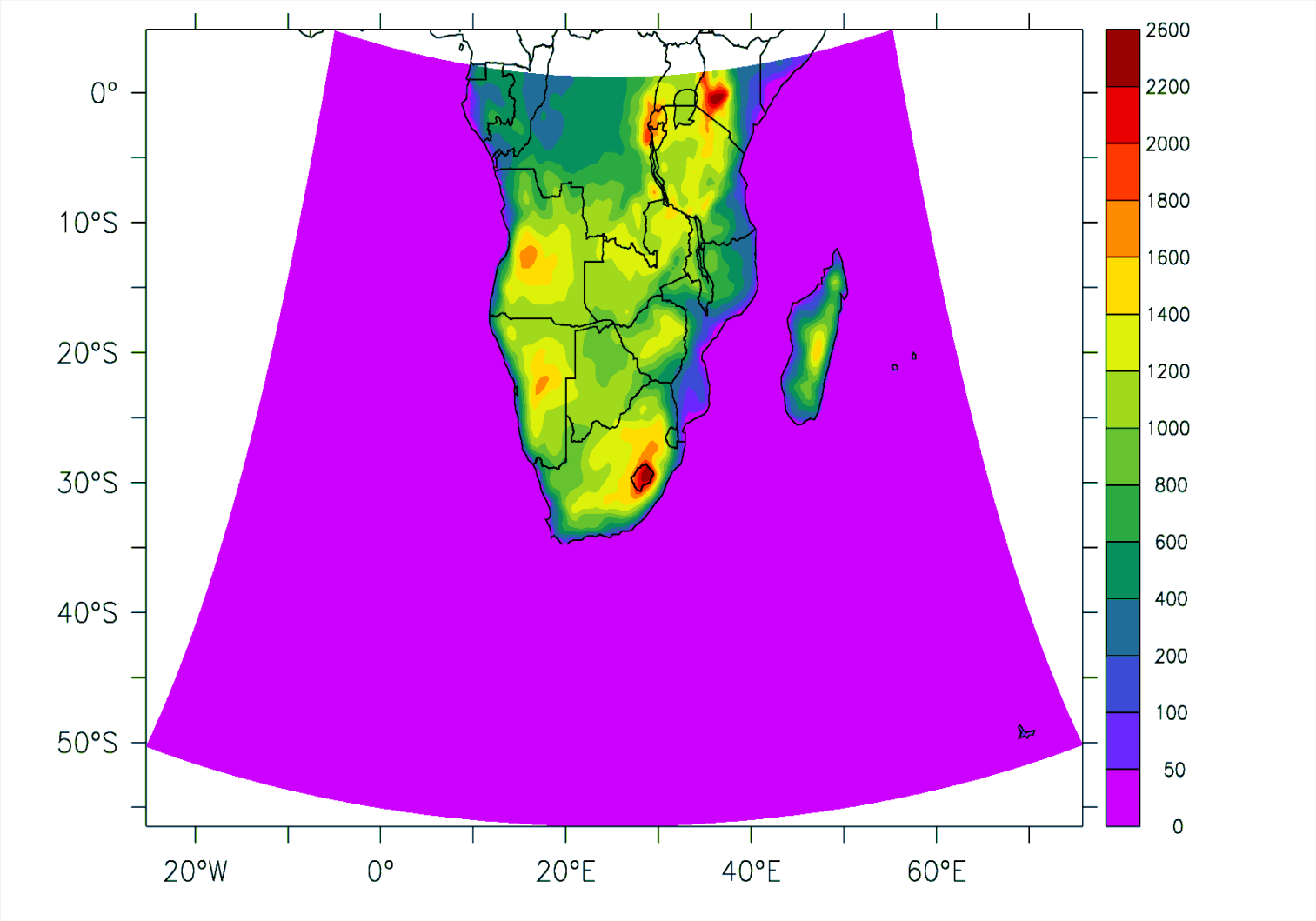

Figure 3-1 The model simulation domain showing Southern African topography (meters) as seen by the models.

3.2.2 WRF

WRF is a mesoscale model designed to be flexible, portable and computationally efficient. This model was developed in a collaborative effort by both scientific research institutions and operational forecasting centres, including the National Centre for Atmospheric Research (NCAR), the National Centres for Environmental Prediction (NCEP), the Forecast Systems Laboratory (FSL), the Air Force Weather Agency (AFWA), and Oklahoma University (OU) (Skamarock *et al.,* 2001). Since the release of the WRF version 2.0 modelling system in 2004, the model has been applied by a large community of users worldwide in a variety of research areas (*e.g.* air pollution simulation, wildfire simulation, tropical storm and numerical weather prediction and regional climate projections), for both operational weather forecasts and climate research purposes (Michalakes *et al.,* 2004). The model has two dynamic core versions; The Nonhydrostatic Mesoscale Model (WRF-NMM) and The Advanced Research (WRF-ARW). In this study, the latter option and most recent version of WRF (v 3.1.1) is used.

WRF is a non-hydrostatic, fully compressible and terrain-following (eta-coordinate) model (Skamarock *et al.,* 2008; Table 3-1). For the simulations used in the study, parameterizations for radiative transfer follow the Rapid Radiative Transfer Model scheme (of Mlawer *et al.,* 1997) for long waves, and the Dudhia (1989) scheme for short waves. The planetary boundary layer (PBL) scheme follows that of Hong *et al.* (2006). The WRF single-moment 5-class scheme (WSM5) is used for cloud microphysics which has prognostic equations for water vapour, cloud water, rain, cloud ice, and snow (Hong *et al.,* 2004). The Kain–Fritsch mass flux scheme (new Eta scheme; Kain, 2004) is used

to represent convection and precipitation processes. The time step used is 180s. The domain and horizontal resolution for WRF simulations is the same as that of RegCM, except that 40 vertical grid points were used. Surface data is taken from the United States Geological Survey (USGS 24 category land dataset, the characteristics of the land cover are in Appendix A; see Table 10-3, Table 10-4). Land surface processes are represented by Unified Noah land-surface model (NOAH). NOAH predicts soil temperature and moisture for four soil categories (10, 30, 60 and 1000 cm thick). Details on the calculations for soil moisture, the surface water budget, surface evaporation, vegetation transpiration, and canopy resistance are described by Chen (2012).

3.3 Experiments

Each RCM was applied to perform four experiments (Table 3-2). The first experiment (PRS) simulated the present day climate, the second experiment (GHG) simulated the future climate without forestation, the third experiment (FRS) simulated the future climate with potential forestation, and the fourth experiment (GRA) simulated the future climate with changes to the Grassland biome. The first two experiments (PRS and GHG) used the present day landcover patterns (Figure 3-2) in simulating present day (1970-2005) and the future climate (2030-2065), respectively. The same landcover distribution was used for each of these two experiments. Each model used their respective landcover/vegetation classes, shown in Figure 3-2 (RegCM used BATS and WRF used NOAH). The difference between these two experiments provided an indication of the future climate change due to increasing atmospheric greenhouse gas concentrations (*i.e.* a projection of global warming due to emissions change, but involving no landcover

changes). The future climate experiments (GHG and FRS) were based on increasing greenhouse gas concentrations under the intermediate-range Representative Concentration Pathway (RCP) 4.5 scenario. This represents an intermediate range scenario of future climate change (with stabilization by the year 2080, and one where the radiative forcing reaches 4.5 Wm^{-2}, or ~526 ppm atmospheric CO_2, by 2100 (Thomson *et al.,* 2011)).

Table 3-2 Summary of the experiments performed with each regional climate model in the study.

No.	Experiment	Boundary Condition Data	Land cover pattern
1.	PRS	Present-day (1970—2005)	Present-day (Figure 3-2 a & Figure 3-2 d)
2.	GHG	Future (2030—2065) RCP4.5	Present-day (Figure 3-2 a & Figure 3-2 d)
3.	FRS	Future (2030—2065) RCP4.5	Forestation along the eastern region of South Africa (Figure 3-2 b & Figure 3-2 e)
4.	GRA	Future (2030—2065) RCP4.5	Change in the extent of The Grassland Biome (Figure 3-2 c and Figure 3-2 f)

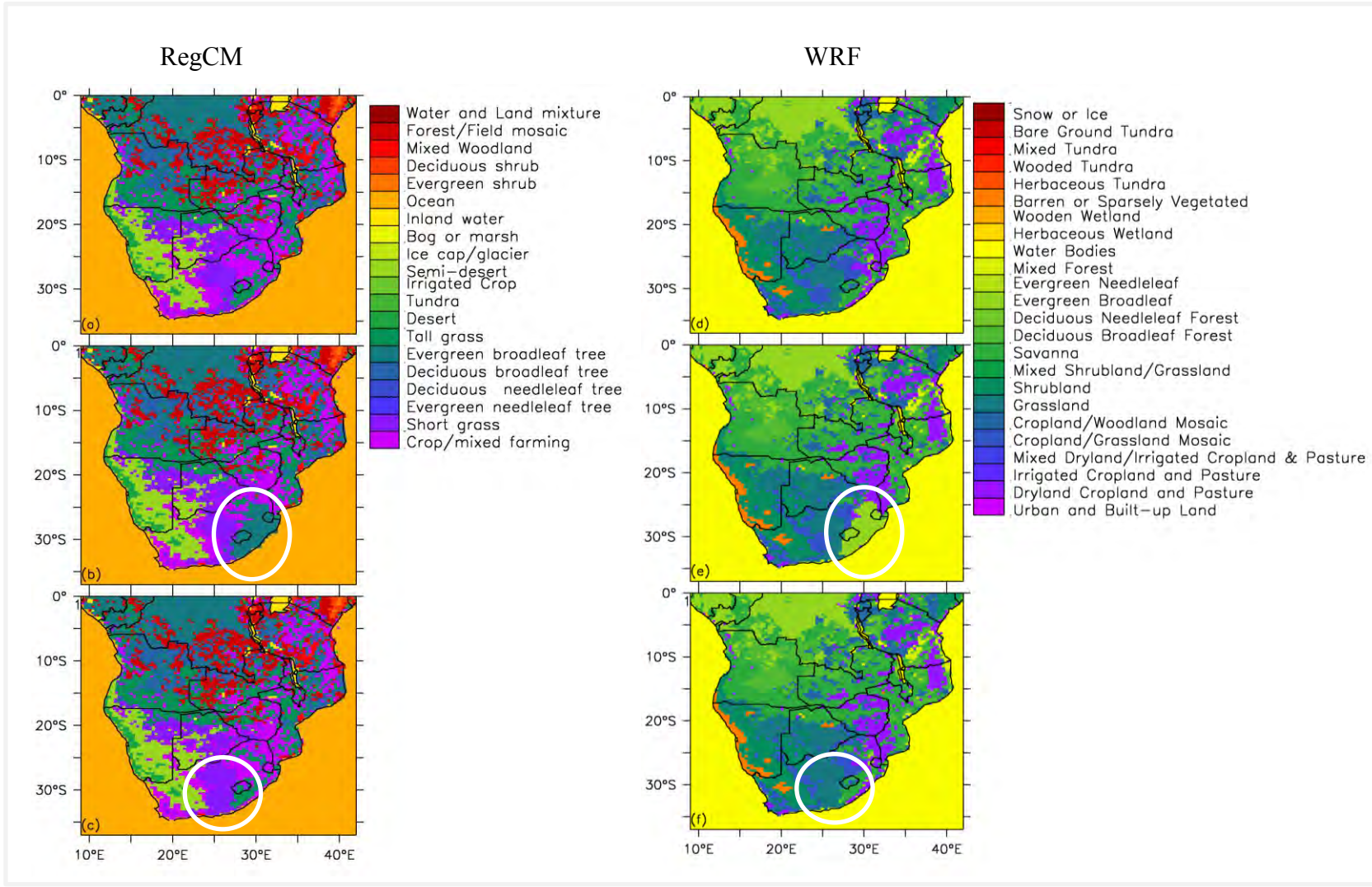

Figure 3-2 Land cover types used in this study for RegCM (left) and for WRF (right) for the present-day and future (PRS and GHG, respectively; (a) and (d), for forestation (FRS) simulations; (b) and (e), and for grass cover (GRA) simulations; (c) and (f).

Two scenarios of vegetation change were identified through a process of stakeholder engagement. Stakeholder input was required to tailor the project in this manner so that the project outcomes would be more relevant to decision making and of more value to end-users, particularly those in natural resource management. Regional experts (from South Africa, Namibia and Botswana) and stakeholders (*e.g.* from the South African Department of Environmental Affairs and the South African National Biodiversity Institute) were consulted. Their input helped to assess the status quo regarding forestation, to identify the environments that are suitable for such activities, and to attain knowledge of existing forestation programs. In focus groups members also discussed the spatial extent of vegetation changes currently occurring, and that have been observed overtime in the past. Other social, ecological and economic ramifications of vegetation change in Southern Africa were also considered. After discussion with the stakeholders, two plausible scenarios of vegetation change were selected for this study. The contextual research that reinforces each scenario is detailed below.

The first scenario of vegetation change describes a forestation experiment (FRS) (Table 3-2). The FRS experiment used landcover patterns in which the biophysically suitable areas in Eastern Cape are forested. It aimed to simulate a future climate with the influence of natural and human-induced forestation in the Eastern Cape and Kwa-Zulu Natal Provinces (Figure 3-3). The forestation area was delineated based on results of previous studies (in particular, that of Gush *et al.,* 2002) that mapped the distribution of Quaternary Catchments and identified regions where the mean annual precipitation was sufficient to sustain forestation (areas exceeding 650 mm) (Figure 3-3). The

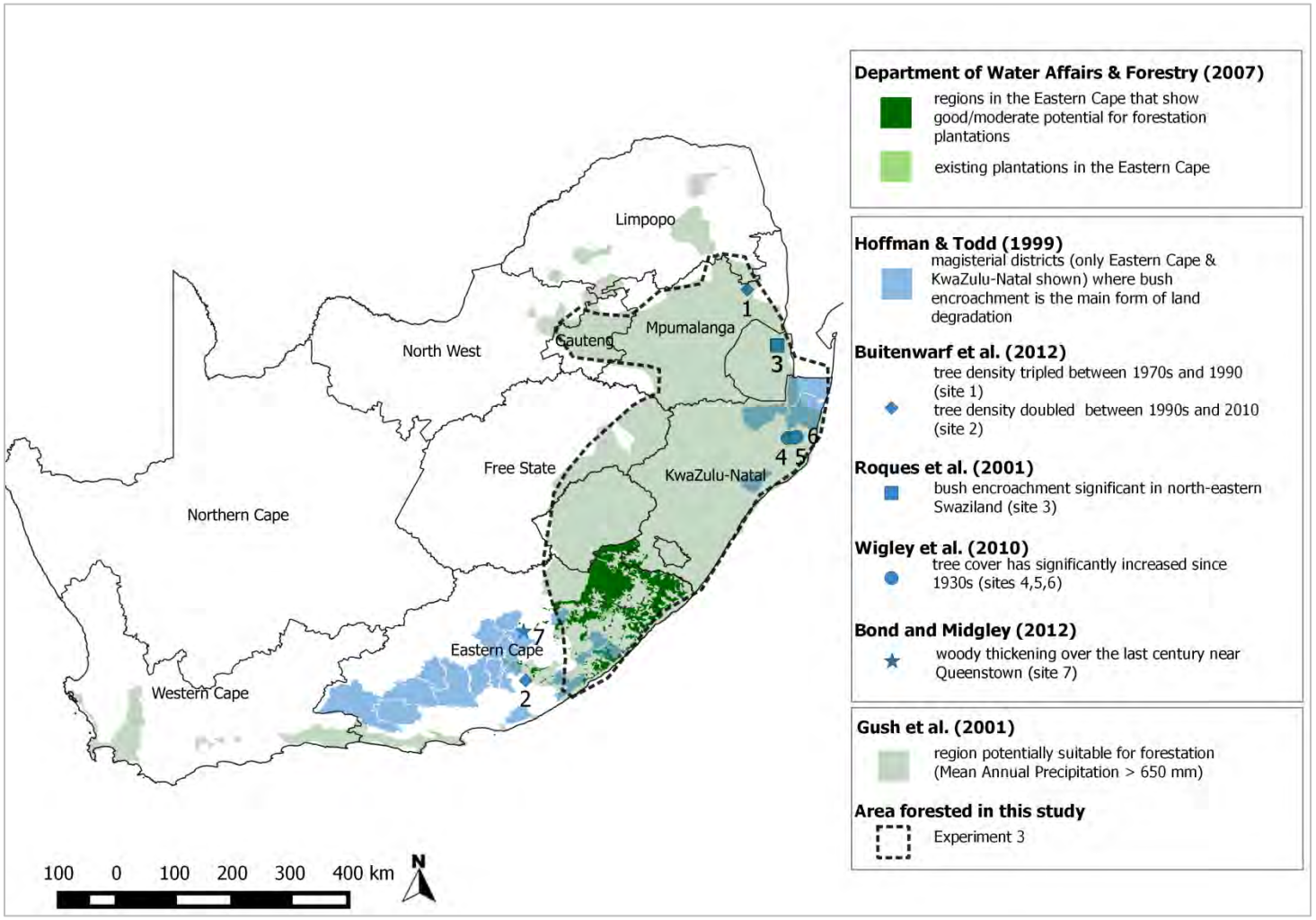

Figure 3-3 Area forested (Experiment 3) for RegCM and for WRF simulations was delineated based on relevant literature. (Adapted from: Department of Water Affairs and Forestry, 2007; Hoffman and Todd, 1999; Buitenwerf *et al.,* 2012; Roques *et al.,* 2001; Wigley *et al.,* 2010; Bond and Midgley 2012; Gush *et al.*, 2001)

difference between this forestation (FRS) experiment and that of no forestation (*i.e.* present day landcover distribution) was used to determine the impact of forest cover on the future climate (*i.e.* FRS minus GHG).

The second scenario of vegetation change describes a grass cover experiment (GRA; Table 3-2). The GRA experiment used landcover patterns that represent an increase in the extent of grass cover along the western border of the South African Grassland Biome (Figure 3-4). This experiment is supported with evidence of vegetation change in the Grassland Biome (Ellery *et al.,* 1991) and a predicted expansion of grass cover in the Karoo Midlands, a region along the ecotone between the Grassland and Nama-karoo biomes (Figure 1-5 and Figure 3-4) (Masubelele, 2012). The difference between this experiment of grass cover (GRA) and that of the present day landcover distribution was used to determine the impact of grass cover on the future climate (*i.e.* GRA minus GHG).

For both vegetation change experiments, forest and grass cover replace 100% of the present day vegetation. Although each scenario is rooted in the scientific literature discussed above, both experiments of vegetation change represent extreme changes compared to present day landcover distribution. However, as it is common in modeling studies in this field of research (see, for example, Wang *et al.,* 2014), the experiments in this study were not designed to simulate accurate scenarios of vegetation change, but rather to assess the magnitude and type of impact on regional climate that could occur from a hypothetical, albeit plausible, change in vegetation.

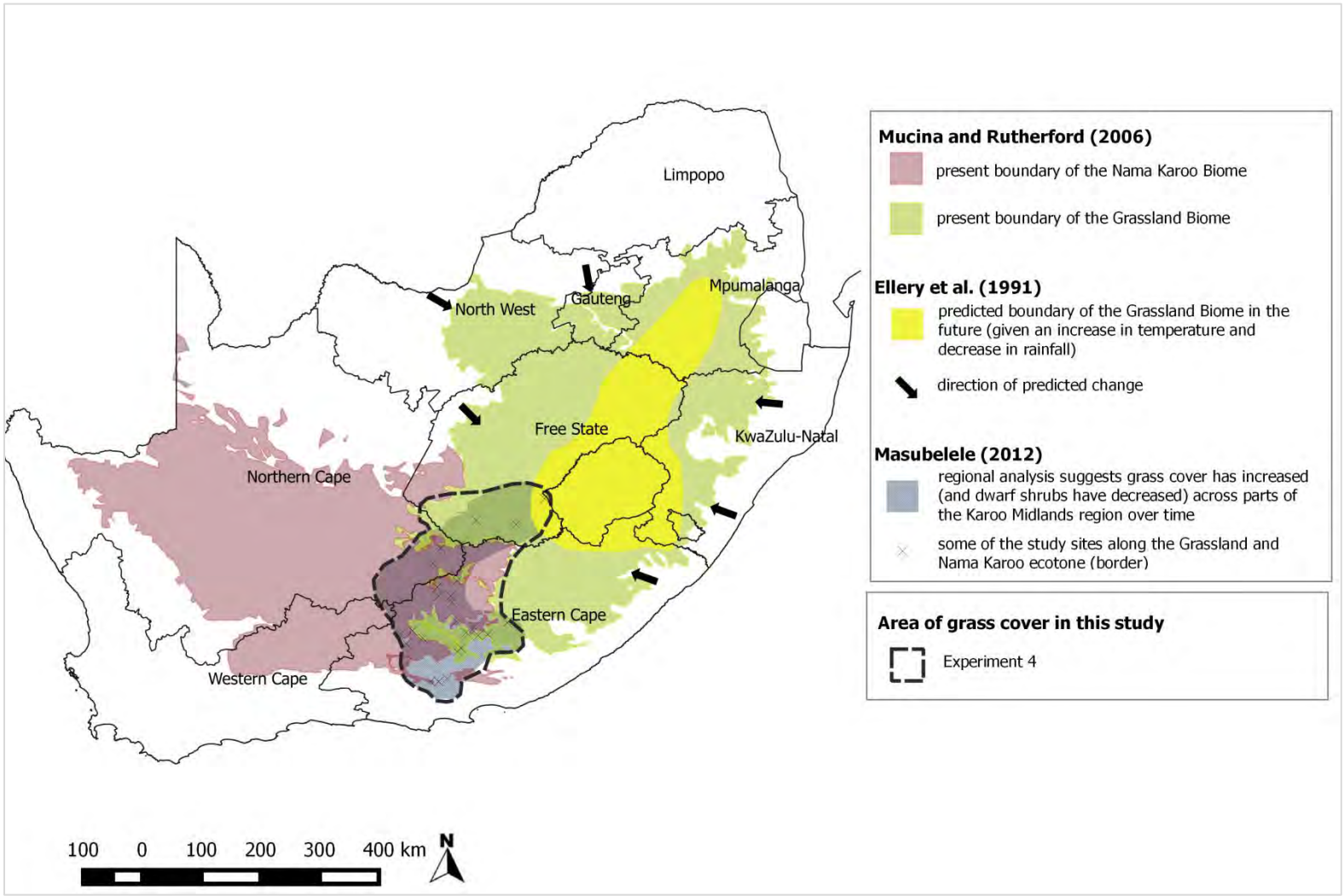

Figure 3-4 Area of grass cover change (Experiment 4) for RegCM and for WRF simulations was delineated based on relevant literature. (Adapted from: Mucina and Rutherford, 2006; Ellery, *et al.,* 1991; Masubelele, 2012)

Each RCM simulation was initialised and forced by the corresponding GCM simulation (*i.e.* RegCM by HAD, and WRF by MPI). All the simulations were run for 35 years, but the simulation of the first year was discarded as the spin up period, and the simulations of the remaining 34 years were analysed for the study. The PRS simulation was analysed to evaluate the performance of the models in simulating the Southern African climate, using the difference between PRS and GHG (*i.e.* GHG minus PRS) results to obtain the projected future climate change, using the difference between GHG and FRS results (*i.e.* FRS minus GHG) to assess the impacts of the forestation on the future climate, and using the difference between GHG and GRA results (*i.e.* GRA minus GHG) to assess the impacts of grass cover on the future climate. Thus, all the future projections of climate are presented as an anomaly (GHG is relative to the PRS experiment, while that of FRS and GRA are relative to that of GHG).

3.4 Calculation of Added Value

The study includes a calculation of added value using the method of Di Luca *et al.* (2013). RCMs offer a potential advantage over GCMs in that they capture small scale features at horizontal and temporal scales that are not explicitly resolved in GCM simulations. The concept of added value represents the ability of the RCM simulation to improve on the driving fields as compared to the observed data sets (Di Luca *et al.,* 2013), and the usefulness of the added value framework in evaluating RCM performance has also been reviewed (see, for example, Feser *et al.,* 2011). The added value provided by each regional model in this study is calculated as the difference between the GCM and RCM errors, where:

$$AV = SE\ (GCM\text{-}OBS)^{2} - SE\ (RCM\text{-}OBS)^{2}$$

and, AV, SE, GCM, RCM and OBS represent the amount of added value, the squared error, the forcing GCM, the RCM performing the downscaling and the observation, respectively (Di Luca et al., 2013).

Thus, the RCMs provide added value to the simulation of the GCM if their contribution of fine-scale details to climate statistics is not negligible (Di Luca *et al.,* 2012). More specifically, the RCM generates some AV if the SE is smaller than that of the GCM, *i.e.* positive values suggest the RCM provides a better approximation of the observation (or some ~~"a~~dded value") compared to the GCM.

3.5 Calculation of Drought

The study also includes a calculation of the 3-month drought frequency over Southern Africa using the Standardized Precipitation-Evapotranspiration Index (SPEI; Vicente-Serrano *et al.,* 2010). SPEI represents the climatic water balance of an area; it is calculated as the difference between the precipitation and potential evapotranspiration. As the SPEI calculation is based on the water balance, it can be used to identify a drought caused by a decrease in rainfall or higher water demand (*i.e.* evaporation) or both. It is also suitable for calculating drought indexes at different time scales, and many studies (Abiodun et al., 2013; Araujo *et al.,* 2014; Meque and Abiodun, 2014; Ujeneza and Abiodun, 2014) have demonstrated the usefulness of the SPEI index in calculations of

drought over Southern Africa. For the present study, SPEI is computed, for both observation and model simulations (PRS, GHG, FRS, GRA), using 1971-2004 as the reference period. The temporal scale for SPEI that is selected for the analyses is in line with a previous studies over Southern Africa that have identified the 3-month SPEI as a suitable timescale for monitoring soil moisture and precipitation during the growing season (Meque and Abiodun, 2014; Potop, 2011). Drought categories for SPEI depict the intensity of dryness; these range from -3 (extreme drought; negative values) to +3 (extreme wet; positive values) (Potop, 2011). For this study, the drought frequency is defined as the number of months when the 3-month SPEI is less than -1.5 per decade.

4 Model evaluation

In this chapter, the RCMs are evaluated by comparing the results of their PRS simulations with observation and with the GCMs simulations that provided the boundary forcing. Previous studies have shown that when using global re-analysis datasets as boundary forcing, both RCMs give a realistic representation of the Southern African climate (see, for example, Kalognomou *et al.,* 2013). However, since the horizontal resolution and lateral boundary conditions used in the present study differ from those used in previous studies, it is necessary to validate the models again in order to show how well the model set-ups used in this study simulate the regional climate. Our validation focuses on the ability of the models to reproduce the temporal and spatial variation of essential climatic features in the temperature, rainfall, and wind fields over Southern Africa. The seasonal timescale was considered for the austral summer (December-January-February; DJF), autumn (March-April-May; MAM), winter (June-July-August; JJA) and spring (September-October-November; SON) seasons.

4.1 Temperature

The models simulate the essential features in the observed temperature field over Southern Africa well, though with some biases (Figure 4-1). The observation (CRU) shows a temperature minimum along the escarpment in the southeast region of South Africa. This topographically induced minimum temperature has its lowest value (< 10°C) in the austral winter (JJA), when the overhead sun is in the Northern Hemisphere. Both

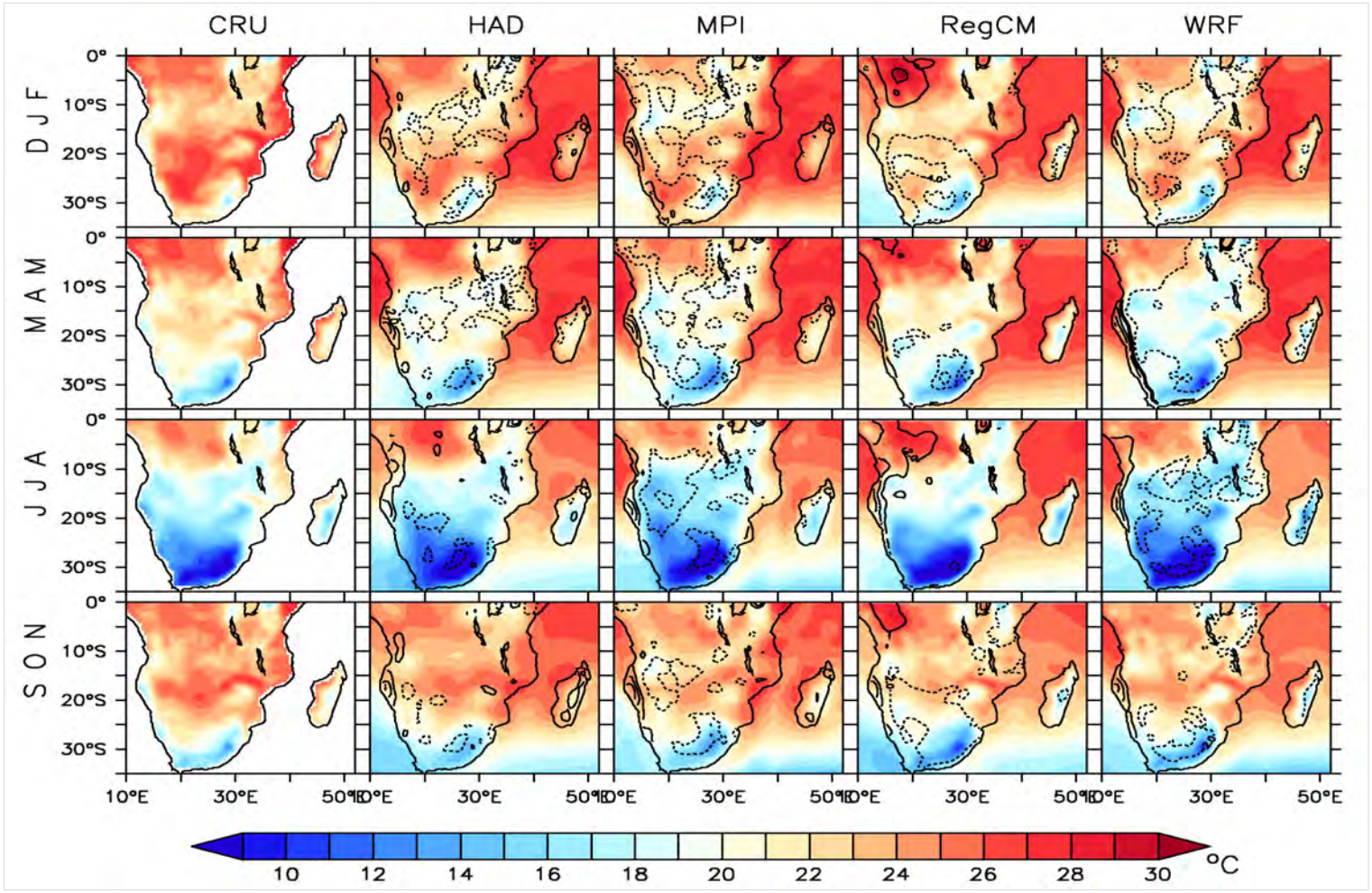

Figure 4-1 Observed and simulated seasonal mean temperature (shaded; degree Celsius) over Southern Africa in 1971-2004. The biases in simulated temperature are indicated with contours at an interval of 2°C; warm biases are indicated with solid contours while cold biases are indicated with dashed contours.

GCMs (HAD and MPI) and RCMs (RegCM and WRF) reproduce the location, the magnitude, and the seasonal variation of the minimum temperature as observed, except that they all show a cold bias, which is up to -2°C in HAD and -4°C in other models. The observation also features two temperature maxima in the tropics: a permanent temperature maximum near the equator (north of 10°S) and a temporal temperature maximum in the sub-tropics (south of 15^{o}S). The location and magnitude of the temporal temperature maximum varies with season. This feature reaches its southern most position (about 30^{o} S) and attains its highest magnitude (about 30°C) in DJF, but disappears in JJA. Whenever it appears, it is linked with the permanent temperature maximum (Figure 4-1) and forms a trough (not shown). All the models reproduce both the permanent and the temporal temperature maxima and capture the seasonal variation of the temporal temperature maximum, except that, in MAM, they all underestimate the magnitude of the temporal temperature maximum and simulate a weaker link between the two temperature maxima. RegCM also tends to produce a warm bias in tropical regions over the DRC and Congo. Both RegCM and WRF exhibit a cold bias over most parts of Southern Africa, but the cold bias is larger in WRF than in RegCM. The cold bias in WRF (> 3°C) may be linked to the cold bias in MPI that provided the boundary forcing; the cold bias is higher in MPI than in HAD. However, all the models produce a warm bias along the west coast, suggesting that they may not resolve the cooling effect of the Benguela current.

4.2 Rainfall

The RCMs reproduce the north-south and east-west spatial gradient in rainfall over Southern Africa well (Figure 4-2). In agreement with the CRU observation, all the

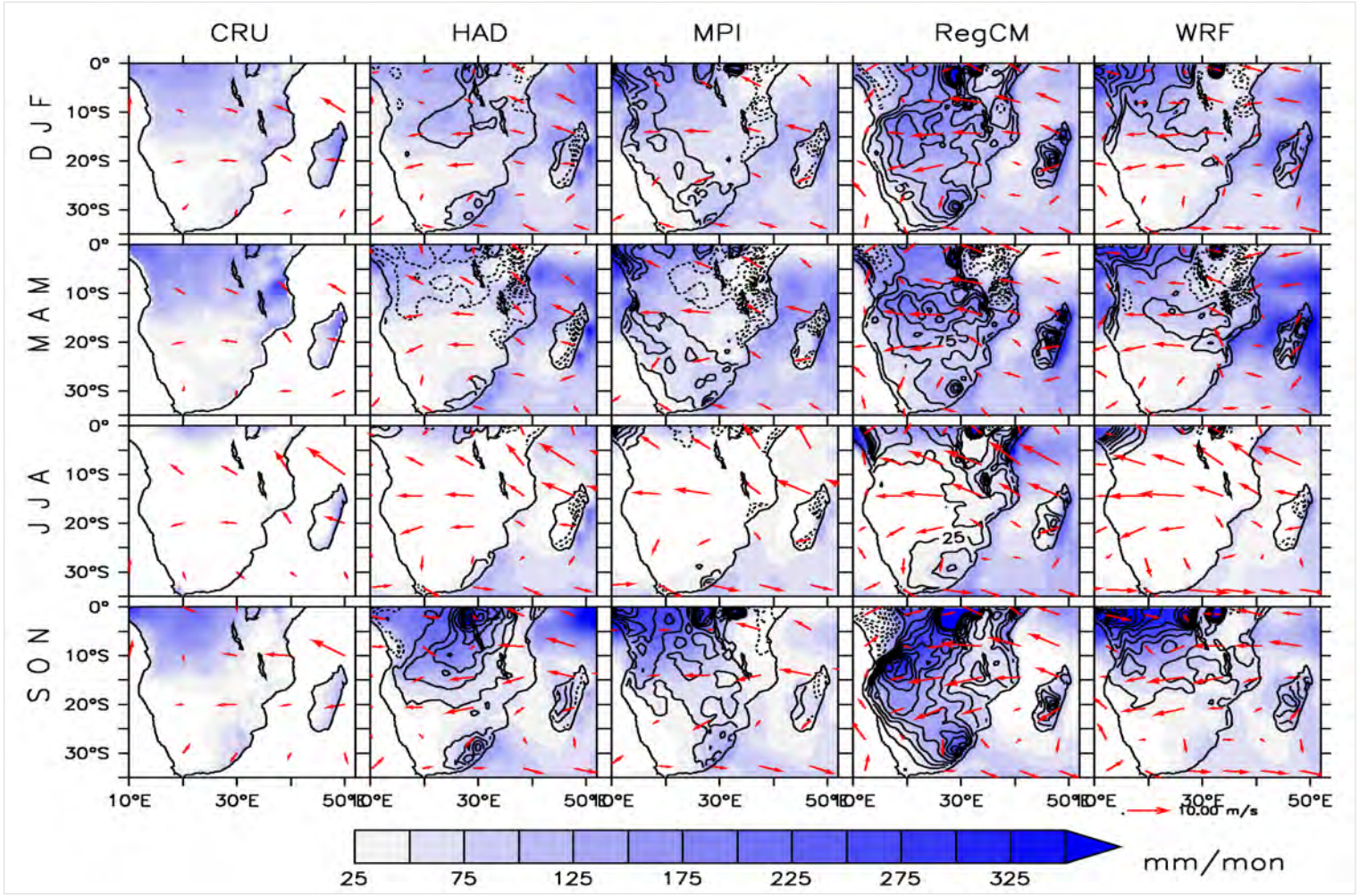

Figure 4-2 Observed and simulated seasonal mean rainfall (shaded; millimeter per month) over Southern Africa in 1971-2004. The biases in the simulated rainfall are indicated with contours at an interval of 25 mm/month; wet biases are indicated with solid contours while dry biases are indicated with dashed contours. The vectors indicate associated wind speed (meter per second) and direction at 850 hPa level.

models simulate dry conditions over most of the subcontinent (between 10°S and 25°S) in JJA, when rainfall is limited to the equatorial region (north of 10°S) and the southwestern edge of Southern Africa. The dry condition is associated with the subsidence arm of the Hadley circulation (Tyson, 1986) and the migration of the ITCZ (Inter-Tropical Convergence Zone) to the Northern Hemisphere. The rainfall at the southwestern edge is from the incursion of mid-latitude frontal systems into the subcontinent, but the incursion is usually limited to the Western Cape, which receives its maximum rainfall in JJA (Reason and Rouault, 2002). However, most parts of Southern Africa (with the exception of Namibia and the Western Cape Province of South Africa) receive at least 25 mm/month in other seasons (SON, DJF and MAM; Figure 4-2). In these seasons, the zone of maximum rainfall (produced by the ITCZ) is located within the tropics, near the equator, coinciding with the area of maximum temperature. Topography (*i.e.* the Great Escarpment) also induces a rainfall maximum over the Eastern Cape and Kwa-Zulu Natal Provinces in South Africa. Although WRF simulates rainfall amounts in this region well, RegCM tends to overestimate rainfall in each season. While the simulated rainfall patterns generally agree with the observed pattern, the models show wet biases in some seasons and dry biases in others (Figure 4-2). Some of these biases also appear in the GCM's simulations that provided the boundary forcing.

4.3 Wind profile

The RCMs also reproduce the location of the Subtropical Jet and the gradient in zonal wind over Southern Africa, though with some biases (Figure 4-3). The observation (NOA) shows strong (+24 m/s) westerly winds in the upper troposphere (200 mb) that

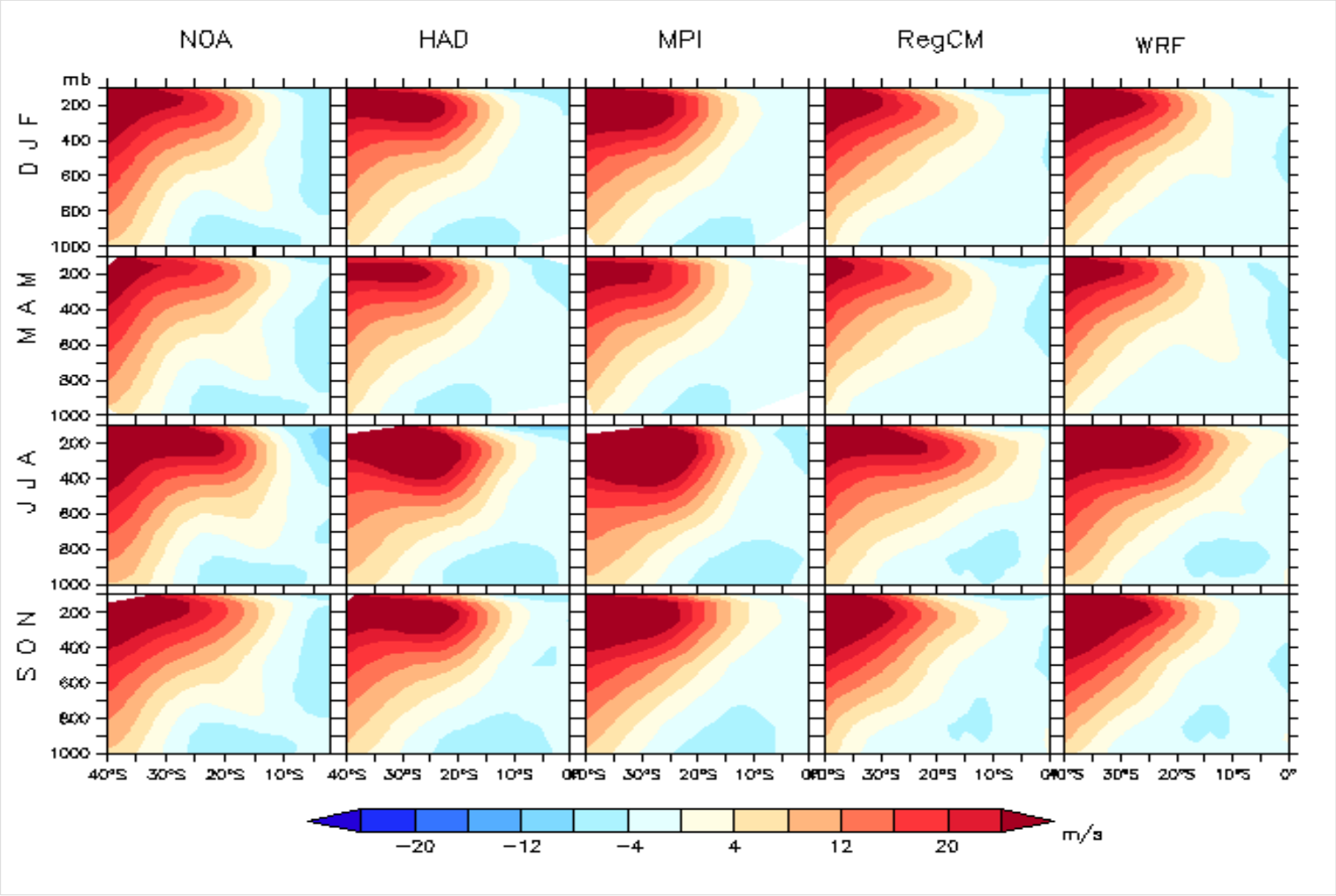

Figure 4-3 Observed and simulated vertical cross section of mean zonal wind speed (shaded; meter per second) over Southern Africa in 1971-2004.

characterize the Subtropical Jet. Both GCMs (HAD and MPI) and RCMs (RegCM and WRF) reproduce the strength of these westerly winds at the core of jet, in the upper troposphere, and the seasonal variation in position (latitude) in DJF (35^{o}S) and JJA (20^{o}S). The observation also features easterly wind flow (-8 m/s) in the mid to upper troposphere at the equator and at the surface, between 10°S to 25°S. All the models tend to underestimate the easterlies at the equator, but both RegCM and WRF also underestimate the strength of the surface easterlies (between 10°S to 25°S) during DJF (the primary rainfall season over much of the region) and MAM.

4.4 Added value

The added value of downscaling provided by each RCM as compared to the observation is presented in Figure 4-4. For temperature, both the RCMs provide added value over Southern Africa, but the performance varies with the model and seasonal differences do occur. For instance, the downscaling by WRF improves the simulation of MPI during SON over Angola, and during DJF over south-central Africa, but RegCM depreciates the simulation of HAD over this region. However, during MAM the opposite pattern occurs over parts of Zimbabwe and Mozambique; RegCM improves the simulation of HAD, but WRF depreciates the value of MPI in this region. In (JJA) the performance of the RCMs is similar.

For rainfall, the added value of downscaling differs between the RCMs (Figure 4-4). The value added by RegCM is negative over many regions of Southern Africa, as the model tends to depreciate the signal produced by HAD in most seasons. However, the added

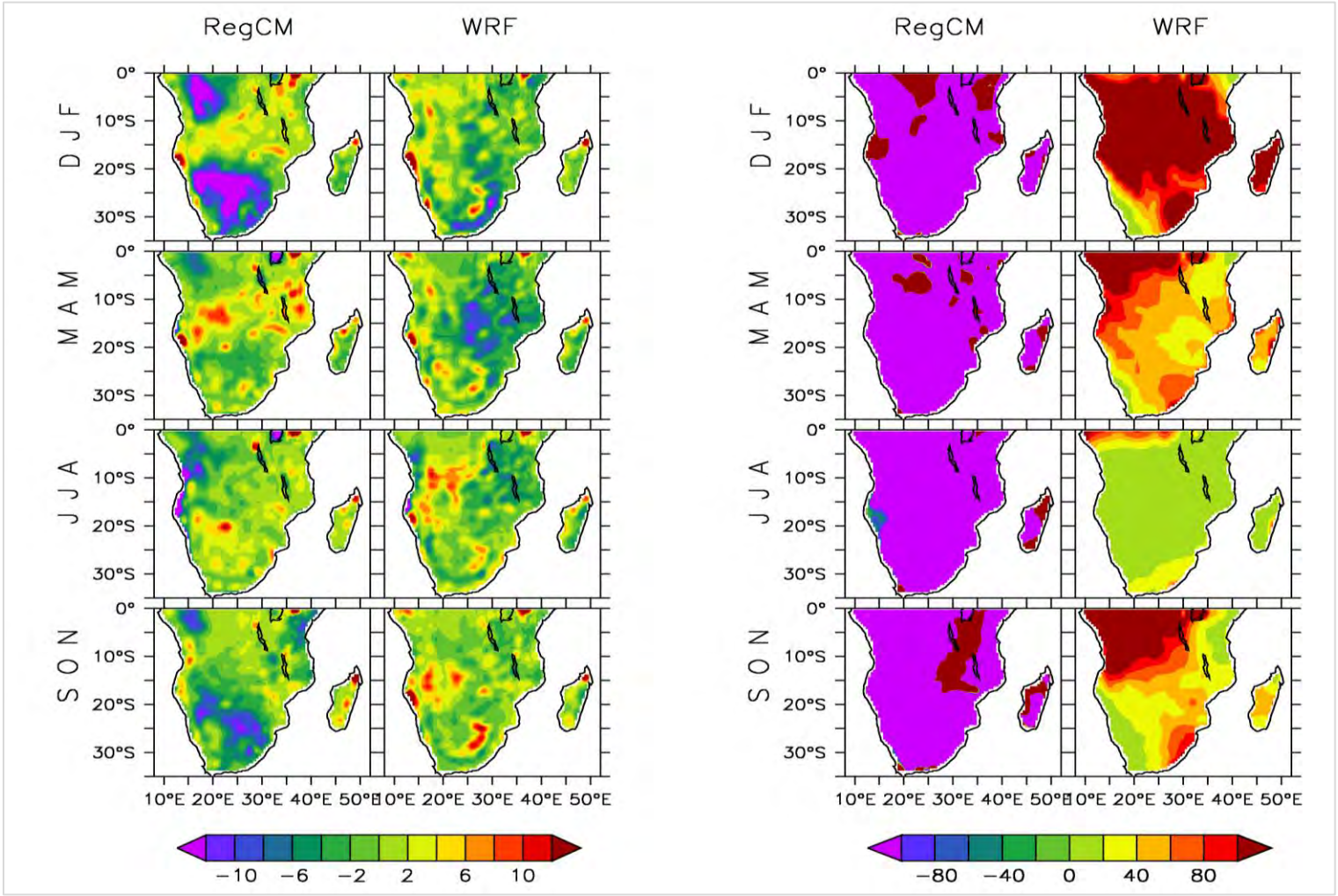

Figure 4-4 Added value for each RCM (shaded) for (a) temperature (left) and (b) rainfall (right).

value by WRF is positive and the model improves on the simulation of MPI. For example, WRF provides an added value (100+) during DJF, SON and MAM over equatorial regions such as Angola and the summer rainfall region of South Africa. However, during JJA the value added by WRF is limited, due to the dry conditions over the region.

It is difficult to explain the cause of the underlying biases in the regional models without a more extensive analysis incorporating other meteorological variables at different timescales. However, results here are comparable to previous studies suggesting that the RCM's ability to provide added value depends on several factors including the season, time scale and variable of interest (Di Luca *et al.,* 2013). Analysis of added value here is also useful since it summarizes the relative performance of the models and underscores the value of using two regional models for the study.

The RCM biases found in this study are similar to those obtained in previous studies where the RCMs were forced with Reanalysis. For instance, the warm biases over DRC and Congo (equatorial forested regions), and cold biases over Kalahari Desert (Figure 4-1) in RegCM were also reported in Sylla *et al.* (2009), where the model was forced with the ERA-Interim dataset. Larger biases may have been expected in the present study, due to the additional error from the driving GCM (*i.e.* HAD) and the tendency of the model to overestimate precipitation at finer horizontal resolution (Sylla *et al.,* 2012). However, annual biases in the present study (not shown) are of about the same magnitude as that of Sylla *et al.* (2009). The strength and location of this Subtropical Jet Stream also

has an important influence on the generation of rainfall over the Southern African region. This is because the low level easterly flow between 15°S to 25°S acts as an important moisture source transporting water vapour from the South Indian Ocean to the interior, where it contributes to the rainfall over the region (Sylla *et al.,* 2009). Previous studies have also found that RegCM produces a wet bias over parts of the Indian Ocean due to simulation of stronger easterly winds north of Madagascar (Sylla *et al.,* 2009). Although this did not occur in the present study, the simulated easterly winds (about -2 m/s) are weaker than observed (-6 m/s) and this difference may have contributed to the accumulation of moisture inland and the positive rainfall bias in RegCM.

The performance of WRF over South Africa also compares well to that of previous studies. These studies suggest the mean biases of the model are influenced by the convective parameterization schemes used in the simulation. For instance, Crétat and Pohl (2012) and Pohl *et al.* (2014) show that the Kain-Fritsch scheme used in the present study produced the largest rainfall overestimation as compared to other parameterizations. The positive biases in rainfall are reported to be the result of atmospheric instability, strong moisture convergence near the surface, and enhanced moisture transport from the tropical regions (Pohl *et al.,* 2014; Ratna *et al.,* 2014). The large biases observed in the present study over regions of complex topography in the eastern region of South Africa were also reported by Ratna *et al.* (2014). Hence, the model biases found in this study are comparable with that of previous studies. The results of the model evaluation suggest RegCM and WRF provide a realistic representation of

the present day climate. This encourages some confidence when interpreting the projections of future climate.

5 Projected impacts of elevated greenhouse gasses

In this chapter, climate change projections due to emissions change without any land cover changes are analysed under the RCP 4.5 scenario (*i.e.* GHG – PRS). The changes are presented as the anomaly between the future climate (2031-2064) and present day (1971-2004) climate. The RCM projections are then contextualized in relevant literature.

5.1 Temperature

The models (GCMs and RCMs) project that elevated greenhouse emissions will increase air temperatures over Southern Africa in the future, but the spatial distribution of the increase differs among the models and varies with the seasons (Figure 5-1). For instance, in SON and MAM, both RCMs show that the largest warming occurs over the western interior of South Africa, but, while RegCM projects a warming that is up to 3.2°C in SON and 2.4°C in MAM, WRF projects lower warming (2.2°C and 1.8°C, respectively). In DJF, the spatial pattern of warming is not consistent between the RCMs. Although both models project higher warming along the western periphery of South Africa (about 2.3^{o}C), RegCM shows a peak warming over northern Mozambique in contrast to WRF‘s projection. In JJA, the RCMs show their largest warming (about 3°C in RegCM and 2°C in WRF) in the equatorial region (between about 0-10°S); but, in addition, RegCM shows another peak warming (about 3°C) over Angola and the DRC. The differences in the RCMs‘ projections reflect the dissimilarity between the GCM projections that forced the

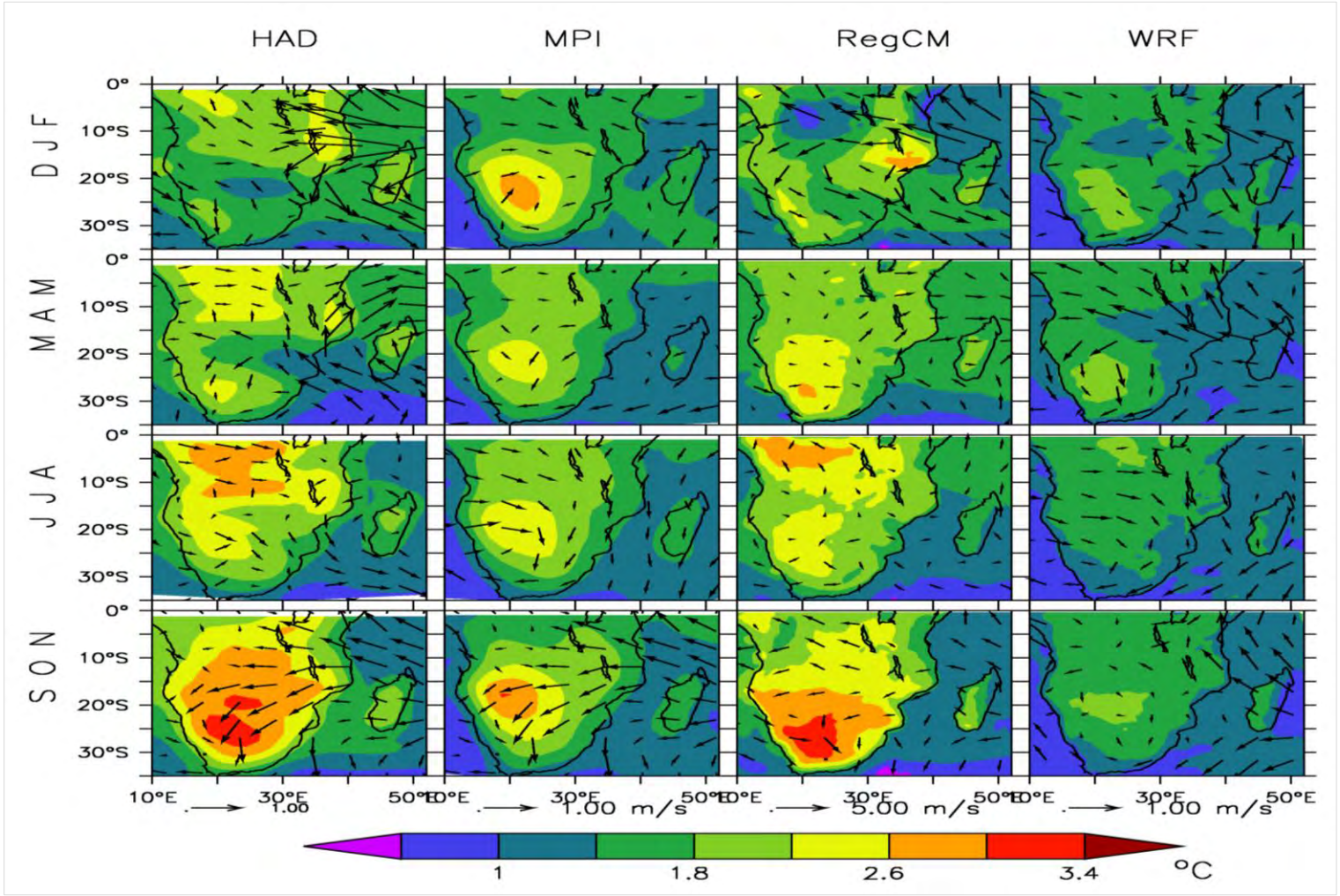

Figure 5-1 Projected differences in mean air temperature (shaded; degree Celsius) as simulated for 2031-2064. The vectors indicate associated wind speed (meter per second) and direction at 850 hPa level.

RCMs. Excepting these few differences, there is agreement between the temperature projections from the two RCMs.

5.2 Rainfall

The projected rainfall changes are more complex than the projections of temperature. All the models feature both wet and dry biases in different seasons and over different areas of the subcontinent (Figure 5-2). The patterns of the rainfall changes produced by each RCM are similar to those of the GCM that forced it, except that the RCM projections show more refined local scale features than those in the GCM projections. In addition, the magnitudes of the changes are higher in the RCMs‘ projections. The level of agreement between RegCM and WRF projections vary with the season. The RCMs agree on the decrease in rainfall over central Southern Africa (including northern Botswana and Zimbabwe and Southern regions of Zambia) in MAM and SON, over Mozambique in SON, and over the DRC and northern Angola in JJA. They also agree on an increase in rainfall over northern Mozambique in MAM. The main disagreement between the RCMs occurs in DJF, when RegCM projects a decrease in rainfall over the eastern part of the subcontinent and an increase in rainfall over the southern and northern parts, while WRF projects the opposite pattern. Furthermore, in SON, RegCM projects a decrease in rainfall over the tropical region (0–10^{o}S) while WRF projects an increase in rainfall over the region. However, on the annual scale, the RCM projections show wetter conditions over the eastern coast of South Africa (not shown).

The RCM projections for both temperature and rainfall over Southern Africa are in line with those in previous studies. For example, using the A2 emissions scenario, Hudson

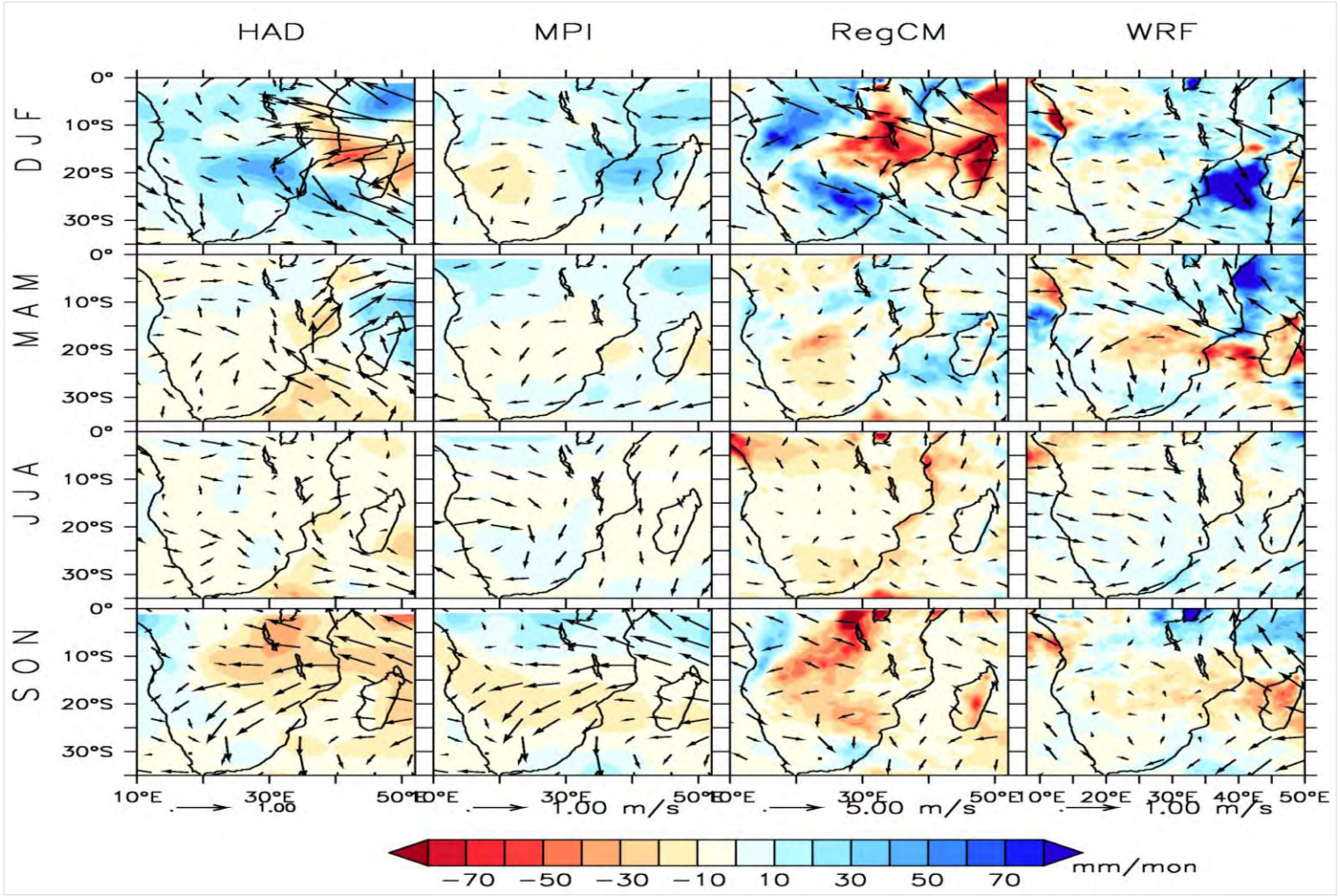

Figure 5-2 Projected differences in mean rainfall (shaded; millimeter per month) as simulated for 2031-2064. The vectors indicate associated wind speed (meter per second) and direction at 850 hPa level.

and Jones (2002) found that by the 2080s the air temperature over Southern Africa would increase by 3.7^{o}C in summer and by 4.0^{o}C in winter. With the same emissions scenario, but with a higher resolution model (REMO), Haensler *et al.* (2011b) found a peak warming over the southwestern interior (over the Kalahari Desert) of about 4^{o}C from 2041-2070 and in excess of 5°C by the end of the century. RegCM projects a peak in mean annual warming over this region to be about 2.5°C (not shown); however, considering the shorter trajectory (2060s) and more conservative future scenario (RCP4.5), projections in the present study are, as expected, of smaller magnitude.

These regional model projections for rainfall also compare well with the literature. Rainfall projections from previous studies suggest increased rainfall over eastern Southern Africa during the summer season (Christensen *et al.,* 2007; Hewitson and Crane, 2006; Tadross *et al.,* 2005). Several studies also project a decrease in winter rainfall over the southwestern Cape (Hewitson and Crane, 2006; Tadross *et al.,* 2005; Tyson and Gatebe, 2001). Projections by Engelbrecht *et al.* (2009), suggest that this may be due to an increase in the intensity and frequency of upper level highs over Southern Africa that would enhance subsidence and decrease rainfall in this region. RegCM projections are in line with these studies and also reflect a reduction in rainfall over the winter rainfall region. However, WRF projections, suggest a weak increase in rainfall over the winter rainfall zone. This may be the result of enhanced cyclonic motion in the WRF model over the region.

6 Potential impacts of vegetation changes

In this chapter the potential impacts of both vegetation change scenarios are discussed. These are impacts of forestation scenario (*i.e.* FRS – GHG) and impacts expansion of grass cover scenario (*i.e.* GRA – GHG) on the future climate. The changes are computed to assess the impact on future climate (2031-2064), under the RCP 4.5 scenario, rather than the present day (1971-2004) climate.

6.1 Impacts of forestation

The RCMs show that the forestation induces both warming and cooling over Southern Africa, but the spatial distribution of the warming and cooling varies with the seasons and slightly differs between models (Figure 6-1). For forestation (FRS), both RegCM and WRF models show that the peak of the warming occurs over the forested area in all seasons. The magnitude of this warming is higher in MAM than in JJA, and the warming covers a broader spatial area with RegCM than with WRF. For instance, with WRF the warming of 0.1^{o}C is confined to the forested area (*i.e.* largely KwaZulu Natal and Eastern Cape Province) in all seasons, but with RegCM it extends to the central part of Southern Africa in DJF and JJA and as far as the Western Cape Province in MAM. However, there is better agreement between the models on the spatial distribution of the cooling, which is most visible over Namibia and Botswana in MAM and stronger in RegCM (about -0.2^{o}C) than in WRF (about -0.15^{o}C). It is also worth mentioning that, for both RCMs, as compared with the natural variability (*i.e.* standard deviation) of the present day climate, the impacts of forestation may not significantly modify the future climate,

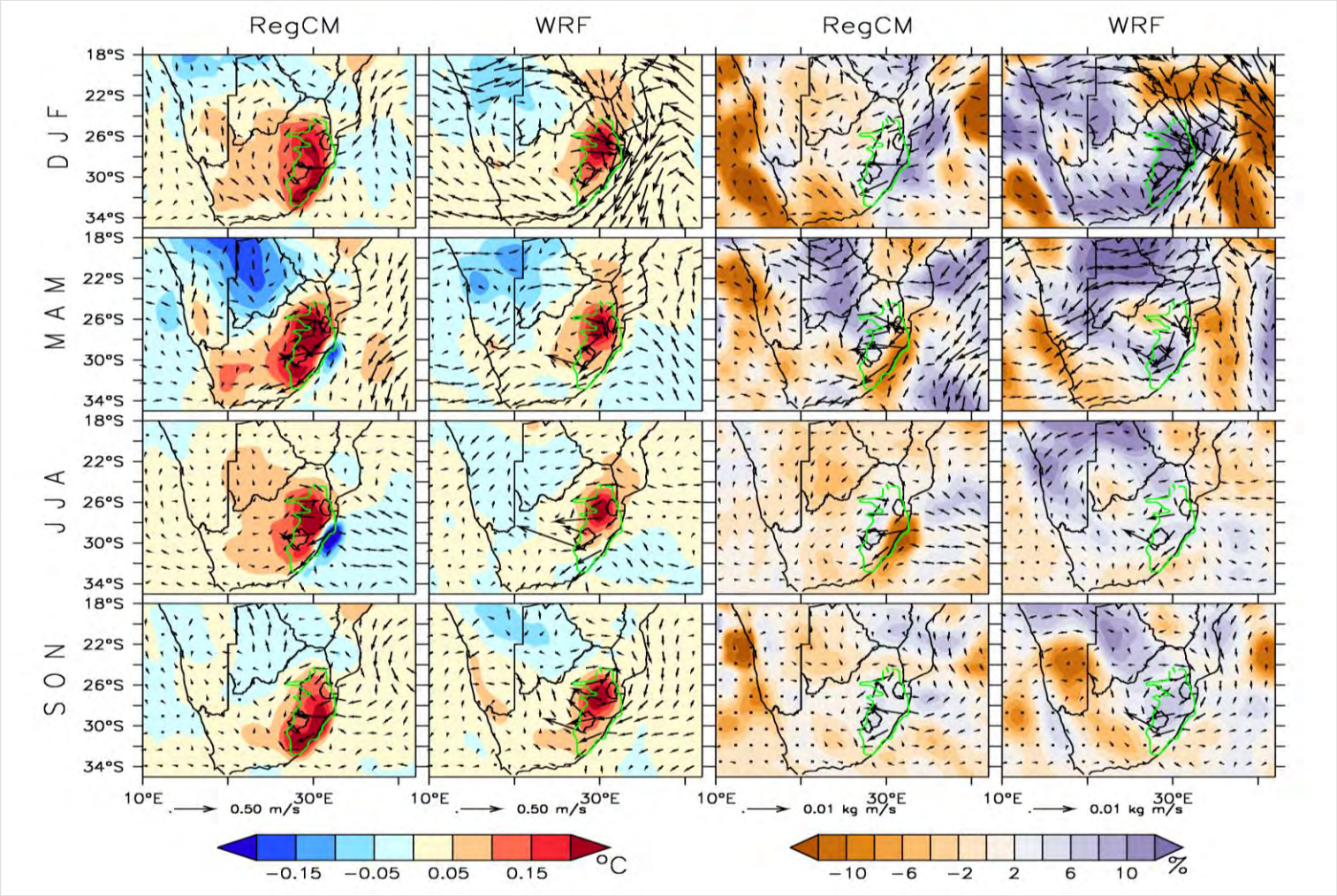

Figure 6-1 Potential impacts of forestation as simulated for surface (2m) temperature (shaded; degree Celsius; left panels), the vectors indicate associated wind speed (meter per second) and direction at 850 hPa level, and rainfall (shaded; percentage change; right panels), the vectors indicate associated moisture flux (kilogram meter per second).

although the changes in temperature due to emission change are significant (Table 6-1 and Table 6-2).

The RCMs also show that changes to forestation induce wet and dry patterns over the different regions of the subcontinent (Figure 6-1). The spatial distribution follows that of the warming and cooling in some seasons, but differs in other seasons. In general, forestation induces wet conditions over the forested area, except in the RegCM simulation where it induces a dry condition along the eastern coast in JJA and MAM. In MAM, both models agree that the forestation enhances rainfall over Botswana. In other seasons, WRF shows that the forestation still increases the rainfall over Botswana, but RegCM suggests that it decreases the rainfall over the country. With the exception of DJF, both models also agree that forestation induces a dry condition over the southwestern half of the subcontinent, although the magnitude of the drying is higher in RegCM than in WRF. Nonetheless, the impact of forestation on rainfall in the future climate is not significant (Table 6-1 and Table 6-2).

The impacts of forestation on the rainfall and temperature fields can be linked to the biogeophysical influence of the vegetation change on the surface energy balance and on the atmospheric dynamics. The warming over the forested area can be attributed to the influence of forestation on surface albedo (Table 6-1 and Table 6-2). The darker tree canopy of the forest absorbs more of the incoming solar radiation, relative to pre-existing vegetation cover. Thus, the forestation decreases surface albedo (*e.g.* for RegCM, by -0.02 in DJF), thereby increasing the amount of net solar radiation at the surface (*i.e.* for RegCM, by 3.83 Wm^{-2} in DJF). The excess energy

Table 6-1 The RegCM simulated mean (μ) and standard deviation (σ) of some climate variables in each season of the present-day (PRS); the projected future changes in the mean relative to the present day climate (GHG), and the impacts of forestation (FRS).The climate variables considered are temperature (Temp), rainfall (Rain), specific humidity (Q), relative humidity (RH), latent heat flux (LHF), surface downward shortwave flux in air (RSDS), net downward shortwave energy flux (RSS), surface albedo to diffuse shortwave radiation (ALBEDO), sensible heat flux (SHF), surface drag force (DRAG), maximum wind speed at 10 m height (WIND), moisture content of the soil layers (MRSO), planetary boundary layer thickness (PBL) and Bowen ratio. The significant GHG values (*i.e.* > σ) are in bold. If GHG is significant, but the impact of forestation (FRS) on future climate (GHG) is not significant, the value is underlined (FRS+GHG < σ *i.e.* forestation will shift the projected climate change signal to within the region's natural climate variability). If GHG is not significant, but the impact of forestation (FRS) on future climate is significant, the FRS value is bold (FRS+GHG > σ *i.e.* the impacts of forestation on future climate would exceed the region's natural climate variability).

Variables	**DJF**				**MAM**				**JJA**				**SON**			
	PRS		GHG	FRS	PRS		GHG	FRS	PRS		GHG	FRS	PRS		GHG	FRS
	μ	σ			μ	σ			μ	σ			μ	σ		
Temp (°C)	24.59	0.52	**1.72**	0.19	23.87	0.49	**1.81**	0.21	20.07	0.78	**5.62**	0.16	22.44	0.84	**2.35**	0.19
Rain (mm mon^{-1})	73.79	42.92	10.10	3.49	31.63	25.87	-0.12	-0.23	17.76	20.64	13.75	0.04	51.98	29.37	0.62	2.06
Q (g kg^{-1})	11.33	0.49	**1.46**	0.05	9.57	0.47	**0.78**	-0.12	6.61	0.48	**3.75**	-0.09	9.17	0.41	**1.02**	0.05
RH (%)	84.85	2.53	1.12	-0.78	77.91	2.13	-1.95	**-2.10**	71.61	4.21	**4.35**	-2.06	80.05	3.31	-2.17	-0.99
LHF (W m^{-2})	139.70	3.70	**4.49**	2.98	97.62	3.88	0.83	**-7.06**	63.87	4.37	**34.58**	-6.66	119.70	4.09	0.13	3.52
RSDS (W m^{-2})	219.40	15.67	-9.92	-4.43	174.00	10.46	3.08	-2.79	142.50	8.67	**34.54**	-1.50	207.40	10.34	2.58	-1.96
RSS (W m^{-2})	228.90	10.14	-6.37	3.83	170.90	6.85	1.32	4.37	135.10	4.78	**37.19**	5.34	209.50	6.37	0.99	**6.42**
ALBEDO	0.08	0.00	0.00	**-0.02**	0.09	0.00	0.00	**-0.02**	0.09	0.00	0.00	**-0.03**	0.08	0.00	0.00	**-0.02**
SHF (W m^{-2})	33.85	5.06	**-5.88**	1.09	9.43	3.48	1.10	**5.52**	-4.11	3.05	**14.65**	4.36	24.47	3.80	1.65	2.02
DRAG	0.07	0.10	0.00	0.04	0.12	2.05	0.01	0.20	0.04	0.02	**0.09**	0.09	0.19	0.34	0.04	-0.01
WIND (m s^{-1})	1.97	0.75	-0.26	-0.50	2.05	0.68	0.03	**-0.87**	4.68	1.12	**-2.60**	-2.10	1.51	0.63	0.44	-0.68
MRSO (kg m^{-2})	29.98	1.26	0.78	**5.00**	26.96	1.07	**-1.16**	3.13	24.35	2.34	1.46	**2.89**	28.61	1.76	-1.08	**4.56**
PBL (m)	742.90	37.76	**-43.71**	47.94	646.40	31.31	10.53	**72.43**	665.70	45.87	-8.70	49.08	758.30	46.61	13.19	**54.66**
BOWEN RATIO	0.25	0.05	-0.05	0.01	0.08	0.04	0.01	**0.08**	-0.08	0.05	**0.17**	0.08	0.21	0.06	0.03	0.02

Table 6-2 Same as Table 6-1, but for WRF simulation.

Variables	**DJF**				**MAM**				**JJA**				**SON**			
	PRS		GHG	FRS	PRS		GHG	FRS	PRS		GHG	FRS	PRS		GHG	FRS
	μ	σ			μ	σ			μ	σ			μ	σ		
Temp (°C)	17.14	0.48	**1.37**	0.20	14.41	0.65	**1.40**	0.14	10.51	0.63	**5.30**	0.12	15.49	0.78	**1.39**	0.15
Rain (mm mon^{-1})	208.20	35.23	-1.78	33.30	89.96	42.68	6.67	7.69	31.69	11.70	**64.94**	1.76	117.20	25.85	4.84	8.81
Q (g kg^{-1})	9.78	0.40	**0.90**	0.20	7.76	0.51	**0.85**	0.18	4.65	0.34	**3.96**	0.08	6.99	0.41	**0.71**	0.13
RH (%)	80.21	9.52	-0.55	0.14	74.18	9.39	0.58	0.92	60.34	9.20	**14.42**	0.61	65.38	8.20	0.59	0.27
LHF (W m^{-2})	124.30	3.73	2.42	**9.16**	78.44	3.92	1.04	**7.09**	39.00	2.60	**40.48**	**5.94**	77.14	4.12	2.57	**9.74**
RSS (W m^{-2})	240.80	10.81	-0.09	**11.60**	166.20	10.42	-1.12	9.92	132.80	4.27	**32.32**	**12.19**	220.70	8.28	0.76	**18.83**
ALBEDO	0.18	0.00	0.00	**-0.06**	0.19	0.00	0.00	**-0.06**	0.21	0.00	**-0.03**	**-0.08**	0.20	0.01	0.00	**-0.08**
SHF (W m^{-2})	51.36	3.64	-0.58	**4.67**	23.75	3.18	-0.04	**3.71**	14.51	1.71	**9.20**	**4.55**	58.57	4.94	-1.27	**8.86**
WIND (m s^{-1})	5.78	2.93	0.91	-0.93	9.07	3.13	-1.67	-1.38	24.25	6.21	**-16.85**	-3.53	6.97	5.58	-0.86	-1.37
PBL (m)	540.20	22.62	-6.08	19.65	458.20	21.84	-11.78	14.81	489.10	21.87	**-42.66**	23.71	613.20	35.95	-17.78	33.92
BOWEN RATIO	0.43	0.03	-0.01	0.00	0.33	0.04	0.00	0.01	0.48	0.10	**-0.15**	0.03	0.88	0.23	-0.03	0.00

influences the surface heat fluxes, such that the increase in the net solar radiation enhances the sensible heat flux from the surface. While the increase in the sensible heat flux over the forested area is consistent with warming over the area, the maximum increase in the sensible heat flux in DJF agrees with the region of peak warming during this season. In addition, the increase in rainfall over the forested area can be attributed to both the albedo-effect and the dynamic-effect of forestation. With the albedo-effect, the increase in the net solar radiation enhances the latent heat flux, but only in DJF (by 2.92 Wm^{-2}) and SON (by 3.52 Wm^{-2}), when the soil moisture is sufficient. This is consistent with the increase in surface moisture (*i.e.* specific humidity) and rainfall in the two seasons. With the dynamic-effect, the increase in temperature and in surface friction induced by forestation encourages convergence and cyclonic flow over the forested area, thereby producing more rain (Figure 6-1 and Table 6-1). This is supported by the decrease in surface pressure and increase in boundary layer height following the forestation. However, while the dynamic-effect increases the rainfall in all seasons, the albedo-effect only contributes to the rainfall increase in DJF and SON. That explains why the rainfall increase is higher during DJF and SON than in other seasons (MAM and JJA).

The influence of forestation on temperature (*i.e.* warming) found in this study agrees with what Swann *et al.* (2012) found in mid-latitude regions and contradicts with what Abiodun *et al.* (2012) found over West Africa. For Abiodun *et al.* (2012), forestation induced cooling over West Africa. The discrepancies between our study and that of Abiodun *et al.* (2012) may be attributed to the differences in the net influence of

forestation on albedo. In Abiodun *et al.* (2012), forestation increases the albedo rather than decreasing it.

6.2 Impacts of grass cover expansion

The RCMs show that changes to grass cover induce both warming and cooling over Southern Africa; however, the spatial distribution of the warming and cooling, varies with the seasons, and differs slightly between models (Figure 6-2). Both RCMs show that a general cooling occurs over the area of grass cover expansion. In RegCM, cooling (about -0.2°C) occurs over the area of grass cover expansion in all the seasons and the magnitude is higher in DJF and SON. In WRF, cooling also occurs over the area of grass cover change in some seasons, but not in others. For instance, during SON and JJA cooling of about -0.2°C occurs, but in DJF and MAM warming of about +0.1°C occurs. There is a good agreement between RegCM and WRF on the spatial distribution of the cooling that occurs over Botswana and Namibia in MAM and SON, although it is stronger in WRF (about -0.2°C) than in RegCM (about -0.05°C). However, there is some disagreement between RegCM and WRF in DJF and JJA, when the models show an opposite pattern: WRF projects cooling over this region while RegCM projects warming. Overall, the RCMs show that locally, grass cover expansion could reduce the projected warming. Nevertheless, for both RCMs, though the changes in temperature due to emission change are significant, the impact of grass cover may not significantly modify the future climate (Table 6-3 and Table 6-4).

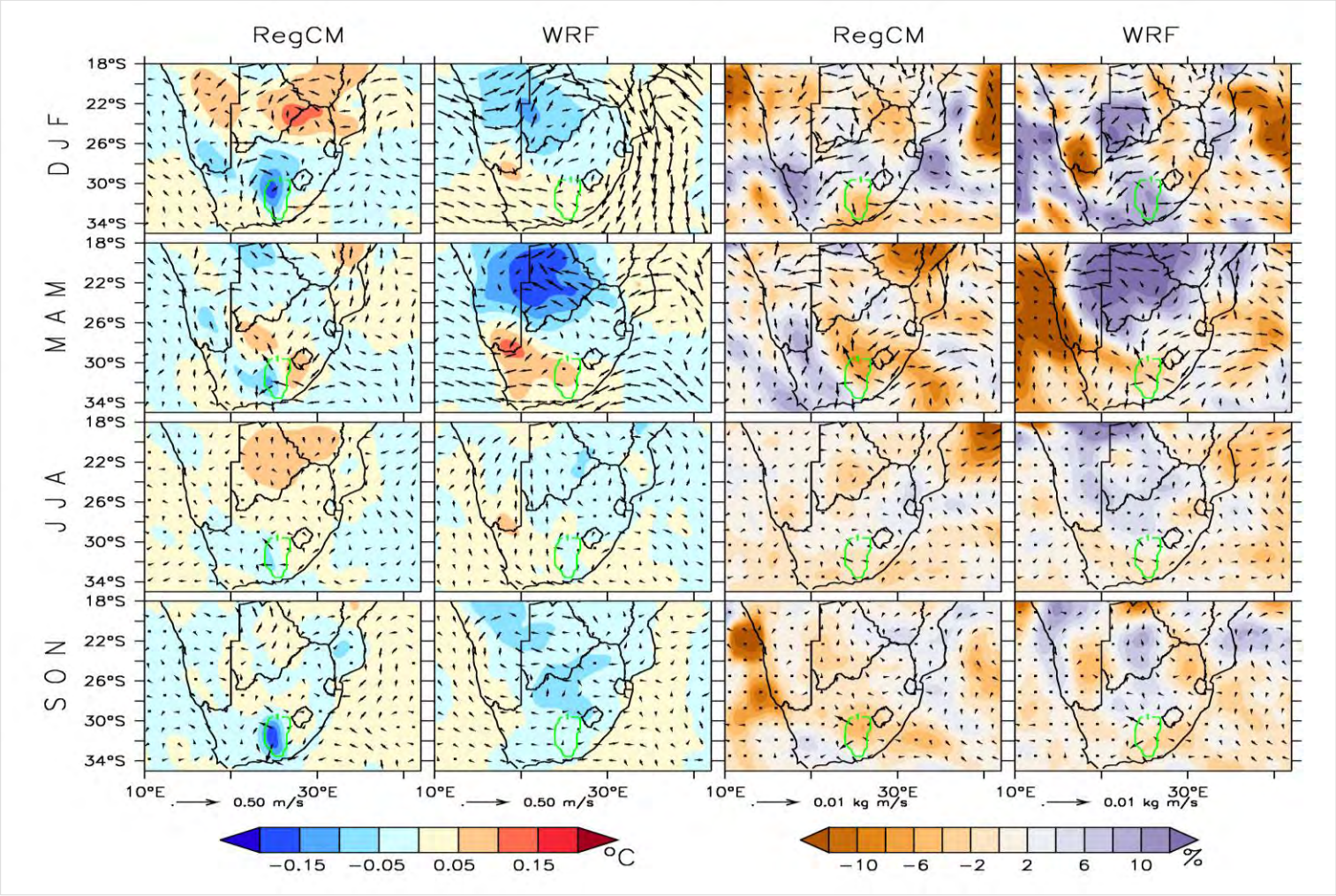

Figure 6-2 Potential impacts of grass cover as simulated for surface (2m) temperature (shaded; degree Celsius; left panels), the vectors indicate associated wind speed (meter per second) and direction at 850 hPa level, and rainfall (shaded; percentage change; right panels), the vectors indicate associated moisture flux (kilogram meter per second).

The expansion of grass cover (GRA) also induces wet and dry patterns over Southern Africa (Figure 6-2). Generally, drier conditions over the area of grass cover change, except in the RegCM simulation, where it induces a wet condition in DJF. In this season, both the RCMs show that the expansion of grass cover could increase rainfall over the western half of South Africa and parts of Botswana. In other seasons, however, although WRF shows that the grass cover expansion still increases the rainfall over Botswana, RegCM suggests that it decreases the rainfall over the country. For instance, in MAM, when the largest changes in rainfall occur, WRF shows that rainfall could increase (+10%) over Botswana, but RegCM shows rainfall could decreases (-5%). In general, the grass cover could decrease rainfall locally, and induce more complex changes in remote regions. Nonetheless, for both RCMs, the impacts of grass cover on rainfall are not significant (Table 6-3 and Table 6-4).

The cooling over the grass expansion can also be attributed to the influence of grass cover on albedo (Table 6-3). The lighter cover of the grass reflects more of the incoming solar radiation, relative to pre-existing vegetation cover. This increase in surface albedo (*i.e.* in DJF, for RegCM: +0.01) decreases the amount of solar radiation absorbed at the earth‘s surface (*i.e.* in DJF, for RegCM: 5.66 Wm^{-2}). The loss of energy influences the surface energy heat fluxes, such that the decrease in the net solar radiation decreases the sensible heat flux from the surface. The changes in the sensible heat flux are consistent with cooling over the grass covered area. The decrease in rainfall over the grass covered area can also be attributed to both albedo-effect and dynamic-effect. With the albedo-

Table 6-3 The RegCM simulated mean (μ) and standard deviation (σ) of some climate variables in each season of the present-day (PRS); the projected future changes in the mean relative to the present day climate (GHG), and the impacts of grass cover (GRA).The climate variables considered are temperature (Temp), rainfall (Rain), specific humidity (Q), relative humidity (RH), latent heat flux (LHF), surface downward shortwave flux in air (RSDS), net downward shortwave energy flux (RSS), surface albedo to diffuse shortwave radiation (ALBEDO), sensible heat flux (SHF), surface drag force (DRAG), maximum wind speed at 10 m height (WIND), moisture content of the soil layers (MRSO), planetary boundary layer thickness (PBL) and Bowen ratio. The significant GHG values (*i.e.* > σ) are in bold. If GHG is significant, but the impact of grass cover (GRA) on future climate (GHG) is not significant, the value is underlined (GRA+GHG < σ *i.e.* forestation will shift the projected climate change signal to within the region's natural climate variability). If GHG is not significant, but the impact of grass cover (GRA) on future climate is significant, the GRA value is bold (GRA+GHG > σ *i.e.* the impacts of forestation on future climate would exceed the region's natural climate variability).

Variables	**DJF**				**MAM**				**JJA**				**SON**			
	PRS		GHG	GRA	PRS		GHG	GRA	PRS		GHG	GRA	PRS		GHG	GRA
	μ	σ			μ	σ			μ	σ			μ	σ		
Temp (°C)	25.83	0.56	**1.81**	-0.13	23.52	0.79	**2.31**	-0.04	17.77	0.87	**8.06**	-0.02	22.23	1.01	**2.70**	-0.15
Rain (mm mon^{-1})	47.26	42.05	4.08	-2.98	25.46	28.53	-2.22	-1.66	13.93	20.13	9.30	-0.18	25.78	21.96	0.72	-1.89
Q (g kg^{-1})	10.17	0.69	**1.22**	0.02	8.97	0.65	0.59	-0.02	5.95	0.51	3.62	-0.05	7.33	0.49	**0.90**	-0.01
RH (%)	74.78	4.23	0.24	0.46	77.49	3.75	**-4.53**	0.21	76.62	5.36	**-3.67**	-0.06	69.29	4.90	-2.56	0.34
LHF (W m^{-2})	127.00	11.48	2.98	-4.50	81.54	5.26	-2.85	**-4.31**	45.53	4.54	**33.16**	-2.61	93.41	7.46	-1.06	-4.47
RSDS (W m^{-2})	273.80	20.28	-3.17	2.77	171.50	14.32	3.00	1.44	131.50	9.38	**43.05**	0.17	257.70	10.84	0.58	1.61
RSS (W m^{-2})	261.10	12.51	-1.73	-5.66	164.60	8.62	0.79	-3.21	123.10	4.99	**42.32**	-1.83	236.10	6.00	-0.16	-4.57
ALBEDO	0.10	0.01	0.00	0.01	0.10	0.00	0.00	**0.01**	0.10	0.01	0.00	0.00	0.10	0.00	0.00	0.00
SHF (W m^{-2})	59.16	12.06	-1.32	0.57	11.31	6.61	2.72	1.55	-2.17	2.86	**16.19**	1.10	53.32	6.41	2.41	1.37
DRAG	0.08	0.10	0.00	**0.07**	0.03	0.03	0.00	0.02	0.02	0.03	0.01	0.00	0.94	0.45	-0.23	-0.21
WIND (m s^{-1})	0.97	0.53	0.03	-0.26	1.77	0.48	0.19	-0.41	3.76	1.05	**-1.79**	-0.51	0.76	0.83	0.22	-0.19
MRSO (kg m-2)	24.80	1.83	0.22	-0.83	24.93	1.75	**-1.93**	-0.77	23.91	3.11	-0.91	-0.11	22.14	2.17	-0.66	-0.93
PBL (m)	922.70	81.56	-9.78	-43.71	617.10	64.74	40.81	-17.81	594.50	44.51	**63.43**	-6.56	950.70	53.77	29.36	-40.22
BOWEN RATIO	0.55	0.24	-0.03	**868.70**	0.12	0.10	0.04	**640.00**	-0.07	0.07	0.23	**615.40**	0.60	0.16	0.05	**939.20**

Table 6-4 Same as Table 6-3, but for WRF simulation.

Variables	**DJF**				**MAM**				**JJA**				**SON**			
	PRS		GHG	GRA	PRS		GHG	GRA	PRS		GHG	GRA	PRS		GHG	GRA
	μ	σ			μ	σ			μ	σ			μ	σ		
Temp (°C)	18.14	0.70	**1.61**	0.05	13.86	0.88	**1.55**	0.07	7.72	0.58	**7.69**	-0.01	14.18	0.93	**1.37**	-0.02
Rain (mm mon^{-1})	100.30	30.08	-8.55	10.09	57.67	27.76	10.65	-2.03	32.26	9.87	**36.06**	0.26	59.80	15.26	0.58	-0.90
Q (g kg^{-1})	8.52	0.56	**0.78**	0.14	7.11	0.61	**0.83**	0.07	4.66	0.33	**3.27**	0.01	5.81	0.39	**0.55**	0.00
RH (%)	0.65	0.08	-0.02	-0.01	0.67	0.075	0.00	0.00	0.67	0.062	0.00	0.00	0.57	0.065	0.00	0.00
LHF (W m^{-2})	81.06	8.27	-0.21	-0.11	47.29	6.32	1.94	0.17	24.74	3.08	**24.49**	-0.10	55.04	5.21	2.89	-0.45
RSS (W m^{-2})	264.30	9.63	0.24	-4.06	157.20	8.18	-2.18	-0.05	108.10	3.91	**46.94**	-0.31	224.20	6.86	1.15	-0.53
ALBEDO	0.20	0.00	0.00	0.00	0.20	0.00	0.00	0.00	0.23	0.00	**-0.03**	0.00	0.22	0.00	0.00	0.00
SHF (W m^{-2})	82.30	8.87	0.54	-1.52	32.25	5.78	-1.84	0.33	11.07	2.49	**19.35**	0.22	67.55	5.51	-1.93	0.53
WIND (m s^{-1})	1.43	1.18	0.93	0.17	11.26	2.40	-1.11	0.27	44.44	11.45	**-34.29**	-0.12	9.13	8.60	-2.38	-0.01
PBL (m)	714.20	43.27	-5.72	-7.09	519.10	28.09	-17.87	2.84	496.00	41.00	5.20	1.76	693.50	35.07	-27.18	3.55
BOWEN RATIO	1.04	0.26	0.01	-0.02	0.67	0.24	-0.08	0.01	0.48	0.20	0.12	0.02	1.24	0.37	-0.09	0.02

effect, the decrease in the net solar radiation decreases the latent heat flux. This is consistent with the decrease in surface moisture and rainfall in each season. With the dynamic-effect, the decrease in temperature and in surface friction induced by the grass cover encourages divergence, subsidence and anti-cyclonic flow over the grass covered area, thereby producing less rain (Figure 6-2, Table 6-3). This is supported by the increase in surface pressure and decrease in boundary layer height. However, while the dynamic-effect increases the rainfall in all seasons, the albedo-effect only contributes to the rainfall increase in DJF, MAM and SON. That explains why the rainfall increase is higher during DJF, MAM and SON than in other seasons (JJA).

The changes to grass cover are also consistent with the findings of Hoffmann and Jackson (2000), finding that the conversion of tropical savanna regions (trees and grasses) to open grassland reduced precipitation by approximately 10%. However, the change in vegetation prescribed by Hoffmann and Jackson (2000) increased surface air temperature, due to the reduction in surface roughness length, while the present study found a decrease in temperature. The impact of changes to grass cover contrast with the findings of New *et al.* (2003) and Cook *et al.* (2006), which found that increases in the amount of soil moisture resulted in increased atmospheric stability and enhanced divergence at the surface, favouring against conditions conducive to rainfall formation over Southern Africa. More specifically, the increase in latent and the decrease in sensible heat increased the near surface pressure at the height of the boundary layer. The authors noted increased subsidence over the region, leading to a decrease of moisture flow into land from surrounding oceans and reduced cloud cover (*i.e.* through a negative feedback

effect). In the present study, although there is a shift from latent to sensible heat, as one might expect, the decrease in precipitation is also associated with a decrease in soil moisture. The extent of vegetation change in this study is not as extensive as compared to the aforementioned studies, and this may contribute to the differences in results.

6.3 Impacts of vegetation changes compared

The main difference between the scenarios of vegetation changes considered in this study (forestation and expansion of grass cover) is that while forestation produces a local warming effect, the extension of grass cover produces a local cooling effect. Moreover, forestation increases the amount of rainfall, while grass cover decreases rainfall. This is due to the contrasting biogeophysical impacts on local climate that are associated with the structural and functional properties of vegetation. More specifically, although both forestation and the expansion of grass modify the surface energy fluxes and alter the regional atmospheric dynamics, the changes to climate are of opposite sign (Figure 6-3).

These results of vegetation change compare well with those of previous studies. The changes in surface temperature are comparable to the findings of Gibbard *et al.*2005 that investigated the effects of global land cover change using a general circulation model. Their study found that replacement of current vegetation with trees would lead to a global mean warming (of 1.3°C), while replacement by grassland would result in cooling (of 0.4°C). The replacement of current vegetation in the present study resulted in similar changes. The vegetation change prescribed by Gibbard *et al.* 2005 was more extensive than the changes applied in this study, however, and considering the limited area of

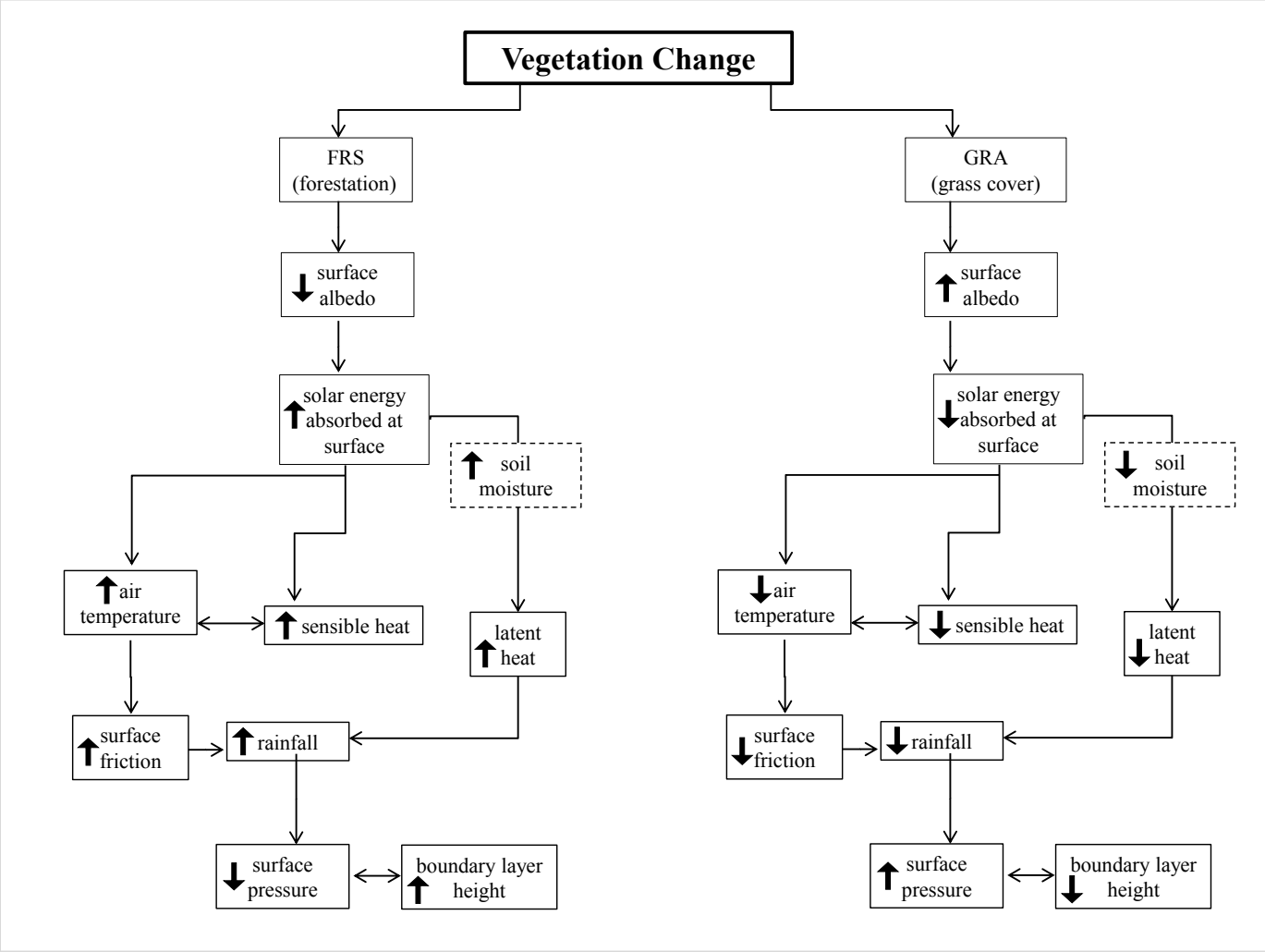

Figure 6-3 Conceptual model of the biogeophysical impacts of vegetation change scenarios (forestation and expansion of grass cover) on local climate in Southern Africa (up or down arrow indicates increase or decrease in a variable, respectively; dashed line for soil moisture represents a limiting factor)

vegetation change in the present study, temperature and rainfall changes are, as expected, of a different magnitude. The regional atmospheric response to vegetation change in this study is also consistent with the findings of Mackellar *et al.* (2008; 2010). Their study over Southern Africa found that a shift from pristine natural state to the present distribution vegetation would increase in surface albedo, induce a cooling effect near the surface, and increase subsidence over the region. As the subsidence increased, moisture convergence reduced and rainfall also decreased in the area. In this study, forestation produces opposite changes, but the expansion of grass cover produces comparable changes, to those in Mackellar *et al.* (2008). More specifically, the decrease in albedo due to forestation induces convergence, while the increase in albedo due to grass cover induces subsidence. It is worth mentioning, however, that Mackellar *et al.* (2008) also found a negative feedback response in this cycle — such that the effect of the initial cooling reduced with time and the decrease in evaporation and latent heat at the surface favoured an increase in surface temperature. However, in contrast, a similar mechanism did not appear to contribute to the changes in temperature observed in the present study.

In agreement with several other global (*e.g.* Chase *et al.*, 2000; Swann *et al.,* 2011; Zhao *et al.,* 2001;) and regional (*e.g.* Abiodun *et al.,* 2013; Gálos *et al.,* 2011) modeling studies, the findings of this study also suggest that the impacts of forestation and the impacts of grass cover change are not limited to the area of vegetation change. Rather, through influence on atmospheric circulation, the changes to vegetation remotely modify the projected regional climatology.

7 Potential impacts of climate and vegetation changes on drought

In this chapter the potential impacts of vegetation change on drought are discussed. The chapter describes the future occurrence of drought due to elevated greenhouse gasses and a description of the potential impacts of the vegetation changes (*i.e.* forestation (FRS – GHG) and grass cover (GRA – GHG)) on drought in the future.

The projected future changes in temperature and rainfall (Figure 6-1, Figure 6-2) caused by the elevated GHG and vegetation change will influence the characteristics of Southern African droughts. In the present day climate (PRS), the RCMs models agree with CRU observation that the drought frequency over Southern Africa ranges from 6-8 events/decade (Figure 7-1a and Figure 7-1b). With the elevated GHG, both models project a future increase in drought frequency and the spatial distributions of the increase are similar in both the models (Figure 7-1c and Figure 7-1d). However, the magnitudes of the increase are generally larger in RegCM than in WRF. For instance, the highest increases, which occur over Namibia, northern Botswana, and northern Mozambique, are about 60-80 events/decade in RegCM, but about 20-40 events/decade in WRF. The lowest increase, which is confined to the southeastern margin of Southern Africa, is about 40 events / decade in RegCM, but 10 events / decade in WRF. The larger increase in drought frequency produced by RegCM (when compared to that of WRF) is consistent with its projection of larger warming and drying in the future.

With forestation (FRS) changes, the spatial distribution of projected drought frequency differs between models (Figure 7-1e and Figure 7-1f). For instance, RegCM (WRF) shows that the forestation increases (decreases) the drought frequency by about 5 events/ decade over much of the forested areas and over South Africa. However, both RCMs agree that although the forestation could increase the occurrence over Congo and the south-central edge of South Africa (about 3 events/decade), it could also decrease the drought frequency over parts of Botswana, northern Namibia, and Mozambique (about four events/decade). The impacts on drought frequency due to forestation for WRF are consistent with those of Gálos *et al.* (2011), where forestation reduced the total number of drought events over northeastern Hungary, but the impacts on drought frequency for RegCM are in line with those of Abiodun *et al.* (2013), where forestation enhanced the occurrence of droughts over northeastern Nigeria.

For grass cover (GRA) changes, the spatial distribution of the projected changes in drought frequency again differs between the RCMs (Figure 7-1g and Figure 7-1h). RegCM (WRF) shows that the grass cover increases (decreases) the drought frequency by about 3 events/decade over much of the region of grass cover change and over many South Africa. Both RCMs suggest that grass cover change could decrease drought frequency over the western and northeastern regions of South Africa. However, for Botswana WRF shows a large decrease in drought frequency (-5 events/decade), but RegCM shows changes of the opposite sign.

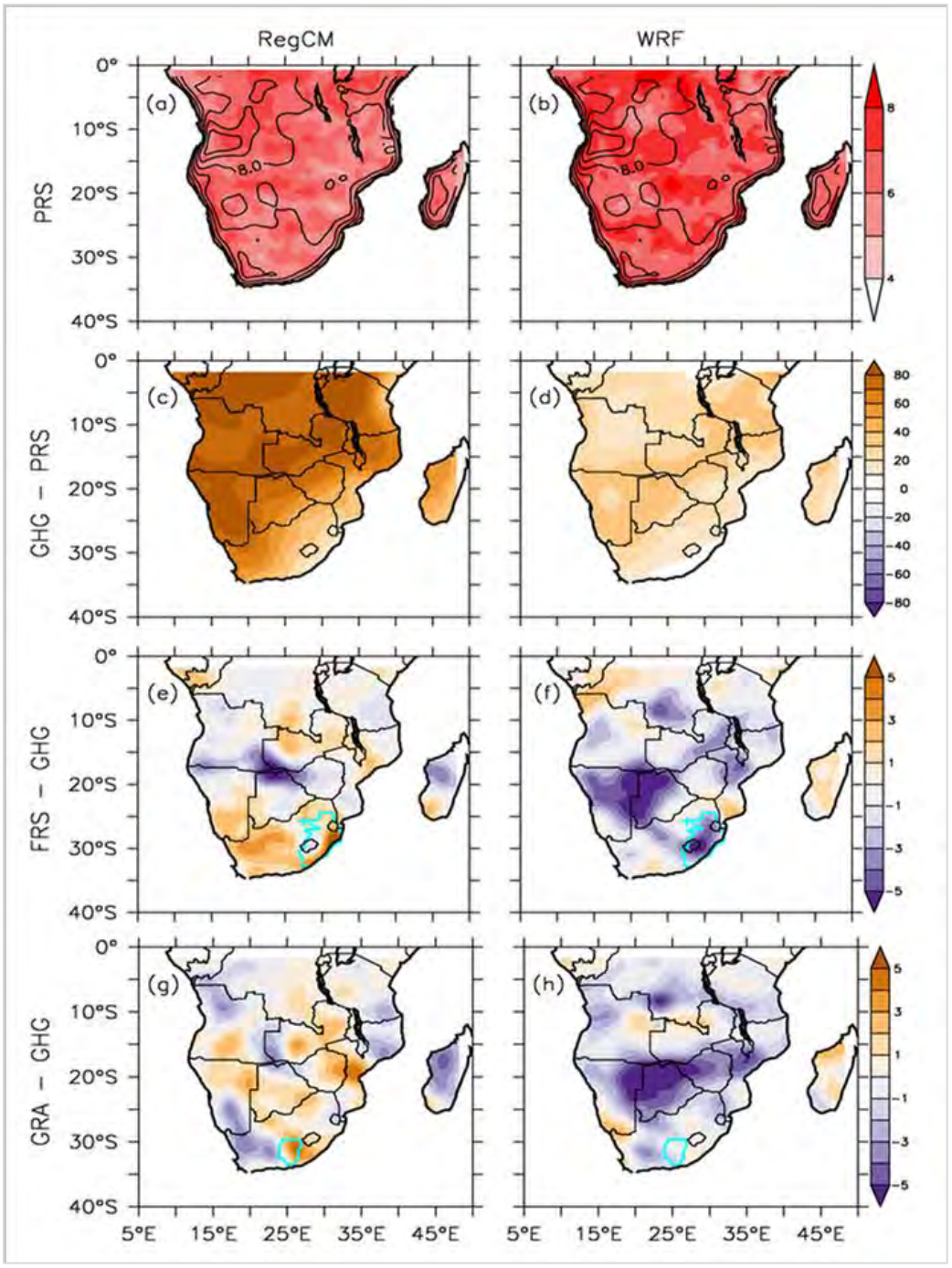

Figure 7-1 The potential impacts on drought frequency (*i.e.* number of months with 3-months SPEI < 1.5 per decade) over Southern Africa, for the present-day values (PRS; the simulations (RegCM and WRF) values are shaded while the observed values are in contours), the impact of the elevated greenhouse gases (GHG minus PRS), the impact of the forestation (FRS minus GHG; the forested area is enclosed with blue line) and the impact of the grass cover (GRA minus GHG; the area of grass cover is enclosed with blue line).

8 Conclusion

8.1 Summary

This study has applied two RCMs (RegCM and WRF) to investigate the potential impacts of vegetation change on future climate in Southern Africa. Forced with GCM simulations, the RCMs were used in four experiments: PRS (present day climate), GHG (future climate without forestation), FRS (future climate with forestation), and GRA (future climate with grass cover changes). The study first evaluated the performance of the RCMs (using PRS) and then presented the projected future changes (GHG minus PRS) before discussing the potential impacts of two scenarios of vegetation change; forestation (FRS minus GHG) and grass cover (GRA minus GHG). In the context of this dissertation‘s objectives, the findings of the study can be summarized as follows:

- Both models (RegCM forced with HAD and WRF forced with MPI) give a realistic simulation of the essential features of the Southern African climate, but with some biases. Both RCMs provide added value over Southern Africa, but the performance of each varies with the location and season. The maximum bias in the temperature field (about 2^{o}C in RegCM and about 4^{o}C in WRF) occurs over the southwest of South Africa in summer, while the maximum bias in the rainfall field (about 75 mm/mon in RegCM and about 50 mm/mon in WRF) occurs over Zimbabwe in summer.

- The RCMs project warming over the entire subcontinent in all seasons and in both models the maximum warming occurs over the southwest of South Africa, but with RegCM the maximum warming occurs in SON (3.2°C), and with WRF it also occurs in DJF and MAM (2.0^{o}C). In summer, RegCM projects drier summer conditions over Mozambique in the future while WRF projects wetter summer conditions over the same region.

- Forestation enhances the projected warming and increases rainfall over the forested area. The darker forest (relative to pre-existing vegetation cover) decreases the surface albedo and increases the amount of solar radiation absorbed at the surface. This extra energy in the system increases the amount of sensible and latent heat, which increases temperature and rainfall, respectively.

- The expansion of grass cover reduces the projected warming and decreases rainfall over the grass covered area. The lighter surface of the grass (relative to pre-existing vegetation cover) increases the surface albedo and decreases the amount of solar radiation absorbed at the surface. This extra energy in the system decreases the amount of sensible and latent heat, and decreases the temperature. This favours conditions conducive to subsidence and a reduction in rainfall.

- Thus, forestation and the expansion of grass modify the surface energy fluxes and alter the regional atmospheric dynamics, but the changes to climate are of opposite sign. Both the vegetation changes induce local (and regional) changes

to temperature and rainfall due to their influences on the surface albedo-effect and atmospheric dynamics.

- The RCMs project that elevated GHG could increase drought frequency over Southern Africa in the future. Forestation and grass cover changes could alleviate the occurrence of droughts projected over some regions, but may also enhance the frequency of drought over other regions in Southern Africa.

8.2 Recommendations

Information from this research has enhanced our understanding of potential vegetation and climate interactions in the future. However, the results and project outcomes obtained in this study could be made more robust from a more extensive analysis. Further research is required to guide decision-making and natural resource management at national and regional levels. Potential avenues of research are outlined below.

Although model evaluation reflects minor differences in the RCM‘s performance, the climate response to each respective scenario of vegetation change is generally similar. This outcome should be emphasized in light of the fact that the RCMs differ, not only in their hydrostatic dynamics, but more importantly in the land surface scheme and the land cover products. The minor inconsistencies between the RCM simulations that occur may be due, at least in part, to the differences in land cover classification and the spatial representation of vegetation distribution across the region (MacKellar, 2007). Further research may simply analyse the experimental results obtained from the simulations produced in the present study and incorporate new variables related to

the vegetation parameters; such as leaf area index, stomatal resistance and green vegetation fraction *etc.* This would provide valuable insight into the land surface processes and the sensitivity of the RCMs to the changes in vegetation class. Future research could also incorporate a dynamic vegetation option for a more detailed description of land surface (for instance, RegCM could be coupled to the Community Land Model (CLM), rather than BATS), or represent less extreme scenarios of vegetation change (*e.g.* 25% or 50% forestation). Such factors were not investigated in the present study due to time constraints and computational expense.

The divergent responses of the two RCMs with respect of the impacts of forestation and grass-cover expansion on projected drought frequency is noteworthy and should deter against the premature application of these results for policy. In the very least, the results obtained indicate substantial sensitivity of the climate projections to land surface characteristics, and suggest human management of vegetation (land use and land cover change) in these biomes could have the potential for regional climate regulation. Future research may be directed at investigating possible reasons for the divergent response and the sensitivity of the models to the differences observed.

While the time-scales for drought analyses that were selected for this study are typical of preliminary assessments in this field of research, and form a foundational analysis of identifying how vegetation might influence projected climate change in the future, further study may also examine the potential impacts related to different temporal scales; for instance, interannual and intraseasonal climate variability. Alternatively, further study may also incorporate a 1-, 6-, 12-monthly SPEI, another drought index (such as SPI) or examine how changes to vegetation cover might influence future

teleconnections important to the Southern African region, such as ENSO events. Such an analysis was not possible due to time constraints of the study, but the potential for agricultural, economic and environmental damage associated with drought events has obvious implications for Southern Africa and this should reinforce the motivation for such work.

More broadly, the additional consequence of each scenario of vegetation change on the ~~"e~~cosystem services" and aspects of ecological functioning of the biomes have not been incorporated in this study. For example, forestation activities in particular are likely to have a considerable impact on soil moisture, streamflow and thereby, the provision of water resources in the affected catchments. There may also be significant adverse effects on the biodiversity (species richness and abundance) associated with the change in vegetation from previously open grassland and savanna ecosystems to forest. Fire is also an important control in Savanna and Grassland ecosystems and is influenced by the composition and structure of vegetation (and soils). Hence, the scenarios of vegetation changes described in the study could have significant impacts on the occurrence of fire and disturbance regime (intensity, frequency, duration and return interval), which in turn could induce various feedbacks (through the amount of fuel available, greenhouse gas emissions, and aerosols *etc.*) to regional climate. While investigation into these processes (hydrology, biodiversity, fire) is beyond the scope of the present study, future research might consider such factors and the potential synergies that could exist between these processes. This would generate further insight into the complex and non-linear relationship between vegetation changes and climate.

Nevertheless, the results from this study suggest that the impacts of forestation and grass cover changes on regional climate are complex and the vegetation changes may produce unexpected impacts on future climate. While it is important to exercise caution so as not to over-interpret the results, the findings suggests that forestation projects in Southern Africa should not be considered for their carbon storage capabilities alone. Rather, the biogeophysical effects need to be carefully weighed against the biogeochemical benefits (*i.e.* carbon sequestration). The findings of this study reinforce previous studies (*e.g.* Anderson *et al.,* 2011; Thompson *et al.,* 2009) which recognize that forestation may not necessarily provide climatic benefits. These studies call for the introduction of more comprehensive climate metrics to assess the impacts of forestation projects and their implementation in climate mitigation strategies. For a more robust analysis, future avenues of research could employ an RCM with active CO_2 or a comprehensive ESM, for example, to incorporate the biogeochemical effects, and thereby examine whether or not the biogeophysical effects forestation would outweigh the carbon drawdown effects. Similarly, the biogeophysical feedbacks effects from expansion of grass cover along the Nama-karoo Biome and Grassland Biome ecotone may have implications for ecosystem assessments on land cover change. It was shown in this study that the biogeophysical feedbacks associated with changes to grass cover may alter the projected climate change signal, the seasonal cycle and the occurrence of drought. Since these impacts are not typically included in regional ecosystem assessments, it may be that the prediction of biome and micro-biome changes in Southern Africa could be improved by incorporating such factors.

9 References

Abiodun, B.J., Adeyewa, Z.D., Oguntunde, P.G., Salami, A.T., Ajayi, V.O., 2012. Modeling the impacts of reforestation on future climate in West Africa. Theor. Appl. Climatol. 110, 77–96.

Abiodun, B.J., Salami, A.T., Matthew, O.J., Odedokun, S., 2013. Potential impacts of afforestation on climate change and extreme events in Nigeria 277–293.

Acocks, J.P.H., 1988. Veld types of South Africa. Memoirs of the Botanical Survey of South Africa.

Alley, W.M., 1984. The Palmer drought severity index: limitations and assumptions. J. Clim. Appl. Meteorol. 23, 1100–1109.

American Meteorological Society, 2004. Statement on meteorological drought. Bull Amer Meteor Soc 85, 771–773.

Anderson, R.G., Canadell, J.G., Randerson, J.T., Jackson, R.B., Hungate, B. a, Baldocchi, D.D., Ban-Weiss, G. a, Bonan, G.B., Caldeira, K., Cao, L., Diffenbaugh, N.S., Gurney, K.R., Kueppers, L.M., Law, B.E., Luyssaert, S., O'Halloran, T.L., 2011. Biophysical considerations in forestry for climate protection. Front. Ecol. Environ. 9, 174–182.

Araujo, J., Abiodun, B.J., Crespo, O., 2014. Impacts of drought on grape yields in Western Cape, South Africa. Theor. Appl. Climatol.

Archer, E., Engelbrecht, F., Landman, W., Le Roux, A., Van Huyssteen, E., Fatti, C., Vogel, C., Akoon, I., Maserumule, R., Colvin, C., 2010. South African risk and vulnerability atlas. Department of Science and Technology.

Arora, V.K., Montenegro, A., 2011. Small temperature benefits provided by realistic afforestation efforts. Nat. Geosci. 4, 514–518.

Bala G Wickett M, Phillips TJ, Lobell DB, Delire C, Mirin A, C.K., 2007. Combined climate and carbon-cycle effects of large-scale deforestation. Proc. Natl. Acad. Sci. U. S. A. 104, 6550–6555.

Bathiany, S., Claussen, M., Brovkin, V., Raddatz, T., Gayler, V., 2010. Combined biogeophysical and biogeochemical e ff ects of large-scale forest cover changes in the MPI earth system model.

Beerling, D.J., Osborne, C.P., 2006. The origin of the savanna biome. Glob. Chang. Biol. 12, 2023–2031.

Beltrán-Przekurat, A., Pielke Sr, R. a., Eastman, J.L., Coughenour, M.B., 2012. Modelling the effects of land-use/land-cover changes on the near-surface atmosphere in southern South America. Int. J. Climatol. 32, 1206–1225.

Betts, R.A., Falloon, P.D., Klein, K., Ramankutty, N., 2007. Biogeophysical effects of land use on climate: Model simulations of radiative forcing and large-scale temperature change 142, 216–233.

Bhaktawar, N., Van Niekerk, L., 2012. South Africa Yearbook 2012/13. Government Communication and Information System (GCIS).

Boko, M., I. Niang, A. Nyong, C. Vogel, A. Githeko, M. Medany, B. Osman-Elasha, R.T. and P.Y., 2007. Africa. Climate Change 2007: Impacts, Adaptation and Vulnerability. Contribution of Working Group II to the Fourth Assessment Report of the Intergovernmental Panel on Climate Change Cambridge, 433–467.

Bonan, G.B., 2008. Forests and climate change: forcings, feedbacks, and the climate benefits of forests. Science 320, 1444–9.

Bond, W.J., Midgley, G.F., 2012. Carbon dioxide and the uneasy interactions of trees and savannah grasses. Philos. Trans. R. Soc. B Biol. Sci. 367, 601–612.

Bond, W.J., Midgley, G.F., Woodward, F.I., 2003. What controls South African vegetation-climate or fire? South African J. Bot. 69, 79–91.

Bond, W.J., Woodward, F.I., Midgley, G.F., 2005. The global distribution of ecosystems in a world without fire. New Phytol. 165, 525–37.

Boulard, D., Pohl, B., Crétat, J., Vigaud, N., Pham-Xuan, T., 2013. Downscaling large-scale climate variability using a regional climate model: the case of ENSO over Southern Africa. Clim. Dyn. 40, 1141–1168.

Bowman, D.M.J.S., Murphy, B.P., Banfai, D.S., 2010. Has global environmental change caused monsoon rainforests to expand in the Australian monsoon tropics? Landsc. Ecol. 25, 1247–1260.

Breman, E., Gillson, L., Willis, K., 2012. How fire and climate shaped grass-dominated vegetation and forest mosaics in northern South Africa during past millennia. The Holocene 22, 1427–1439.

Bryant, R.G., Bigg, G.R., Mahowald, N.M., Eckardt, F.D., Ross, S.G., 2007. Dust emission response to climate in southern Africa. J. Geophys. Res. Atmos. 112, D09207.

Buitenwerf, R., Bond, W.J., Stevens, N., Trollope, W.S.W., 2012. Increased tree densities in South African savannas: >50 years of data suggests CO_2 as a driver. Glob. Chang. Biol. 18, 675–684.

Canadell, J.G., Raupach, M.R., 2008. Managing forests for climate change mitigation. Science 320, 1456–7.

Charney, J., Quirk, W.J., Chow, S.-H., Kornfield, J., 1977. A comparative study of the effects of albedo change on drought in semi-arid regions. J. Atmos. Sci. 34, 1366–1385.

Chase, T.N., Pielke Sr, R.A., Kittel, T.G.F., Nemani, R.R., Running, S.W., 2000. Simulated impacts of historical land cover changes on global climate in northern winter. Clim. Dyn. 16, 93–105.

Chen, F., 2012. The Noah Land Surface Model in WRF A short tutorial. In: Proc. of Land Surface Modeling Group Meeting. Web.

Chen, G.-S., Notaro, M., Liu, Z., Liu, Y., 2012. Simulated Local and Remote Biophysical Effects of Afforestation over the Southeast United States in Boreal Summer. J. Clim. 25, 4511–4522.

Chikoore, H., 2005. Vegetation feedback on the boundary layer climate of Southern Africa, Thesis for. ed. University of Zululand (South Africa).

Chishakwe, N.E., 2010. Southern Africa Sub-Regional Framework on Climate Change Programmes Report (1st Draft, working document).

Christensen, J.H., Hewitson, B., Busuioc, A., Chen, A., Gao, X., Held, R., Jones, R., Kolli, R.K., Kwon, W.K., Laprise, R., 2007. Regional climate projections. Clim. Chang. 2007 Phys. Sci. Basis. Contrib. Work. Gr. I to Fourth Assess. Rep. Intergov. Panel Clim. Chang. Univ. Press. Cambridge, Chapter 11 847–940.

Claussen, M., Brovkin, V., Ganopolski, A., 2001. Biogeophysical versus biogeochemical feedbacks of large-scale land cover change. Geophys. Res. Lett. 28, 1011–1014.

Compo, G.P., Whitaker, J.S., Sardeshmukh, P.D., 2006. Feasibility of a 100-Year Reanalysis Using Only Surface Pressure Data. Bull. Am. Meteorol. Soc. 87, 175–190.

Compo, G.P., Whitaker, J.S., Sardeshmukh, P.D., Matsui, N., Allan, R.J., Yin, X., Gleason, B.E., Vose, R.S., Rutledge, G., Bessemoulin, P., Bronnimann, S., Brunet, M., Crouthamel, R.I., Grant, A.N., Groisman, P.Y., Jones, P.D., Kruk, M.C., Kruger, A.C., Marshall, G.J., Maugeri, M., Mok, H.Y., Nordli, O., Ross, T.F., Trigo, R.M., Wang, X.L., Woodruff, S.D., Worley, S.J., 2009. NOAA CIRES Twentieth Century Global Reanalysis Version 2.

Compo, G.P., Whitaker, J.S., Sardeshmukh, P.D., Matsui, N., Allan, R.J., Yin, X., Gleason, B.E., Vose, R.S., Rutledge, G., Bessemoulin, P., Brönnimann, S., Brunet, M., Crouthamel, R.I., Grant, A.N., Groisman, P.Y., Jones, P.D., Kruk, M.C., Kruger, A.C., Marshall, G.J., Maugeri, M., Mok, H.Y., Nordli, Ø., Ross, T.F., Trigo, R.M., Wang, X.L., Woodruff, S.D., Worley, S.J., 2011. The Twentieth Century Reanalysis Project. Q. J. R. Meteorol. Soc. 137, 1–28.

Cook, B.I., Bonan, G.B., Levis, S., 2006. Soil Moisture Feedbacks to Precipitation in Southern Africa. J. Clim. 19, 4198–4206.

Cooper, P.J.M., Dimes, J., Rao, K.P.C., Shapiro, B., Shiferaw, B., Twomlow, S., 2008. Coping better with current climatic variability in the rain-fed farming systems of sub-Saharan Africa: An essential first step in adapting to future climate change? Agric. Ecosyst. Environ. 126, 24–35.

CORDEX, 2015. Coordinated Regional Climate Downscaling Experiment. Available at: http://wcrp-cordex.ipsl.jussieu.fr/.

Crétat, J., Macron, C., Pohl, B., Richard, Y., 2011. Quantifying internal variability in a regional climate model: a case study for Southern Africa. Clim. Dyn. 37, 1335–1356.

Crétat, J., Pohl, B., 2012. How physical parameterizations can modulate internal variability in a regional climate model. J. Atmos. Sci. 69, 714–724.

Di Luca, A., de Elía, R., Laprise, R., 2012. Potential for added value in precipitation simulated by high-resolution nested Regional Climate Models and observations. Clim. Dyn. 38, 1229–1247.

Di Luca, A., de Elía, R., Laprise, R., 2013. Potential for small scale added value of RCM‘s downscaled climate change signal. Clim. Dyn. 40, 601–618.

Dickinson, R.E., Henderson-Sellers, A., Kennedy, P.J., 1993. Biosphere– atmosphere transfer scheme (BATS) version 1 as coupled to the NCAR Community Climate Model. 72.

Drew, G., 2004. Modelling vegetation dynamics and their feedbacks over southern Africa in response to climate change forcing.

Dudhia, J., 1989. Numerical Study of Convection Observed during the Winter Monsoon Experiment Using a Mesoscale Two-Dimensional Model. J. Atmos. Sci. 46, 3077–3107.

DWAF, 2007. Department of Water Affairs and Forestry, Eastern Cape Forestry Sector Profile.

Ehleringer, J.R., Cerling, T.E., Helliker, B.R., 1997. C4 photosynthesis, atmospheric CO_2 , and climate. Oecologia 112, 285–299.

Ehleringer, J.R., Cerling, T.E., Munn, T., 2002. C3 and C4 Photosynthesis. Edited by Professor Harold A Mooney and Dr Josep G Canadell C3 and C4 Photosynthesis 2, 186–190.

Elguindi, N., Bi, X., Giorgi, F., Nagarajan, B., Pal, J., Solmon, F., Rauscher, S., Zakey, A., Giuliani, G., 2011. Regional climatic model RegCM user manual version 4.1. ITCP, Trieste, Italy.

Ellery, W. N., Scholes, R. J., and Mentis, M.T., 1991. An Initial approach to predicting the sensitivity of the South African Grassland biome to climate change. S. Afr. J. Sci. 87, 499–503.

Emanuel, K.A., 1991. A Scheme for Representing Cumulus Convection in Large-Scale Models. J. Atmos. Sci. 48, 2313–2329.

Engelbrecht, F.A., Landman, W.A., Engelbrecht, C.J., Landman, S., Bopape, M.M., Roux, B., 2011. Multi-scale climate modelling over Southern Africa using a variable-resolution global model 37.

Engelbrecht, F.A., Mcgregor, J.L., Engelbrecht, C.J., 2009. Dynamics of the Conformal-Cubic Atmospheric Model projected climate-change signal over southern Africa 1033, 1013–1033.

ESLR, 2015. Earth System Research Laboratory Physical Sciences Division. National Oceanic and Atmospheric Administration. Available at: http://www.esrl.noaa.gov/psd/ [Accessed February 5, 2015].

Feser, F., Rockel, B., von Storch, H., Winterfeldt, J., Zahn, M., 2011. Regional climate models add value to global model data: a review and selected examples. Bull. Am. Meteorol. Soc. 92, 1181–1192.

Field, C.B., 2012. Glossary of terms in: Managing the risks of extreme events and disasters to advance climate change adaptation: special report of the intergovernmental panel on climate change. Cambridge University Press.

GADM, 2015. Global Administrative Areas database. Boundaries without limits. Available at: http://gadm.org/ [Accessed February 5, 2015].

Gálos, B., Mátyás, C., Jacob, D., 2011. Regional characteristics of climate change altering effects of afforestation. Environ. Res. Lett. 6, 044010.

Gibbard, S., Caldeira, K., Bala, G., Phillips, T.J., Wickett, M., 2005. Climate effects of global land cover change. Geophys. Res. Lett. 32, L23705.

Giorgi, F., Coppola, E., Solmon, F., Mariotti, L., Sylla, M., Bi, X., Elguindi, N., Diro, G., Nair, V., Giuliani, G., Turuncoglu, U., Cozzini, S., Güttler, I., O'Brien, T., Tawfik, A., Shalaby, a, Zakey, A., Steiner, A., Stordal, F., Sloan, L., Brankovic, C., 2012. RegCM4: model description and preliminary tests over multiple CORDEX domains. Clim. Res. 52, 7–29.

Giorgi, F., Jones, C., Asrar, G.R., 2009. Addressing climate information needs at the regional level: the CORDEX framework. World Meteorol. Organ. Bull. 58, 175.

Giorgi, F., Mearns, L.O., 1991. Approaches to the simulation of regional climate change: a review. Rev. Geophys. 29, 191–216.

Gush, M.B., Scott, D.F., Jewitt, G.P.W., Schulze, R.E., Hallowes, L.A., 2002. A new approach to modelling streamflow reductions resulting from commercial afforestation in South Africa A new approach to modelling streamflow reductions resulting from commercial afforestation in South Africa. South African For. J. 196, 27–36.

Haensler, A., Hagemann, S., Jacob, D., 2011a. Dynamical downscaling of ERA40 reanalysis data over southern Africa : added value in the simulation of the seasonal rainfall characteristics 2349, 2338–2349.

Haensler, A., Hagemann, S. and Jacob, D., 2011b. The role of the simulation setup in a long-term high-resolution climate change projection for the southern African region. Theor. Appl. Climatol. 106, 153–169.

Hansingo, K., Reason, C.J.C., 2008. Modelling the atmospheric response to SST dipole patterns in the South Indian Ocean with a regional climate model. Meteorol. Atmos. Phys. 100, 37–52.

Harris, I., Jones, P.D., Osborn, T.J., Lister, D.H., 2014. Updated high-resolution grids of monthly climatic observations – the CRU TS3.10 Dataset. Int. J. Climatol. 34, 623–642.

Hewitson, B.C., Crane, R.G., 2006. Consensus between GCM climate change projections with empirical downscaling: precipitation downscaling over South Africa. Int. J. Climatol. 26, 1315–1337.

Higgins, S.I., Scheiter, S., 2012. Atmospheric CO_2 forces abrupt vegetation shifts locally, but not globally. Nature 488, 209–12.

Hoffman, M.T., Cowling, R.M., 1990. Vegetation change in the semi-arid eastern Karoo over the last 200 years: an expanding Karoo-fact or fiction? S. Afr. J. Sci. 86, 286–294.

Hoffman, T., Ashwell, A., 2001. Nature divided: land degradation in South Africa. University of Cape Town Press.

Hoffman, T., Todd, S., Ntshona, Z., Turner, S., 1999. Land Degradation in South Africa.

Hoffmann, W.A., Jackson, R.B., 2000. Vegetation-climate feedbacks in the conversion of tropical savanna to grassland. J. Clim. 13, 1593–1602.

Holtslag, A.A.M., De Bruijn, E.I.F., Pan, H.-L., 1990. A High Resolution Air Mass Transformation Model for Short-Range Weather Forecasting. Mon. Weather Rev. 118, 1561–1575.

Hong Dudhia, Jimy, Chen, Shu-Hua, S.-Y., 2004. A Revised Approach to Ice Microphysical Processes for the Bulk Parameterization of Clouds and Precipitation. Mon. Weather Rev. 132, 103–120.

Hong, S.-Y., Noh, Y., Dudhia, J., 2006. A New Vertical Diffusion Package with an Explicit Treatment of Entrainment Processes. Mon. Weather Rev. 134, 2318–2341.

Houspanossian, J., Nosetto, M., Jobbágy, E.G., 2013. Radiation budget changes with dry forest clearing in temperate Argentina. Glob. Chang. Biol. 19, 1211–22.

Hudson, D.A. and R.G.J., Jones, R.G., 2002. Regional climate model simulations of Present-dat and future climates of Southern Africa. London Road, Bracknell, RG12 2SY, U.K.

Hurry, L., Van Heerden, J., 1982. Southern Africa‘s weather patterns : a guide to the interpretation of synoptic maps. Via Afrika, Goodwood.

ICTP, 2014. The Abdus Salam International Centre for Theoretical Physics. Available at: http://www.ictp.it/research/esp/models/regcm4.aspx [Accessed September 13, 2014].

Joubert, A.M., Katzfey, J.J., Mcgregor, J.L., Nguyen, K.C., 1999. Simulating midsummer climate over southern Africa using a nested regional climate model analyses 104, 15–19.

Kain, J.S., 2004. The Kain–Fritsch Convective Parameterization: An Update. J. Appl. Meteorol. 43, 170–181.

Kalognomou, E.-A., Lennard, C., Shongwe, M., Pinto, I., Favre, A., Kent, M., Hewitson, B., Dosio, A., Nikulin, G., Panitz, H.-J., Büchner, M., 2013. A Diagnostic Evaluation of Precipitation in CORDEX Models over Southern Africa. J. Clim. 26, 9477–9506.

Kandji, S.T., Verchot, L., Mackensen, J., 2006. Climate change and variability in Southern Africa: impacts and adaptation in the agricultural sector. World Agroforestry Centre.

Kgatuke, M.M., Landman, W.A., Beraki, A., Mbedzi, M.P., 2008. The internal variability of the RegCM3 over South Africa 520, 505–520.

Kiehl, Jeffrey T., James J. Hack, Gordon B. Bonan, Byron A. Boville, and B.P.B., 1996. Description of the NCAR Community Climate Model (CCM3). Technical Note. Clim. Glob. Dyn. Div.

Kjellström, E., Nikulin, G., Gbobaniyi, E., Jones, C., 2013. Future changes in African temperature and precipitation in an ensemble of Africa-CORDEX regional climate model simulations. In: EGU General Assembly Conference Abstracts. p. 4703.

Kruger, A.C., Shongwe, S., 2004. Temperature trends in South Africa: 1960–2003. Int. J. Climatol. 24, 1929–1945.

Kruger, A.C., South African Weather Service, 2004a. Climate of South Africa: Climate controls. Pretoria: South African Weather Service.

Kruger, A.C., South African Weather Service, 2004b. Climate of South Africa - Climate Regions. Pretoria: South African Weather Service.

Laprise, R., 2008. Regional climate modelling. J. Comput. Phys. 227, 3641–3666.

Lennard, C., Kalognoumou, L., 2013. Analysis of the Cordex evaluation runs (ERA_Interim) over Southern Africa. In: EGU General Assembly Conference Abstracts. p. 200.

Lenton, T.M., Vaughan, N.E., 2009. The radiative forcing potential of different climate geoengineering options. Atmos. Chem. Phys. Discuss. 9, 2559–2608.

Li, J., Pósfai, M., Hobbs, P. V, Buseck, P.R., 2003. Individual aerosol particles from biomass burning in southern Africa: 2, Compositions and aging of inorganic particles. J. Geophys. Res. Atmos. 108, 8484.

Low, A.B., 1998. Vegetation of South Africa, Lesotho and Swaziland: a companion to the vegetation map of South Africa, Lesotho and Swaziland. Department of Environmental Affairs & Tourism.

MacKellar, N., New, M., Jack, C., 2014. Observed and modelled trends in rainfall and temperature for South Africa: 1960-2010. S. Afr. J. Sci. 110, 51–63.

MacKellar, N., Tadross, M., Hewitson, B., 2010. Synoptic-based evaluation of climatic response to vegetation change over southern Africa. Int. J. Climatol. 30, 774–789.

MacKellar, N.C., 2007. Simulating the effects of land-surface change on southern Africa‘s climate. University of Cape Town.

Mackellar, N.C., Tadross, M.A., Hewitson, B.C., 2008. Effects of vegetation map change in MM5 simulations of southern Africa‘s summer climate. Int. J. Climatol.

Mahmood, R., Pielke, R.A., Hubbard, K.G., Niyogi, D., Dirmeyer, P.A., McAlpine, C., Carleton, A.M., Hale, R., Gameda, S., Beltrán- Przekurat, A., 2014. Land cover changes and their biogeophysical effects on climate. Int. J. Climatol. 34, 929–953.

Marsland, S.J., Haak, H., Jungclaus, J.H., Latif, M., Röske, F., 2003. The Max-Planck-Institute global ocean/sea ice model with orthogonal curvilinear coordinates. Ocean Model. 5, 91–127.

Martin G. M., Bellouin, N., Collins, W.J., Culverwell, I.D., Halloran, P.R., Hardiman, S.C., Hinton, T.J., Jones, C.D., McDonald, R.E., McLaren, A.J., O‘Connor, F.M., Roberts, M.J., Rodriguez, J.M., Woodward, S., Best, M.J., Brooks, M.E., Brown, A.R., Butchart, N., Dearden, C., Derbyshire, S.H., Dharssi, I., Doutriaux-Boucher, M., Edwards, J.M., Falloon, P.D., Gedney, N., Gray, L.J., Hewitt, H.T., Hobson, M., Huddleston, M.R., Hughes, J., Ineson, S., Ingram, W.J., James, P.M., Johns, T.C., Johnson, C.E., Jones, A., Jones, C.P., Joshi, M.M., Keen, A.B., Liddicoat, S., Lock, A.P., Maidens, A. V, Manners, J.C., Milton, S.F., Rae, J.G.L., Ridley, J.K., Sellar, A., Senior, C.A., Totterdell, I.J., Verhoef, A., Vidale, P.L., Wiltshire, A., 2011. The HadGEM2 family of Met Office Unified Model Climate configurations. Geosci. Model Dev. Discuss. 4, 765–841.

Mason, S., Waylen, P., Mimmack, G., Rajaratnam, B., Harrison, J.M., 1999. Changes in Extreme Rainfall Events in South Africa. Clim. Change 41, 249–257.

Masubelele, M.L., 2012. Understanding the past to conserve the future: Long-term Environmental and Vegetation Change in the Karoo Midlands, South Africa over the 20th Century, Dissertation. University of Cape Town.

Masubelele, M.L., Hoffman, M.T., Bond, W.J., Gambiza, J., 2014. A 50 year study shows grass cover has increased in shrublands of semi-arid South Africa. J. Arid Environ. 104, 43–51.

McGregor, J.L., 1997. Regional climate modelling. Meteorol. Atmos. Phys. 63, 105–117.

McKee, T.B., Doesken, N.J., Kleist, J., 1993. The relationship of drought frequency and duration to time scales. In: Proceedings of the 8th Conference on Applied Climatology. American Meteorological Society Boston, MA, pp. 179–183.

Meque, A., Abiodun, B., 2014. Simulating the link between ENSO and summer drought in Southern Africa using regional climate models. Clim. Dyn. 1–20.

Michalakes, J., Dudhia, J., Gill, D., Henderson, T., Klemp, J., Skamarock, W., Wang, W., 2004. The Weather Research and Forecast Model: Software Architecture and Performance.

Midgley GF, Chapman RA, Mukheibir P, Tadross M, Hewitson B, W.S., Schulze RE, Lumsden T, Horan M, Warburton M, Kgope B, M.B., Knowles A, Abayomi A, Ziervogel G, C.R. and T.A., 2007. Impacts, vulnerability and adaptation in key South African sectors: An input into the Long Term Mitigation Scenarios process, LTMS Input Report 5. Cape Town.

Midgley, G.F., Thuiller, W., 2010. Potential responses of terrestrial biodiversity in Southern Africa to anthropogenic climate change. Reg. Environ. Chang. 11, 127–135.

Mishra, A.K., Singh, V.P., 2010. A review of drought concepts. J. Hydrol. 391, 202–216.

Mitchell, T.D., Jones, P.D., 2005. An improved method of constructing a database of monthly climate observations and associated high- resolution grids. Int. J. Climatol. 25, 693–712.

Mlawer, E.J., Taubman, S.J., Brown, P.D., Iacono, M.J., Clough, S.A., 1997. Radiative transfer for inhomogeneous atmospheres: RRTM, a validated correlated-k model for the longwave. J. Geophys. Res. Atmos. 102, 16663–16682.

Molen, M.K., Hurk, B.J.J.M., Hazeleger, W., 2011. A dampened land use change climate response towards the tropics. Clim. Dyn. 37, 2035–2043.

Mucina, L., Rutherford, M.C., 2006. The vegetation of South Africa, Lesotho and Swaziland. Veg. South Africa, Lesotho Swazil.

Neumann, F.H., Scott, L., Bousman, C.B., Van As, L., 2010. A Holocene sequence of vegetation change at Lake Eteza, coastal KwaZulu-natal, South Africa. Rev. Palaeobot. Palynol. 162, 39–53.

New, M., Washington, R., Jack, C., Hewitson, B., 2003. Sensitivity of southern African climate to soil-moisture. Clivar Exch. 8.

Nikulin, G., Jones, C., Giorgi, F., Asrar, G., Büchner, M., Cerezo-Mota, R., Christensen, O.B., Déqué, M., Fernandez, J., Hänsler, A., 2012. Precipitation climatology in an ensemble of CORDEX-Africa regional climate simulations. J. Clim. 25, 6057–6078.

Ogier, D.B., 2014. Characteristics of inertial gravity waves over Southern Africa as simulated with CAM-EULAG.

Ornstein, L., Aleinov, I., Rind, D., 2009. Irrigated afforestation of the Sahara and Australian Outback to end global warming. Clim. Change 97, 409–437.

Pal, J.S., Small, E.E., Eltahir, E.A.B., 2000. Simulation of regional-scale water and energy budgets: Representation of subgrid cloud and precipitation processes within RegCM. J. Geophys. Res. Atmos. 105, 29579–29594.

Pal, J.S., F. Giorgi, X. Bi, N. Elguindi, F. Solmon, X.J. Gao, R. Francisco, A. Zakey, J. Winter, M. Ashfaq, F. Syed, J. Bell, N. Diffenbaugh, J. Karmacharya, A. Konare, D. Martinez-Castro, R. Porfirio da Rocha, L.S. and A.S., 2007. Regional climate modeling for the developing world: The ICTP RegCM3 and RegCNET. Bull. Am. Meteorol. Soc. 88, 1395–1409.

Palmer, W.C., 1965. Meteorological drought. US Department of Commerce, Weather Bureau Washington, DC, USA.

Pielke, R.A., Marland, G., Betts, R.A., Thomas, N., Eastman, J.L., Niles, J.O., Niyogi, D.S., Running, S.W., 2002. The influence of land-use change and landscape dynamics on the climate system : relevance to climate-change policy beyond the radiative effect of greenhouse gases.

Pinto, I., Lennard, C., Hewitson, B., 2013. Intercomparison of precipitation extremes over southern Africa in CORDEX simulations. In: EGU General Assembly Conference Abstracts. p. 8872.

Pitman, a. J., 2004. Impact of land cover change on the climate of southwest Western Australia. J. Geophys. Res. 109, D18109.

Pohl, B., Rouault, M., Sen, S., 2014. Simulation of the annual and diurnal cycles of rainfall over South Africa by a regional climate model. Clim. Dyn.

Potop, V., 2011. Evolution of drought severity and its impact on corn in the Republic of Moldova. Theor. Appl. Climatol. 105, 469–483.

Quantum, G.I.S., 2011. Development Team, 2012. Quantum GIS Geographic Information System. Open Source Geospatial Foundation Project. URL[http//qgis. osgeo. org].

Ratna, S.B., Ratnam, J. V, Behera, S.K., Ndarana, T., Takahashi, K., Yamagata, T., 2014. Performance assessment of three convective parameterization schemes in WRF for downscaling summer rainfall over South Africa. Clim. Dyn. 42, 2931–2953.

Reason, C.J.C., Rouault, M., 2002. ENSO- like decadal variability and South African rainfall. Geophys. Res. Lett. 29, 11–16.

Richard, Y., Poccard, I., 1998. A statistical study of NDVI sensitivity to seasonal and interannual rainfall variations in Southern Africa. Int. J. Remote Sens. 19, 2907–2920.

Ringrose, S., Chipanshi, a C., Matheson, W., Chanda, R., Motoma, L., Magole, I., Jellema, a, 2002. Climate- and human-induced woody vegetation changes in Botswana and their implications for human adaptation. Environ. Manage. 30, 98–109.

Roques, K.G., O'connor, T.G., Watkinson, A.R., 2001. Dynamics of shrub encroachment in an African savanna: relative influences of fire, herbivory, rainfall and density dependence. J. Appl. Ecol. 38, 268–280.

Rouault, M., Richard, Y., 2003. Intensity and spatial extension of drought in South Africa at different time scales. Water SA 29, 489–500.

Rummukainen, M., 2010. State-of-the-art with Regional Climate Models. Wiley Interdiscip. Rev. Clim. Chang. 1, 82–96.

Rutherford, M.C., Midgley, G.F., Bond, W.J., Powrie, L.W., Musil, C.F., Roberts, R., Allsopp, J., 1999. South African country study on climate change. Pretoria, South Africa, Terr. Plant Divers. Sect. Vulnerability Adapt. Dep. Environ. Aff. Tour.

Rutherford, M.C., Westfall, R.H., 1994. Biomes of southern Africa: an objective categorization. Mem. Bot. Surv. S. Afr.

SADC, 2001. Southern African Development Community. Annual Report 2001-2002.

SADC, 2012. Southern African Development Community. Facts and Figures. Available at: http://www.sadc.int/about-sadc/overview/sadc-facts-figures/ [Accessed February 5, 2015].

Sankaran, M., Hanan, N.P., Scholes, R.J., Ratnam, J., Augustine, D.J., Cade, B.S., Gignoux, J., Higgins, S.I., Le Roux, X., Ludwig, F., Ardo, J., Banyikwa, F.,

Bronn, A., Bucini, G., Caylor, K.K., Coughenour, M.B., Diouf, A., Ekaya, W., Feral, C.J., February, E.C., Frost, P.G.H., Hiernaux, P., Hrabar, H., Metzger, K.L., Prins, H.H.T., Ringrose, S., Sea, W., Tews, J., Worden, J., Zambatis, N., 2005. Determinants of woody cover in African savannas. Nature 438, 846–9.

Scholvin, S., 2014. South Africa‘s Energy Policy: Constrained by Nature and Path Dependency. J. South. Afr. Stud. 40, 185–202.

Shongwe, M.E., Lennard, C., Liebmann, B., Kalognomou, E., Ntsangwane, L., Pinto, I., 2014. An evaluation of CORDEX regional climate models in simulating precipitation over Southern Africa. Atmos. Sci. Lett.

Silva, L.C.R., Sternberg, L., Haridasan, M., Hoffmann, W. a., Miralles-Wilhelm, F., Franco, A.C., 2008. Expansion of gallery forests into central Brazilian savannas. Glob. Chang. Biol. 14, 2108–2118.

Skamarock, W.C., Klemp, J.B., 2008. A time-split nonhydrostatic atmospheric model for weather research and forecasting applications. J. Comput. Phys. 227, 3465–3485.

Skamarock, W.C., Klemp, J.B., Dudhia, J., 2001. Prototypes for the WRF (Weather Research and Forecasting) model. In: Preprints, Ninth Conf. Mesoscale Processes, J11–J15, Amer. Meteorol. Soc., Fort Lauderdale, FL.

Skamarock, W. C., J. B. Klemp, J. Dudhia, D. O. Gill, and D.M.B.C., 2008. A description of the Advanced Research WRF version 3. NCAR Tech. note NCAR/TN/u2013475.

Smith, B., 2014. Land-cover dynamics and feedbacks in RCMs: state-of-the-art, outlook, and lessons learned. In: International Baltic Earth Secretariat Publication No. 3. 21st Century Challenges in Regional Climate Modelling. Lund, Sweden., p. 63.

Solman, S.A., 2013. Regional climate modeling over South America: a review. Adv. Meteorol. 2013.

South Africa Travel, 2015. Southern Domain Online Travel Guides. Available at: http://www.southafrica-travel.net/pages/e_geolog.htm [Accessed February 3, 2015].

South, D.B., Lee, X., Messina, M.G., 2011. Will afforestation in temperate zones warm the Earth ? J. Hortic. For. 3, 195–199.

Swann, A.L., Fung, I.Y., Levis, S., Bonan, G.B., Doney, S.C., 2010. Changes in Arctic vegetation amplify high-latitude warming through the greenhouse effect. Proc. Natl. Acad. Sci. U. S. A. 107, 1295–300.

Swann, A.L.S., Fung, I.Y., Chiang, J.C.H., 2012. Mid-latitude afforestation shifts general circulation and tropical precipitation. Proc. Natl. Acad. Sci. U. S. A. 109, 712–6.

Sylla, M., Giorgi, F., Stordal, F., 2012. Large-scale origins of rainfall and temperature bias in high-resolution simulations over southern Africa. Clim. Res. 52, 193–211.

Sylla, M.B., Coppola, E., Mariotti, L., Giorgi, F., Ruti, P.M., Dell'Aquila, a., Bi, X., 2009. Multiyear simulation of the African climate using a regional climate model (RegCM3) with the high resolution ERA-interim reanalysis. Clim. Dyn. 35, 231–247.

Tadross, M., Jack, C., Hewitson, B., 2005. On RCM-based projections of change in southern African summer climate. Geophys. Res. Lett. 32, L23713.

TDRP, 2015. Transitional Demobilization and Reintegration Program. Regional Economic Communities. SADC: Southern African Development Community. Available at: http://www.tdrp.net/SADC.php [Accessed February 5, 2015].

Tewari, M., F. Chen, W. Wang, J. Dudhia, M. A. LeMone, K. Mitchell, M. Ek, G. Gayno, J. Wegiel, and R. H. Cuenca, 2004. Implementation and verification of the unified NOAH land surface model in the WRF model. 20th Conf. Weather Anal. Forecast. Conf. Numer. Weather Predict. 11–15.

Thompson, M.P., Adams, D., Sessions, J., 2009. Radiative forcing and the optimal rotation age. Ecol. Econ. 68, 2713–2720.

Thomson, A., Calvin, K., Smith, S., Kyle, G.P., Volke, A., Patel, P., Delgado-Arias, S., Bond-Lamberty, B., Wise, M., Clarke, L., Edmonds, J., 2011. RCP4.5: a pathway for stabilization of radiative forcing by 2100. Clim. Change 109, 77–94.

Topfer, K., 2001. What do we know about reducing greenhouse gas emissions? A simplified guide to the IPCC's ―Climate Change 2001 : Mitigation ."

Tozuka, T., Abiodun, B., Engelbrecht, F., 2014. Impacts of convection schemes on simulating tropical-temperate troughs over southern Africa. Clim. Dyn. 42, 433–451.

Trail, M., Tsimpidi, A.P., Liu, P., Tsigaridis, K., Hu, Y., Nenes, A., Stone, B., Russell, A.G., 2013. Potential impact of land use change on future regional climate in the Southeastern US: Reforestation and crop land conversion. J. Geophys. Res. Atmos. 118, 11–577.

Trenberth, K.E., 1992. Climate System Modeling. Cambridge University Press.

Tummon, F., 2011. Direct and semi-direct aerosol effects on the southern African regional climate during the austral winter season.

Tyson, P.D., 1986. Climatic change and variability in southern Africa.

Tyson, P.D., Gatebe, C.K., 2001. The atmosphere, aerosols, trace gases and biogeochemical change in southern Africa: a regional integration: START Regional Syntheses. S. Afr. J. Sci. 97, p–106.

Ujeneza, E., Abiodun, B., 2014. Drought regimes in Southern Africa and how well GCMs simulate them. Clim. Dyn. 1–15.

Unganai, L.S., Kogan, F.N., 1998. Drought monitoring and corn yield estimation in Southern Africa from AVHRR data. Remote Sens. Environ. 63, 219–232.

Usman, M.T., Reason, C.J.C., 2004. Dry spell frequencies and their variability over southern Africa. Clim. Res. 26, 199–211.

Van Rooyen, J., Sigwele, H., 1998. Towards regional food security in southern Africa: a (new) policy framework for the agricultural sector. Food Policy 23, 491–504.

Vicente-Serrano, S.M., Beguería, S., López-Moreno, J.I., 2010. A multiscalar drought index sensitive to global warming: the standardized precipitation evapotranspiration index. J. Clim. 23, 1696–1718.

Vigaud, N., Pohl, B., Crétat, J., 2012. Tropical-temperate interactions over southern Africa simulated by a regional climate model. Clim. Dyn. 39, 2895–2916.

Viterbo, P., 2002. The role of the land surface in the climate system 1–19.

Walker, N.D., 1989. Sea surface temperature-rainfall relationships and associated ocean-atmosphere coupling mechanisms in the southern African region. University of Cape Town.

Wang, Y., Yan, X., Wang, Z., 2014. The biogeophysical effects of extreme afforestation in modeling future climate. Theor. Appl. Climatol. 1–11.

Wang, Y., Yan, X., Wang, Z., 2015. Global warming caused by afforestation in the Southern Hemisphere. Ecol. Indic. 52, 371–378.

Warner, T.T., 2010. Numerical weather and climate prediction. Cambridge University Press.

West, A.G., Midgley, G.F., Bond, W.J., 2012. The reforestation of Africa? S. Afr. J. Sci. 108, 2–4.

Wigley, B.J., Bond, W.J., Hoffman, M.T., 2010. Thicket expansion in a South African savanna under divergent land use: local vs. global drivers? Glob. Chang. Biol. 16, 964–976.

Williams, C.J.R., Kniveton, D.R., 2011. Atmosphere-land surface interactions and their influence on extreme rainfall and potential abrupt climate change over southern Africa. Clim. Change 112, 981–996.

World Bank., 2010. Development and climate change. World Bank, Washington, DC.

Worthington, P., Maluleke, M., 2014. Challenges amid a stagflationary bind. South Africa Q2 14 Q. Perspect. Emerg. Mark. Res.

Yuan, C., Tozuka, T., Landman, W.A., Yamagata, T., 2013. Dynamical seasonal prediction of Southern African summer precipitation. Clim. Dyn. 1–18.

Zhao, K., Jackson, R.B., 2014. Biophysical forcings of land-use changes from potential forestry activities in North America. Ecol. Monogr. 84, 329–353.

Zhao, M., Pitman, A.J., Chase, T., 2001. The impact of land cover change on the atmospheric circulation.

Zinyengere, N., Crespo, O., Hachigonta, S., 2013. Crop response to climate change in southern Africa: A comprehensive review. Glob. Planet. Change 111, 118–126.

9.1 GIS Map References

QGIS, the open source Geographic Information System (Quantum G.I.S., 2011) software program was used to generate the maps presented in Figure 1-1, Figure 1-2, Figure 2-2, Figure 2-3, Figure 2-5, Figure 3-3 and Figure 3-4. Provincial and political boundaries for South Africa and the SADC region were extracted from the Global Administrative Areas and Boundaries database (GADM, 2015). Each figure is adapted from the information and/or map provided by the source cited (see Reference list).

10 Appendix A

Table 10-1: Land Cover/Vegetation classes (in BATS, RegCM) used in the study. (Adapted from: Elguindi *et al.,* 2011)

	Land Cover/Vegetation Class
1	Crop/mixed farming
2	Short grass
3	Evergreen needle leaf tree
4	Deciduous needle leaf tree
5	Deciduous broadleaf tree
6	Evergreen broadleaf tree
7	Tall grass
8	Desert
9	Tundra
10	Irrigated Crop
11	Semi-desert
12	Ice cap/glacier
13	Bog or marsh
14	Inland water
15	Ocean
16	Evergreen shrub
17	Deciduous shrub
18	Mixed Woodland
19	Forest/Field mosaic
20	Water and Land mixture

Table 10-2: Vegetation Parameters for each land cover class (in BATS, RegCM). (Adapted from: Elguindi *et al.,* 2011)

Parameter	Land Cover/Vegetation Type																			
Class	1	2	3	4	5	6	7	8	9	10	11	12	13	14	15	16	17	18	19	20
Max fractional vegetation cover	0.85	0.80	0.80	0.80	0.80	0.90	0.80	0.00	0.60	0.80	0.35	0.00	0.80	0.00	0.00	0.80	0.80	0.80	0.80	0.80
Difference between max fractional vegetation cover land cover at 269 K		0.6	0.1	0.1	0.3	0.5	0.3	0.0	0.2	0.6	0.1	0.0	0.4	0.0	0.0	0.2	0.3	0.2	0.4	0.4
Roughness length (m)	0.08	0.05	1.00	1.00	0.80	2.00	0.10	0.05	0.04	0.06	0.10	0.01	0.03	0.0004	0.0004	0.10	0.10	0.80	0.3	0.3
Displacement height (m)	0.0	0.0	9.0	9.0	0.0	18.0	0.0	0.0	0.0	0.0	0.0	0.0	0.0	0.0	0.0	0.0	0.0	0.0	0.0	0.0
Min stomatal resistance (s/m)	45	60	80	80	120	60	60	200	80	45	150	200	45	200	200	80	120	100	120	120
Max Leaf Area Index	6	2	6	6	6	6	6	0	6	6	6	0	6	0	0	6	6	6	6	6
Min Leaf Area Index	0.5	0.5	5	1	1	5	0.5	0	0.5	0.5	0.5	0	0.5	0	0	5	1	3	0.5	0.5
Stem (dead matter area index)	0.5	4.0	2.0	2.0	2.0	2.0	2.0	0.5	0.5	2.0	2.0	2.0	2.0	2.0	2.0	2.0	2.0	2.0	2.0	2.0
Inverse square root of leaf dimension ($m^{-1/2}$)	10	5	5	5	5	5	5	5	5	5	5	5	5	5	5	5	5	5	5	5
Light sensitivity factor ($m^2\ W^{-1}$)	0.02	0.02	0.06	0.06	0.06	0.06	0.02	0.02	0.02	0.02	0.02	0.02	0.02	0.02	0.02	0.02	0.02	0.06	0.02	0.02
Upper soil layer depth (mm)	100	100	100	100	100	100	100	100	100	100	100	100	100	100	100	100	100	100	100	100
Root zone soil layer depth (mm)	1000	1000	1500	1500	2000	1500	1000	1000	1000	1000	1000	1000	1000	1000	1000	1000	1000	2000	2000	2000
Depth of total soil (mm)	3000	3000	3000	3000	3000	3000	3000	3000	3000	3000	3000	3000	3000	3000	3000	3000	3000	3000	3000	3000
Soil texture type	6	6	6	6	7	8	6	3	6	6	5	12	6	6	6	6	5	6	6	0
Soil colour type	5	3	4	4	4	4	4	1	3	3	2	1	5	5	5	4	3	4	4	0
Vegetation albedo for wavelengths $< 0.7\ \mu$ m	0.10	0.10	0.05	0.05	0.08	0.04	0.08	0.20	0.10	0.08	0.17	0.80	0.06	0.07	0.07	0.05	0.08	0.06	0.06	0.06
Vegetation albedo for wavelengths $> 0.7\ \mu$ m	0.30	0.30	0.23	0.23	0.28	0.20	0.30	0.40	0.30	0.28	0.34	0.60	0.18	0.20	0.20	0.23	0.28	0.24	0.18	0.18

Table 10-3: Land Cover/Vegetation classes (USGS for WRF) used in the study. (Adapted from: Chen 2012)

	Land Cover/Vegetation Class
1	Urban and Built-Up Land
2	Dryland Cropland and Pasture
3	Irrigated Cropland and Pasture
4	Mixed Dryland/Irrigated Cropland and Pasture
5	Cropland/Grassland Mosaic
6	Cropland/Woodland Mosaic
7	Grassland
8	Shrubland
9	Mixed Shrubland/Grassland
10	Savanna
11	Deciduous Broadleaf Forest
12	Deciduous Needle leaf Forest
13	Evergreen Broadleaf Forest
14	Evergreen Needle leaf Forest
15	Mixed Forest
16	Water Bodies
17	Herbaceous Wetland
18	Wooded Wetland
19	Barren and Sparsely Vegetated
20	Herbaceous Tundra
21	Wooded Tundra
22	Mixed Tundra
23	Bare Ground Tundra
24	Snow or Ice

Table 10-4: Vegetation Parameters for each land cover class (in USGS, WRF). (Adapted from: Chen, 2012)

Parameter	Land cover/Vegetation Type																						
Class	1	2	3	4	5	6	7	8	9	10	11	12	13	14	15	16	17	18	19	20	21	22	23	24
Albedo (%)	0.15	0.19	0.15	0.17	0.19	0.19	0.19	0.25	0.23	0.2	0.12	0.11	0.11	0.1	0.12	0.19	0.12	0.12	0.12	0.16	0.16	0.16	0.17	0.7
Roughness Length (m)	1	0.07	0.07	0.07	0.07	0.15	0.08	0.03	0.05	0.86	0.8	0.85	2.65	1.09	0.8	0.001	0.04	0.05	0.01	0.04	0.06	0.05	0.03	0.001
Green vegetation fraction	0.1	0.8	0.8	0.8	0.8	0.8	0.8	0.7	0.7	0.5	0.8	0.7	0.95	0.7	0.8	0	0.6	0.6	0.01	0.6	0.6	0.6	0.3	0
Number of root layers	1	3	3	3	3	3	3	3	3	3	4	4	4	4	4	0	2	2	1	3	3	3	2	1
Stomatal resistance ($s\ m^{-1}$)	200	40	40	40	40	70	40	300	170	70	100	150	150	125	125	100	40	100	999	150	150	150	200	999
Radiation stress function	999	100	100	100	100	65	100	100	100	65	30	30	30	30	30	30	100	30	999	100	100	100	100	999
Vapour pressure deficit	999	36.25	36.25	36.25	36.25	44.14	36.35	42	39.18	54.53	54.53	47.35	41.69	47.35	51.93	51.75	60	51.93	999	42	42	42	42	999
Threshold depth for 100% snow cover	0.04	0.04	0.04	0.04	0.04	0.04	0.04	0.03	0.035	0.04	0.08	0.08	0.08	0.08	0.08	0.01	0.01	0.02	0.02	0.025	0.025	0.025	0.02	0.02
Leaf area index (dimensionless)	4	4	4	4	4	4	4	4	4	4	4	4	4	4	4	4	4	4	4	4	4	4	4	4
Upper bound on max albedo snow	40	64	64	64	64	60	64	69	67	45	58	54	32	52	53	70	35	30	69	58	55	55	65	75